Deanship of Graduate Studies
Al-Quds University

"Sucrose Myristate Micellar Systems: Formulation, Characterization and Cefuroxime Axetil Solubilization"

Muhammad "Abed-AlRhman" Taea Fanun

M.Sc. Thesis

Jerusalem-Palestine

1436/2015

"Sucrose Myristate Micellar Systems: Formulation, Characterization and Cefuroxime Axetil Solubilization"

Prepared by:

Muhammad “Abed-AlRhman” Taea Fanun

B.Sc: Food Science and Technology, Al-Quds University Palestine

Supervisor: Monzer Fanun, PhD

A thesis submitted in partial fulfillment of requirements for the degree of Food Processing Technology Master Degree in Applied and Industrial Technology

Al-Quds University/ Palestine
1436/2015

Deanship of Graduate Studies
Al-Quds University
Applied and Industrial Technology
Science and Technology Department

Thesis Approval

" Sucrose Myristate Micellar Systems Formulation, Characterization and Cefuroxime Axetil Solubilization "

Prepared by: Muhammad "Abed-AlRhman" Taea Fanun

Registration No: 21120170

Supervisor: Dr. Monzer Fanun

Master Thesis Submitted and Accepted, Date:13/5/2015

The names and signatures of the examining committee members are as follows:

1- Head of Committee: Dr. Monzer Fanun **Signature:**

2- Internal Examiner: Dr. *Sameer Barghouthi* **Signature:**

3- External Examiner: Dr. Dr.Alfred Abed Rabbo **Signature:**

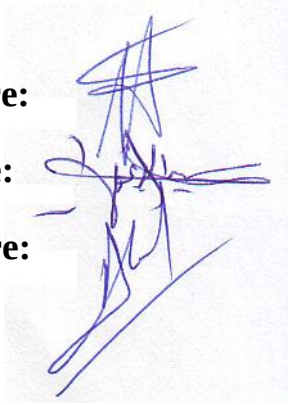

Jerusalem-Palestine

1436/2015

Dedication

I would like to dedicate this thesis to my parents for their diligent encouragement and believing in me all the time: my friends, and my supervisor Dr. Monzer Fanun.

My deep gratitude to The Department of Food Science and The Deanship of Graduate Studies at Al-Quds University

Finally, this thesis is dedicated to all those who believe in the richness of learning.

Declaration:

I Certify that this thesis submitted for the degree of master is the result of my own research, except where otherwise acknowledged, and that this thesis (or any part of the same) has not been submitted for a higher degree to any other university or institution.

Signed: 

Muhammad “Abed-AlRhman” Taea Fanun

Date:13/5/2015

Acknowledgements:

I would like first of all to express my deep gratitude to my supervisor Dr. Monzer Fanun for his special tremendous efforts on my experiments that I respect and admire the most.
I would also like to thank the Department of Food Science at Al-Quds University for their help through this work.

Finally, but by no means least, I wish to thank all of my family, friends and colleagues for the support and encouragement they generously provided through my study period.
Lastly, I offer my regards and blessings to all of those who supported me in any respect during the completion of the project.

Muhammad “Abed-AlRhman” Taea Fanun

Abstract:

In this study, the reserch estimated the food grade sugar ester, nonionic, sucrose myristate M1695, food grade emulsifiers, and the quality standards for food application. Sucrose myristate M1695 has unique properties (biodegradable, nontoxic, and capable of forming temperature-insensitive microemulsions) which make it suitable for a variety of food-based and pharmaceutical application.

Different types of oils are used in this study such as the cyclic oils, peppermint oil (MNT) and R(+)-limonene oil(LIM), and the linear isopropylmyristate (IPM) oil, and caprylic-capric triglyceride (CCT).

Surfactant molecules are used in microemulsion to bring down the water/oil interfacial tension (IFT) to a very low value, but if surfactant does not bring the interfacial tension down to the required value, other substance must be added to obtain the required interfacial tension for the formation of a stable microemulsion such as short chain alcohols, cosurfactant. The cosurfactants used in this study are propylene glycol, propionic acid, ethanol and, glycerol. The cosurfactants added to the mixture to increase solubilizing power of surfactant system, all cosurfactants used in this study are food, cosmetic, and pharmaceutical grade.

The simplest microemulsion used in this research consisted from water, surfactant, and oil (W/S/O). Single surfactant and, a single oil are used to study the effect of different types and percentages of surfactant on the phase behavior of each system. Firstly, single surfactant with single oil are used at different temperatures 25, 37, and 45°C. Another type of microemulsion used in this research consisted of water, surfactant, and a mixture of oils and cosurfactant at different concentrations.

We explored the effect of mixing oil with cosurfactant on the phase behavior, water solubilization capacity and the area of the microemulsion region A_T (%), It was found that mixing oils and cosurfactant increased the water solubilization capacity; this depended on the type and percentage of oil and cosurfactant.

Cyclic peppermint and R(+)-limonene oils have higher water solubilization capacity than other types of oil due to its cyclic structure that enhances penetration on the surfactant surface and due to its low molecular volume, caprylic-capric triglyceride and linear

isopropylmyristate oil have low total monophasic area because of their high molecular volume, so their ability to penetrate the interfacial film is very low and does not assist to obtain the optimum curvature of surfactants.

When temperature was changed from 25°C to 45°C, the total monophasic region A_T (%) was not affected, indicating the formulation of temperature insensitive microemulsions.

Electrical conductivity was used in this research to determine microemulsion microstructure. Electrical conductivity measurements were performed to determine the type of formed microemulsion droplets (i.e. water-in-oil (W/O), bicontinues, or oil-in-water (O/W).

In this research, Sucrose myristate M1695 microemulsion system were used to solubilize active pharmaceutical ingredients (cefuroxime axetil)

Cefuroxime axetil is used to reduce the development of drug-resistant bacteria. Cefuroxime axetil should be used only to treat or prevent infections that are proven or strongly suspected to be caused by bacteria.

It was found that the solubilization capacity of the drug is structure dependent. Maximum drug solubilization was absorbed in the micelle system that decrease as the system passes to water-in-oil microemulsions and continued to decrease as the system passed to the bicontinuous and oil-in-water microemulsions. The oil and cosurfactant type and percentage used in the formulation of the microemulsion are considered the major components that affect cefuroxime axetil solubilization.

نظم المستحلبات الدقيقة لسكر الميرستات: تحضير و تشخيص و إذابة السفيروكسيم اكستل

الملخص

اسم الطالب : محمد عبد الرحمن طايع فنون

اسم المشرف: الدكتور منذر فنون

تقوم هذه الدراسة على خلط مكونات لا تختلط ببعضها البعض، لتدخل في الصناعات الغذائية والدوائية وعلوم البيئة وغيرها. هذه المواد هي ماء وزيت حيث يتم خلطها باستخدام مادة تسمى المستحلبات وهي خوافض التوتر السطحي مما يجعل الزيت والماء يبدوان بالعين المجردة كأنهما حالة واحدة، حيث تسمى هذه المركبات مستحلبات دقيقة (Microemulsion). تتميز المستحلبات الدقيقة بانها شفافة، ثابتة (ثيرموميكانيكيا) لمدة طويلة من الزمن وقليلة اللزوجة، وذات توتر سطحي صغير.

تهدف هذه الدراسة الى تكوين مركبات من الزيت والماء تسمى مستحلبات دقيقة (Microemulsions) وذلك باضافة مادة لخفض التوتر السطحي بين الزيت والماء تسمى مستحلب (surfactant) وتهدف ايضا الى إذابة أدوية فيها كنوع من أنواع التطبيقات العملية لهذه الأنظمة ويتم تشخيصها و التعرف على تركيبها الداخلي بطريقة التوصيل الكهربائي.

تناولت هذه الدراسة عدة انظمة تختلف فيما بينها في التركيب والنوعية وايضا نسب المواد المضافة، حيث تناول البحث نظام مبسط يحتوي على (ماء /خوافض توتر سطحي لاأيونية / زيت)، ونظام مكون من (ماء/ خوافض توتر سطحي لاأيونية / زيت / مساعدات خوافض التوتر السطحي) ، تستخدم هذه المساعدات لزيادة قدرة خوافض التوتر السطحي على اذابة الماء بالزيت وهي عادةً تتكون من الكحول.

استخدم نوع واحد من خوافظ التوتر السطحي يسمى سكروز ميرستسيت (M1695)، أما الزيوت المستخدمة والتي تناولتها هذه الدراسة هي :أولا زيوت عطرية حلقية مثل زيت نعناع (MNT) و زيت الحمضيات(LIM)، ثانيا زيوت خطية التركيب مثل الأيزوبروبيل مريستي (IPM) ، ثالثا زيوت ثلاثية الجليسيرايد مثل الكابريلك-كابرك ثلاثي الجليسريد (CCT)،أما مساعدات خوافض التوتر السطحي المستخدمة في هذه الدراسة والتي أيضا تدخل في مجالات الغذاء ومواد التجميل والصناعات الدوائية فهي مادة البروبلين جلايكول (PG) التي تتميز بسهولة ذوبانها في الماء،وكذلك الايثانول (ETOH) وحمض بروبيونك (PRA) الذي يستعمل كذلك كمضاد للبكتيريا والجليسرول.

في هذه الدراسة تم خلط السكروز ميرستيت مع الماء وزيت الحمضيات، زيت النعناع، زيت الكابريلك-كابرك ثلاثي الجليسريد و زيت الأيزوبروبيل مريستيت كل على حدى فوجد أن المستحلبات الدقيقة المبنية في تركيبها على زيت الحمضيات والنعناع تعطي اكبر قدر من المستحلبات الدقيقة في رسومات الحالات (Phase diagram) للمستحلب الدقيق من أي زيت اخر ويعود ذلك بسبب الشكل الحلقي وحجمها الجزيئي (Molecular volume) لهذه الزيوت الذي يجعل لها قدرة افضل على اختراق اسطح خوافض التوتر السطحي، في الجزء الثاني من هذا البحث خلط السكروز ميرستيت مع الماء والكابريلك-كابرك ثلاثي الجليسريد وزيت الأيزوبروبيل مريستيت مع مساعدات خوافض التوتر السطحي المذكورة سابقا فوجد ان الايزو بروبيل ميرستيت مع البروبلين جلايكول له اكبر مساحة وحيدة الحالة ((Monophasic region A_T(%) في رسومات الحالات للمستحلب الدقيق، ولوحظ ايضا ان المساحة وحيدة الحالة في رسومات الحالات للمستحلب الدقيق زادت بشكل كبير في جميع الانظمة عند اضافة مساعدات خوافض التوتر السطحي بكافة انواعها.

تتكون المستحلبات الدقيقة (Microemulsions) من بناء جزيئي دقيق مكون من طبقة واحدة. تهدف هذه الدراسة الى تبيان وتوضيح البناء الجزيئي الدقيق لهذه الطبقة باستخدام تقنية التوصيل الكهربائي، حيث وجد أن التوصيل الكهربائي للمستحلبات الدقيقة سواء كانت مبنية من مركب مستحلب منفرد أو مزيج من المستحلبات تعتمد بشكل أساسي على محتوى الماء داخل المستحلبات الدقيقة. كذلك وجد أن أعلى قيمة للتوصيل الكهربائي للمستحلبات الدقيقة التي تمت دراستها تحدث عندما تزيد كمية الماء على الزيت مما يدلّ على تحول في شكل التركيب الدقيق للمستحلبات الدقيقة من (ماء في زيت) إلى (زيت في ماء).

من اهم اهداف هذه الدراسة هوَ استكشاف قدرة المستحلبات الدقيقة (Microemulsions) على إذابة عقاقير (ذات ذائبيّة منخفضة جدا في الماء) وذلك بسبب الخواص الفريدة التي تتمتع بها المستحلبات الدقيقة، حيث انها شفافة، ثابتة(ثيرموميكانيكيا) لمدة طويلة من الزمن وايضا قدرتها العالية على تذويب عقاقير ذات ذائبية منخفضة. في هذا البحث تم استخدم دواء السيفروكسيم اكستل وهو دواء قليل الذائبية يستخدم كمضاد حيوي.

تم اضافة دواء السيفروكسيم اكستل على الانظمة المبنية من السكروز ميرستيت مع الماء والزيوت ومساعدات خوافض التوتر السطحي، حيث وجد أن سعة الذائبية للعقاقير المستخدمة في الدراسة تقل مع زيادة محتوى الماء في المستحلب الدقيق وهذا دليل على حدوث تغير في التركيب الداخلي للمستحلبات الدقيق، ولوحظ ايضا انه اصبح بالامكان انتاج منتجات جديدة لهذا العقار مثل المراهم لتستخدم كمضاد حيوي في حالة الجروح والحروق حيث اصبح بالامكان اذابته وانتناجه باشكال مختلفة .

Table of Contents

Page number

List of Tables:

List of Figures

Abbreviations, Symbols & Terminology:

A_T (%): Total one-phase microemulsion area (total monophasic area)

CCT: Caprylic-capric triglyceride oil

Co-S: Cosurfactant

ETOH: Ethanol

GLY: Glycerol

HLB: Hydrophilic-lipophilic balance

IFT: Interfacial tension

IPM: Isopropylmyristate oil

LIM: R (+)-limonene oil

M1695: Sucrose myristate

ME: Microemulsion

MNT: Peppermint oil

NaCl: Sodium chloride

O/W: Oil-in-water

O: Oil

PAIS: Pharmaceutical active ingredient

PG: Propylene glycol

PIT: Phase inversion temperature

PRA: Propionic acid

S: Surfactant

W/O: Water-in-oil

W: Water

Winsor I: Oil-in-water microemulsion coexists with excess oil

Winsor II: Water-in-oil microemulsion coexists with excess water

Winsor III: Bicontinuous middle phase microemulsion

Winsor IV: Microemulsion which is not in equilibrium with oil or water

Winsor II: Water-in-oil microemulsion coexists with excess water

Winsor III: Bicontinuous middle phase microemulsion

Winsor IV: Microemulsion which is not in equilibrium with oil or water

μS: Microsiemens

ρ: Density

σ: Electrical conductivity

1.Introduction

Microemulsions are clear, thermodynamically stable mixtures of two immiscible liquids brought together by the means of surfactant or a mixture of surfactants forming a film separating the immiscible phases. The unique properties of microemulsions that include ultralow interfacial tension, large interfacial area, low viscosity, and high solubilization capacity attracted researchers [Fanun. M, 2009], [Kumar. P, Mittal. K.C, 1999], [Kunieda. H, Solans. C,1996], [Bourrel. M, Schechter. R.S,1988].

The interfacial tension between oil and water is reduced to a very low value by the presence of an amphiphile, [Prince. L.M ,1977], but if the amphiphile doesn't bring the interfacial tension down to the required value, another substance must be added to obtain the required interfacial tension for the formation of a stable microemulsion; e.g. short chain alcohols (cosurfactant). Microemulsions are composed of four components water, oil, surfactant, and a short chain substance called a cosurfactant. Fanun and Salah Al-Diyn 2006a investigated the phase behavior of the systems water/sucrose laurate/ethoxylated mono-di-glyceride/oil as a function of temperature and the weight ratio of ethoxylated mono-di-glyceride in the mixed surfactants. The oils were R(+)-limonene, isopropylmyristate, and caprylic-capric triglyceride, they found that the phase inversion temperature decreases and the efficiency of the mixed surfactants increases as the weight ratio of the ethoxylated mono-di-glyceride in the mixed surfactants increases. R(+)-limonene gave lower phase inversion temperatures and higher efficiencies compared to isopropylmyristate and caprylic-capric triglyceride. The solubilization capacity of the system water/sucrose laurate/oil increased upon the addition of ethoxylated mono-di-glyceride which stabilizes the surfactant layer and increases the interfacial area.

Microemulsions have been intensively studied during the last decades [2004-2014] by many scientists and technologists because of their great potential in many applications, [Fanun. M, 2008, Kumar. P, Mittal. K.C, 1999, Solans.C. and Kunieda. H 1997]. The first paper on microemulsions appeared in 1943, but it was Schulman and coworkers who first proposed the word "microemulsion" in 1959, [Fanun. M, 2008]. Since then, the term "microemulsions" has been used to describe multicomponent systems comprising nonpolar, aqueous, surfactant, and cosurfactant components. The application areas of microemulsions have increased dramatically during the past decades. For example, the

major industrial areas are fabricating nanoparticles, oil recovery, pollution control, and food and pharmaceutical industries, [Fanun. M ,2008].

An interesting characteristic of microemulsion is that when even a small amount of a mixture, of surfactant and cosurfactant, is added to biphasic water-oil system, a thermodynamically stable mixture forms spontaneously, [Hsiao. Ho et al., 1996], due to their unique properties, microemulsions have been used in a variety of technological applications including environmental protection, nanoparticle formation, personal care product formulations, drug delivery systems, and chemical reaction media, [Solans .C, and Kunieda. H, 1997], [Brusseau. M.L, Sabatini. D.A, Gierke. J.S, and Annable. M.D,1999], [Sabatini. D.A, and Knox. R.C,1992], [Texter. J, 2001], [Terjarla. S, 1999] and [Lawrence. M.J, and Rees , 2000]. When the microemulsion components being used are safe for human consumption, microemulsions become important in fields such as foods, cosmetics, pharmaceuticals, and medicine, [Kunieda. H, Shinoda. J, 1982], [Attwood. D, 1994], [Shah. D.O, Bansal. V.K, Chan. K.S, and Hsich. C.W. 1977]. Microemulsions have found extensive uses and applications in important fields such as biotechnology, pharmacy and oil recovery, [Kunieda. H, Solans. C, 1996].

Sucrose ester (SE), a nonionic surfactant, contains sucrose as the hydrophilic group and a fatty acid as the hydrophobic, [Rosen. M.J, 1989] and the microemulsions formed using sucrose ester can be temperature insensitive [Pes. M.A, Aramaki. K, Nakamura. N, and Kunieda. H, 1996].

Numerous groups have studied the phase behavior and properties of water/sucrose esters/cosurfactant/oil microemulsions; it was found that sucrose esters in the presence of C2-C8 alcohols as cosurfactants, can form microemulsions used for pharmaceutical and food applications, [Fanun. M, Wachtel. E, Antalek. B, Aserin. A, and Garti. N.A, 2001], [Thevenin. M.A, Grossiord. J.L, and Poelman. M.C, 1996].

An advantageous property of sucrose ester surfactants is their weak temperature dependence of the head group hydration, biodegradable, nontoxic, and capable of forming temperature-insensitive microemulsions, which make them suitable for a variety of food-based and pharmaceutical application. This property makes it difficult to tune the spontaneous curvature of the surfactant film in ternary water sucrose ester/oil systems by

changing the temperature [Fanun. M, Wachtel. E, Antalek. B, Aserin. A, Garti.N, 2001], [Garti. N, Aserin. A, Fanun. M, 2000] .

Microemulsion systems can be one of three types depending on the relative ratios of the constituting components: oil-in-water (o/w ME) systems comprise water as the continuous medium; water-in-oil (w/o ME), where oil is the continuous medium and bicontinuous microemulsion [Garti. N, Fanun. M, Aserin. A, et al, 2001].

The surfactant used in this research was sucrose myristate M1695, which is a sugar ester (sugar base surfactant), nonionic, food grade emulsifier. Sucrose myristate (M1695) has unique properties, it is biodegradable, nontoxic and capable of forming temperature-insensitive microemulsions, which make them suitable for a variety of food-based and pharmaceutical application.

The oils used in this research peppermint oil (MNT), R (+)-limonene oil (LIM), isopropylmyristate (IPM), and caprylic/capric triglyceride oil (CCT). Different types of oils were used (liner, cyclic, and triglyceride) to study the effect of the type of oils on chemical formula, effective carbon number, and molecular volume on solubility and phase diagram (A_T), then the cosurfactant is often added to the mixture to increase solubilizing power of surfactant system, different substance can be used as cosurfactant, mainly alcohols, amines or ether alcohols, the cosurfactant used are propylene glycol (PG), ethanol (ETOH), propionic acid (PRA) and glycerol (GLY).

Microemulsions are fundamental in the pharmaceutical field due to their high stability, ease of preparation, and particularly their ability to considerably increase the bioavailability of sparingly water-soluble drugs, [Malmsten. M,1996] and [Müller, R. H, Benita. S, Böhm. B, 1998].

The properties of drug-loaded microemulsions can reveal the presence of molecular interactions between the loaded drug and the microemulsion. These properties include the electrical conductivity, [Cametti.C et al, 1992], [Kahlweit.M, et al, 1993], viscosity [Berghenholtz et al., 1995], [Matsumoto and Sherman, 1969], [Ray et al., 1992], and diffusion, [Berghenholtz.J, et al, 1995], [Matsumoto. S. P, and Sherman. P, 1969, Ray. S, et al, 1992], [Fanun. M, 2007, Fanun.M and Salah Al-Diyn. W, 2006, 2007], [Olsson.U, et al, 1986], [Soderman. O, and Nyden. M,1999].

In this research, we use microemulsions to dissolve active pharmaceutical ingredients (cefuroxime axetil) that are normally poor soluble, microemulsions have unique properties that include the high mutual solubilization of water and oil.

Cefuroxime axetil (CA) is a broad-spectrum/lactamase stable, second generation cephalosporin antibiotic with a proven record of efficacy and safety in the parenteral management of various infections including urinary tract infections, cefuroxime axetil poor soluble in biological fluids, which results in poor bioavailability after oral administration [Adams .D.H, Wood .M.J, Farre .D 1985], [Keith B. Holten. M.D, and Edward. M, Onusko. M.D 2000], [Akira.Y, Junichi. M, et al, 1988]. Cephalosporins work the same way as penicillins.

Since cefuroxime is not absorbed orally, cefuroxime axetil (CA) (1-acetoxyethyl ester of a β-lactamase-stable cephalosporin), an orally absorbed pro-drug of cefuroxime is used in the treatment of common community acquired infections because of its in-vitro antibacterial activity against several gram-positive and gram-negative organisms, [Nighute A. B., Bhise S. B, 2009].

Cefuroxime axetil is used to reduce the development of drug-resistant bacteria and maintain the effectiveness of CA and other antibacterial drugs, CA should be used only to treat or prevent infections that are proven or strongly suspected to be caused by bacteria.

Indeed, a large amount of a lipophilic drug can be dissolved in the microemulsion oil droplets, so that drug solubility in the whole system is considerably enhanced. Drug diffusion from the oil droplets to the living tissues can take place by crossing the surrounding aqueous medium which essentially acts as a barrier to drug transport owing to the very low drug solubility in water. In this case, microemulsion speeds up the drug uptake by the living tissues as in the case of oil droplet phagocytosis [Thiele. L, Rothen-Rutishauser. B, et al, 1999].

Moreover, drug-loaded microemulsions are fundamental for delivery systems devoted to topial and transdermal administration, [Lapasin. R, Grassi. M, Coceani. N, 2001], [Gasco. M.R, Gallarate. M, Pattarino. F, 1991], [Osborne. D.U, Ward. A.J, and O'Neill. K.J,

1998], for solid nanoparticles preparation, [Viswanathan. N.B, Thomas. P.A, et al,1999], [Song. S, Labhasetwar. V, et al, 1998] and for loading process of a lipophilic drug into hydrophilic carriers, [Chiellini. C, Coceani. N, et al, 2000], technologies that have a wide employment in the treatment of many diseases and that could have a considerable impact also in the gene delivery field, [Roy. K, Huang. S, and Leong. K 1999].

In the first step was to formulate different systems containing water / sucrose myristate M1695 / and oils without adding cosurfactant, then to add the cosurfactants to oils in different percentages to study the effect of cosurfactant on phase diagram. Then to study the effects of changing the relative amounts of microemulsion components on the transport, diffusion, and structural properties of these self-assemblies were investigated using electrical conductivity.

The formulation of microemulsion system and its ability to solubilize active pharmaceutical ingredients CA was investigated by dissolving in microemulsion that are normally poor soluble, we used different types of oils (cyclic, linear and triglyceride) that were mixed with cosurfactant in different percentages.

2. Objectives

2.1 Formulation of microemulsion systems using different components which include biologically compatible oil phase (cyclic oils; peppermint and R (+)-limonene, linear oil; isopropyl myristate and triglyceride oil; caprylic capric triglyceride), nonionic surfactant (food and pharmaceutical grade) sucrose myristate M1695 with or without addition of cosurfactant at different temperatures. This is accomplished by multi component system phase diagrams.

2.2 Evaluation of the water solubilization capacity of the formulated microemulsion systems by evaluating the area of the one-phase microemulsion region (A_T) that is limited by the micro-emulsification failure boundaries.

3.3 Exploring the microstructures of the formed microemulsion by electrical conductivity. These techniques will be used to study how changes (in the relative amounts of the surfactant and in the chain length of the surfactants or oil, the presence of cosurfactant and the addition of water) influence the microemulsion microstructure within the one-phase region.

3.4 Evaluation the maximum solubilization capacity of the pharmaceutical active ingredients (cefuroxime axetil) CA and define the relationship between the microstructure of the formulated microemulsions and the quantity of solubilized material.

3 Materials and Methods

3.1 Materials

3.1.1 Surfactants

Surfactants (surface active agents) sucrose myristate M1695

Sucrose ester are food grade emulsifiers, they are sucrose fatty acid ester (sugar ester), nonionic, ultra-mild, highly pure and strong water binders, they have an hydrophilic-lipophilic balance scale (HLB) 16 and surface tension 41.5 mille newton per meter at 20°C .

Sucrose myristate M1695 present in Figure 3.1 were obtained from Mitsubishi-Kasei Food Corp. (Mie, Japan).

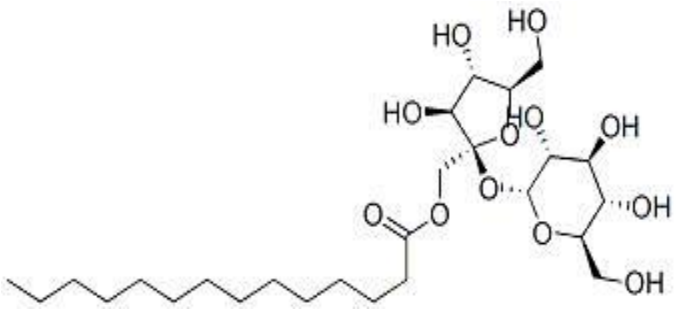

Figure 3.1: The chemical structure of sucrose myristate M1695.

Chemical structure data base that could be found in the web site (http://www.chemspider.com/StructureSearch.aspx)

3.1.2 Oils

Different types of oils were used in this research., including (liner , cyclic , and triglyceride oils) in different concentration, these oils differ in their molecular volumes and effective carbon number, this plays an important role in water solubilization and the total monophasic area A_T.

Cyclic oils: peppermint oil and R (+)-limonene oil.

3.1.2. a Peppermint oil (MNT), (98%).

Peppermint oil (Mentha piperita) is derived from the peppermint plant- a cross between water mint and spearmint - that thrives in Europe and North America. The major compound of peppermint oil is menthol, the chemical structure of peppermint oil presented in Figure 3.2.

Peppermint oil is commonly used as flavoring in foods and beverages and as a fragrance in soaps and cosmetics. Peppermint oil is also used for a variety of health conditions and can be taken orally in dietary supplements or topically as a skin cream or ointment, peppermint oil (MNT), (98%) was purchased from Sigma Chemicals Co. (St. Louis, USA).

Some evidence suggests that peppermint oil may help relieve symptoms of irritable bowel syndrome and indigestion. But despite the promising research, there is no clear-cut evidence to support its use for other health conditions. When it is used directly, dietary supplements and skin preparations containing peppermint oil are likely safe for most adults.

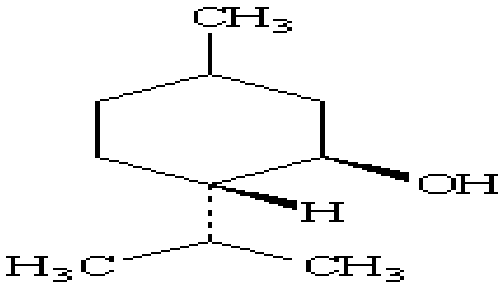

Figure 3.2: The chemical structure of menthol major compound of peppermint oil.

Chemical structure data base that could be found in the web site
(http://www.chemspider.com/StructureSearch.aspx)

3.1.2.b R (+)-limonene (LIM)

R-limonene is the major component of the oil extracted from citrus rind. When citrus fruits are juiced, the oil is pressed out of the rind. This oil is separated from the juice, and distilled to recover certain flavor and fragrance compounds. The bulk of the oil is left

behind and collected. This is food grade R-limonene. After the juicing process, the peels are conveyed to a steam extractor. This extracts more of the oil from the peel. When the steam is condensed, a layer of oil floats on the surface of the condensed water. This is technical grade R-limonene, the chemical structure of R (+)-limonene oil presented in Figure 3.3, R (+)-limonene (98%) was purchased from Sigma Chemicals Co. (St. Louis, USA).

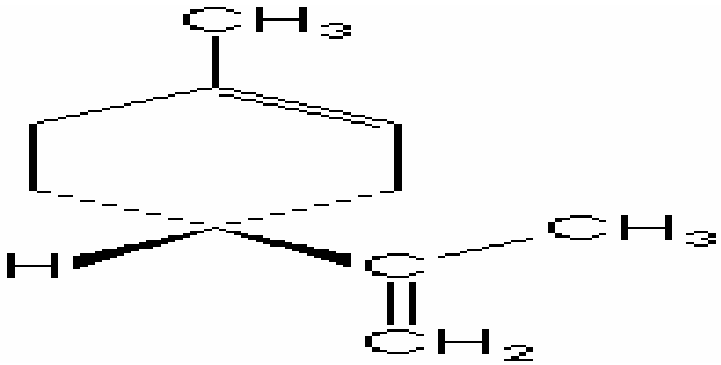

Figure 3.3: The chemical structure of R (+)-limonene oil

Chemical structure data base that could be found in the web site
(http://www.chemspider.com/StructureSearch.aspx)

3.1.2.d Linear oils: isopropylmyristate (IPM), (tetradecanoic acid, 1-methyethyl ester (99%)).

Isopropyl myristate is a synthetic oil widely used in the cosmetics and pharmaceutical industries as a lubricant, emollient and as a non-toxic alternative for controlling head lice. The oil is manufactured by condensing myristic acid with isopropyl alcohol presented in Figure 3.4 , it is colorless and mild in odor. It is readily absorbed by the skin and lessens the greasy nature of cosmetics while lending them a sheer, slick feel. In addition, it is commonly used as an additive in oral hygiene products, such as mouthwash. Although generally considered to be safe, isopropyl myristate may cause mild allergic reactions and could aggravate skin conditions, such as acne, isopropylmyristate (IPM)(99%), was purchased from Sigma Chemicals Co. (St. Louis, MO).

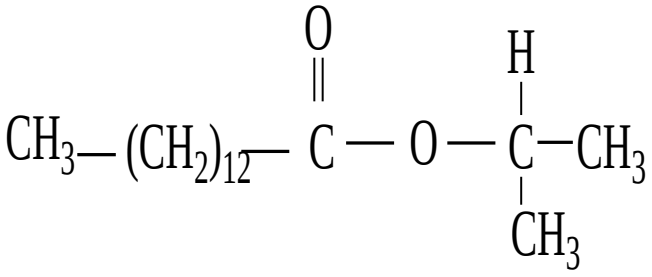

Figure3.4: The chemical structure of isopropylmyristate oil

Chemical structure data base that could be found in the web site
(http://www.chemspider.com/StructureSearch.aspx)

3.1.2.c Triglyceride oils: caprylic/capric triglyceride oil (CCT).

Caprylic/capric triglycerides are produced by the esterification of glycerol (plant sugars) with mixtures of caprylic (C:8) and capric (C:10) fatty acids from coconut or palm kernel oils. The special combination and esterification are responsible for the silky oil feel. This is a specialized process used to achieve the skin benefits of the specific fatty acid esters that also results in superior oxidative stability, low color and odor, as it is then further refined to remove residual fatty acids resulting in a pure ester, with a silky oil feel, that is a great choice for sensitive skin and oil free applications. The unique metabolic and functional properties of caprylic/capric triglycerides are a consequence of their chemical structure presented in Figure 3.5, and makes them a versatile ingredient in numerous pharmaceutical and cosmetic applications, Caprylic-Capric triglyceride (CCT) “Neobee M5” a food grade triglyceride containing 66 wt% C7 and 34 wt% C9, was obtained from Stepan Europe (Voreppe, France).

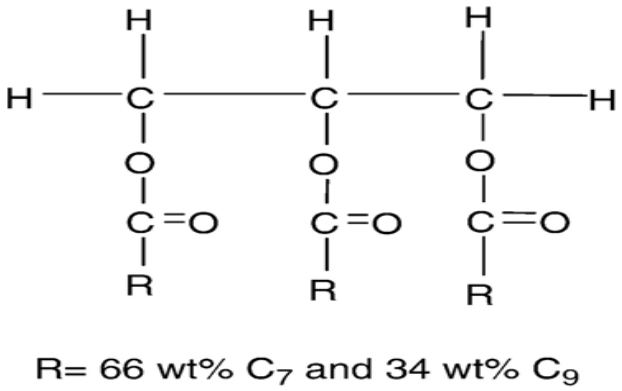

Figure 3.5: The chemical structure of caprylic/capric triglyceride oil

Chemical structure data base that could be found in the web site
(http://www.chemspider.com/StructureSearch.aspx)

Caprylic/capric triglyceride oil is found in two structures: caprylic/capric triglyceride compressed, they contine C_{11} or caprylic/capric triglyceride extended fork and they contain C_{16y} .

3.1.3 Co-surfactants

3.1.3.a Ethanol

Ethanol is a straight-chain alcohol, and its molecular formula is C_2H_5OH, absolute ethanol (minimum 99.8%) has the structural formula (CH_3CH_2OH) presented in Figure 3.6. In general, they are unsuitable for food uses, but using a small amounts (about 5%) of ethanol in food products is acceptable, ethanol (minimum 99.8%) were purchased from Was obtained from Frutarom (Haifa, Israel

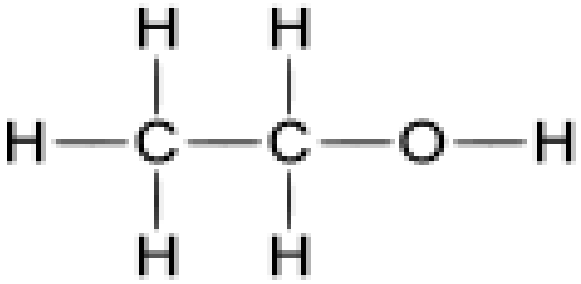

Figure 3.6: The chemical structure of ethanol.

Chemical structure data base that could be found in the web site
(http://www.chemspider.com/StructureSearch.aspx)

3.1.3.b Propylene glycol, PG

Propylene glycol like water form hydrogen bonds has relatively high dielectric constants and is immiscible with hydrocarbon solvents.

The co-surfactant used was 1,2-propandiol (propylene glycol, PG) (99.5%), is shown in Figure 3.7, 1,2-Propandiol (Propylene glycol, PG) (99.5%) was purchased from BDH (Poole, UK).

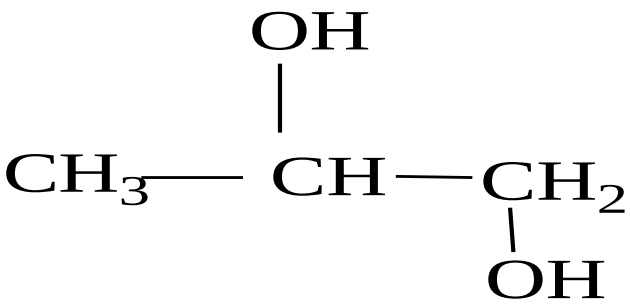

Figure 3.7: The chemical structure propylene glycol, PG.

Chemical structure data base that could be found in the web site
(http://www.chemspider.com/StructureSearch.aspx)

3.1.3.c Propionic acid

It is a naturally occurring carboxylic acid with chemical formula CH_3CH_2COOH. It is a clear liquid with a pungent odor. The anion CH_3CH_2COO as well as the salts and esters of propionic acid are known as propionates (or propionates), the chemical structure of propionic acid presented in Figure 3.8 . Propionic acid is inhibits the growth of mold and some bacteria at the levels between (0.1 and 1% by weight). Propionic acid was purchased from Sigma Chemicals Co. (St. Louis, USA).

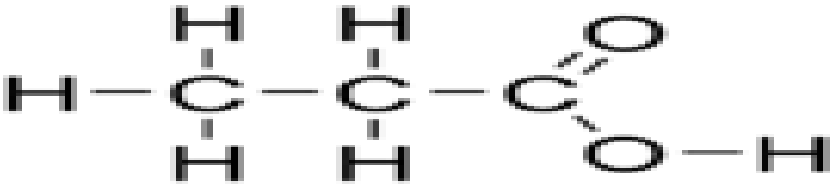

Figure 3.8: The chemical structure of propionic acid.

Chemical structure data base that could be found in the web site
(http://www.chemspider.com/StructureSearch.aspx)

3.1.3.d Glycerol

Known as simple polyol compound. Glycerol is colorless, odorless and viscous liquid that is widely used in pharmaceutical formulations. Glycerol has three hydroxyl groups that are responsible for its solubility in water and its hygroscopic nature. The glycerol backbone is central to all lipids known as triglycerides. Glycerol is sweet-tasting and of low toxicity. Like ethylene glycol and propylene glycol, when dissolved in water, glycerol disrupts the hydrogen bonding between water molecules such that the mixture cannot form a stable crystal structure unless the temperature is significantly lowered, the viscosity of the aqueous solution is increased by glycerol, the chemical structure of glycerol presented in Figure 3.9. Glycerol (99%) was purchased from Sigma Chemicals Co. (St. Louis, USA).

Figure 3.9: The chemical structure glycerol (1, 2, 3-trihydroxypropane).

Chemical structure data base that could be found in the web site
(http://www.chemspider.com/StructureSearch.aspx)

3.1.4 Water

Mill Q water with $\sigma < 3$ μS was used.

Table 3.1 : All materials used in this research.

Oil phase	Surfactants	Cosurfactant	Aqueous phase
Peppermint oil R (+)-limonene oil Isopropyl myristate oil Caprylic/capric triglyceride oil	M1695	Prop ionic acid Propylene glycol Ethanol Glycerol	MQ water

3.1.5 Pharmaceutical Active Ingredients (PAI), cefuroxime axetil (CA).

Poorly water soluble drug, Its molecular formula is $C_{20}H_{22}N_4O_{10}S$ presented in Figure 3.10, and it has a molecular weight of 510.48 Daltons. Cefuroxime axetil is used orally for the treatment of patients with mild-to-moderate infections, caused by susceptible strains of the designated microorganisms.

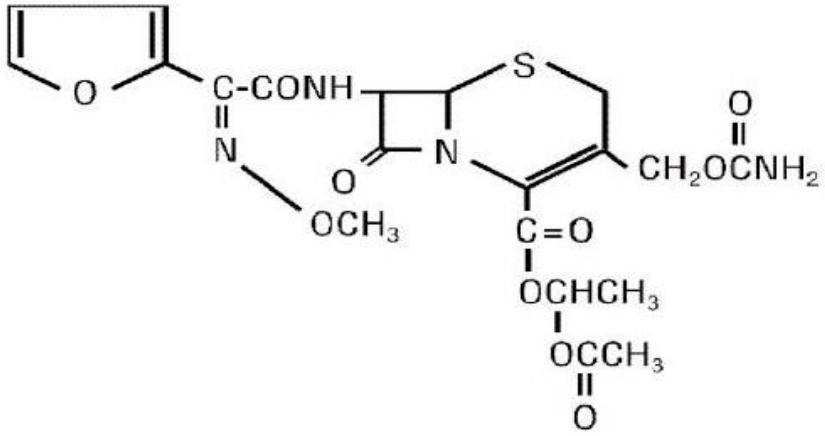

Figure 3.10: Chemical structure of cefuroxime axetil.

Chemical structure data base that could be found in the web site (http://www.chemspider.com/StructureSearch.aspx)

3.2 Methods

3.2.1 Construction of phase diagrams

The phase behavior of the systems consisting of water, oil , surfactant may be described on a phase tetrahedron whose apexes respectively represent the pure components.
1g of a mixture consisting of oil, surfactant were prepared in culture tubes sealed and stirred at high temperature (45°C) by vortex until clear solution was obtained.

Titration these samples with M.q water which was added dropwise until its solubilization limit was reached. Vigorous stirring followed all of the aqueous phase additions on a vortex mixer. The time for equilibration between each addition was typically, from a few minutes up to 24 h.
Phase transitions were detected visually by the appearance of cloudiness or sharply
All phase diagrams were investigated at three temperatures (25°C, 37°C and 45°C).

The Total monophasic area $A_{T(\%)}$ was calculated using the program Auto CAD 2007 software after drawing the phase diagrams using Origin Pro 8.1 software.

Table 3.2**:** The materials used in the construction of phase diagrams of (Surfactants – Single Oil)

Aqueous phase	Surfactant	Oil
W	M1695	MNT
W	M1695	LIM
W	M1695	CCT
W	M1695	IPM

Table 3.3: The materials used in the construction of phase diagrams of (Single Surfactants – Mixed Oils with cosurfactant) MNT Oil.

Aqueous phase	Surfactant	Oil	Cosurfactant	Ratio
W	M1695	MNT	ETOH	(1/1)
W	M1695	MNT	PG	(1/1)
W	M1695	MNT	GLY	(1/1)
W	M1695	MNT	PRA	(1/1)

Table 3.4**:** The materials used in the construction of phase diagrams of (Single Surfactants – Mixed Oils with cosurfactant) LIM Oil.

Aqueous phase	Surfactant	Oil	Cosurfactant	Ratio
W	M1695	LIM	ETOH	(1/1)
W	M1695	LIM	PG	(1/1)
W	M1695	LIM	GLY	(1/1)
W	M1695	LIM	PRA	(1/1)

Table 3.5: The materials used in the construction of phase diagrams of (Single Surfactants – Mixed Oils with cosurfactant) CCT Oil.

Aqueous phase	Surfactant	Oil	Cosurfactant	Ratio
W	M1695	CCT	ETOH	(1/1)
W	M1695	CCT	PG	(1/1)
W	M1695	CCT	GLY	(1/1)
W	M1695	CCT	PRA	(1/1)

Table 3.6: The materials used in the construction of phase diagrams of (Single Surfactants – Mixed Oils with cosurfactant) IPM Oil.

Aqueous phase	Surfactant	Oil	Cosurfactant	Ratio
W	M1695	IPM	ETOH	(1/1)
W	M1695	IPM	PG	(1/1)
W	M1695	IPM	GLY	(1/1)
W	M1695	IPM	PRA	(1/1)

3.2.2 Determination of water solubilization capacity

The water solubilization capacity of different amphiphilic systems should be compared at optimal conditions (Garti, N., Clement, V., Fanun, M. et al, 2000). Li et al, 1989 have employed as a solubilization parameter the area of the one-phase microemulsion region (A_T) that is area limited by the microemulsification failure boundaries. In this research we used the one phase microemulsion region to compare the water solubilization capacity in the studied systems. The relative error in determining the A_T (%) was estimated to be ±2% for all of the systems studied. The following figure presents a schematic phase diagram where we indicated the one phase region, the microemulsification failure and the multiple phase regions.

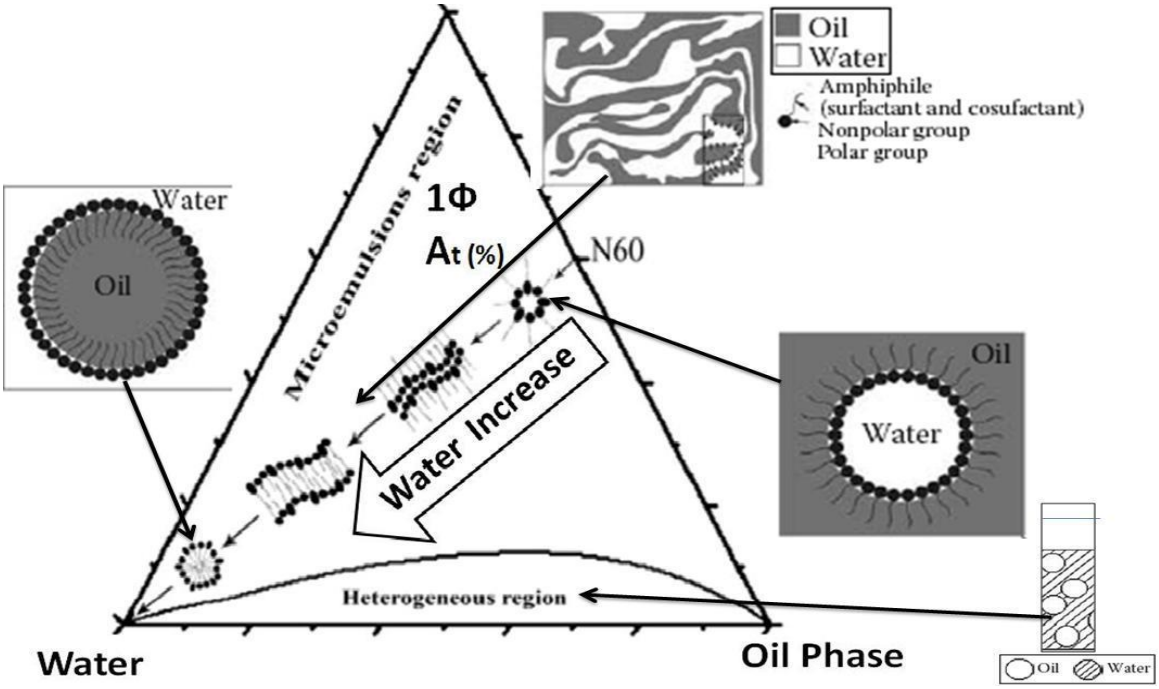

Figure 3.11**:** Schematic presentation (not for scale) of the structural transitions along the N60 dilution line (Fanun M., 2010).

3.2.3 Electrical conductivity measurements

Conductivity measurements were performed at temperatures ±0.3 °C on samples the compositions of which lie along the one phase channel, using conductivity meter, the conductivity cell used is Tetra Con® 325, the electrode material is graphite and the cell constant is 0.475 cm^{-1} ±1.5%.the temperature range is from 14 to 50 °C. In the case of nonionic microemulsions, a small amount of an aqueous electrolyte must be added for electrical conduction (Eicke, H.F., Meier, W. and Hammerich, H. 1994). the electrode was dipped in the microemulsion sample until equilibrium was reached and reading becomes stable at 1 min.

Reproducibility was checked for certain samples and no significant differences were observed. The constant of the conductivity cell was calibrated using standard KCl solutions at the first of every month during the Characterization or when the conductivity meter needs that.

Electrical conductivity measurements are performed to determine the type of microemulsion droplets formed (i.e. water-in-oil (W/O), Bicontinues, or oil-in-water (O/W)).

Table 4.7: The system used for determination of electrical conductivity.

Aqueous phase	Surfactant	Oil	Cosurfactant	Ratio
W	M1695	LIM	PG	(1/1)
W	M1695	CCT	PG	(1/1)
W	M1695	IPM	PG	(1/1)

3.2.4 Determination of drugs Solubilization capacity

Solubilization of cefuroxime axetil has been studied in different microemulsion systems, 3 g of microemulsion was prepared in a test tube and then a small amount of CA (about 10 mg in each step) was added and dissolution was performed by mixing through a vortex in water bath at 45°C for 120 min and then stored at 25°C in water bath. Samples which remained transparent for at least 5 days were loaded step-wise with additional CA to its maximum solubilization. The appearance of turbidity, or a precipitate, indicates that the microemulsions were drug saturated (or supersaturated). No further drug loading in such samples was done. The dissolved amount of CA was estimated by calculated the accumulate weight of CA which was added before the appearance of turbidity, or a precipitate, after they hold in water bath at 25 °C for at least 5 days.

Table 3.8: The system used for determination of cefuroxime axetil solubilization capacity (Single surfactant / single oil)

Aqueous phase	Surfactant	Oil
W	M1695	MNT
W	M1695	LIM
W	M1695	CCT
W	M1695	IPM

Table 3.9**:** The system used for determination of cefuroxime axetil solubilization capacity (Single surfactant / Oil + ETOH)

Aqueous phase	Surfactant	Oil	Cosurfactant	Ratio
W	M1695	MNT	ETOH	(1-1)
W	M1695	LIM	ETOH	(1-1)
W	M1695	CCT	ETOH	(1-1)
W	M1695	IPM	ETOH	(1-1)

Table 3.10**:** The system used for determination of cefuroxime axetil solubilization capacity (Single surfactant / Oil + PG)

Aqueous phase	Surfactant	Oil	Cosurfactant	Ratio
W	M1695	MNT	PG	(1-1)
W	M1695	LIM	PG	(1-1)
W	M1695	CCT	PG	(1-1)
W	M1695	IPM	PG	(1-1)

Table 3.11**:** The system used for determination of cefuroxime axetil solubilization capacity (Single surfactant / Oil + PRA)

Aqueous phase	Surfactant	Oil	Cosurfactant	Ratio
W	M1695	MNT	PRA	(1-1)
W	M1695	LIM	PRA	(1-1)
W	M1695	CCT	PRA	(1-1)
W	M1695	IPM	PRA	(1-1)

Table 3.12**:** The system used for determination of cefuroxime axetil solubilization capacity (Single surfactant / Oil + GLY)

Aqueous phase	Surfactant	Oil	Cosurfactant	Ratio
W	M1695	MNT	GLY	(1-1)
W	M1695	LIM	GLY	(1-1)
W	M1695	CCT	GLY	(1-1)
W	M1695	IPM	GLY	(1-1)

4. Result and Discussion

4.1 Phase behavior

The phase diagram approach to microemulsions was introduced decades ago by gillberg and collaborators, [Gillberg. G, Lehtinen. H, and Friberg. S. E,1970]. Phase diagrams are shown to provide valuable information on the role that structure of the surfactant, cosurfactant and oil play in determining the properties of the system at any composition. Phase diagram describes the experimental conditions in which it is possible to combine the components in order to obtain transparent, one-phase and low-viscous systems. A number of factors influence the water solubilization in mixed nonionic surfactant/oil mixtures that include the type of surfactants, surfactants mixing ratio, and the presence of additives such as alcohols or electrolytes at a given temperature, [Ogino. K,1992]. Phase behavior of nonionic amphiphiles is characterized by the change in the distribution of the amphiphile between the water-rich and oil-rich phase with the change in temperature, [Kahlweit. M, Strey. R, and Busse. G, 1990], [Kahlweit. M, Strey. R, Schomacker. R, and Hasse.D, 1989]. The miscibility of water, oil, surfactant, or mixed surfactants and cosurfactant is a composition dependent variable, [Kunieda. H, Nakano. A, Pes. M, 1995], [Kunieda. H, Nakano. A, Akimura. M, 1995], and [Kunieda. H, Yamagata. M, 1993]. The role of alcohol in microemulsions to delay the occurrence of liquid crystalline phases, to increase the fluidity of the interfacial layer separating oil and water, to decrease the interfacial tension between the microemulsion phase and excess oil and water and to increase the disorder in these interfacial layers as well as their dynamic character. Other studies, [Fanun. M, 2007], [Fanun. M, Salah Al-Diyn. W, 2006], [Szekeres. S, Acosta. E, Sabatini.D.A, and Harwell. J.H, 2006] and [Mehta. S.K, Bala. K, 2000] studied cyclic hydrocarbons effect on microemulsions formation.

Fanun and coworks reported on the effect of polar oils (such as triglycerides, middle- or long-chain alcohols or fatty acids, fatty acid ester) on the water solubilization and properties of microemulsions for different technological applications. These oils influence the surfactant layer curvature in aggregates or self-organized structures when solubilized, [Fanun. M, 2007], [Fanun. M, and Salah Al-Diyn. W, 2007], [Fanun. M, and Salah Al-Diyn. W, 2006], [Paul. B, Mitra. R, 2005].

One of the goals of this research was to incorporate a large amount of water into the microemulsions. Thus, the water solubilization was estimated as the monophasic area of the relevant pseudoternary phase diagrams.

4.1.1 Water / sucrose myristate M1695 /oil phase behavior

4.1.1.a Water / sucrose myristate M1695 / peppermint oil

This section, study the phase behavior of the system: water / sucrose myristate M1695 / peppermint oil in order to determine the boundary of one phase region at different temperatures (25°C,37°C,45°C). Based on results of phase diagram, the total area of the one phase microemulsion region A_T (±2%), was determined.

Figure 4.1 presents the phase diagram of the system: water/ sucrose myristate M1695 / peppermint oil at 25°C, The single phase appears for surfactant contents above 60% wt from the first addition of water. For surfactant contents below 60% wt, the system extends multiple phase regions.

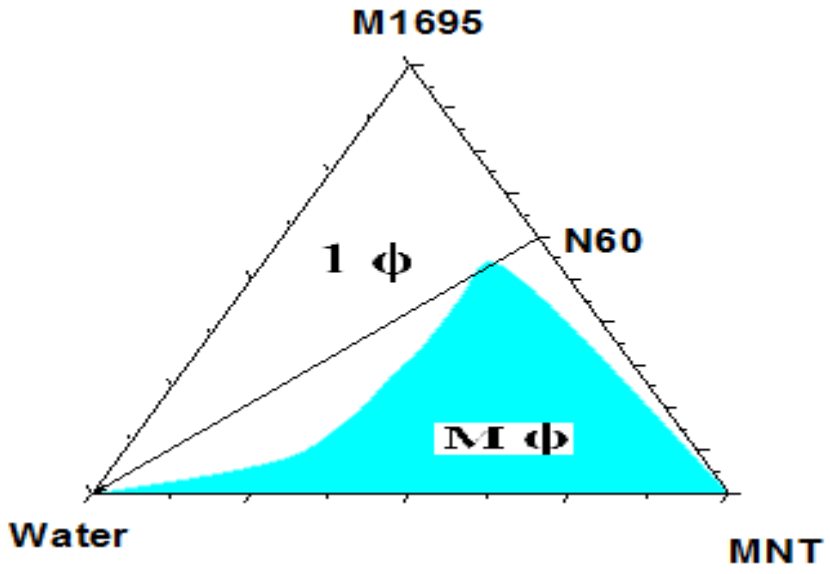

Figure 4.1: Phase diagram of the system: water / sucrose myristate M1695 / peppermint oil at 25 °C

[The one phase region is designated by 1Φ, and the multiple phase regions are designated by M Φ]. N60 is the dilution line where the weight ratio of surfactant / single oil equals 60/40.

4.1.1.b Water / sucrose myristate M1695 / R (+)-limonene

This section, study the phase behavior of the system: water / sucrose myristate M1695 / R (+)-limonene oil in order to determine the boundary of one phase region at different temperatures (25°C,37°C,45°C). Based on results of phase diagram, the total area of the one phase microemulsion region A_T (±2%), was determined.

Figure 4.2 presents the phase diagram of the system: water / sucrose myristate M1695 / R (+)-limonene at 25°C. The single phase appears for surfactant contents above 60% wt from the first addition of water. For surfactant contents below 60% wt, the system extends multiple phase regions.

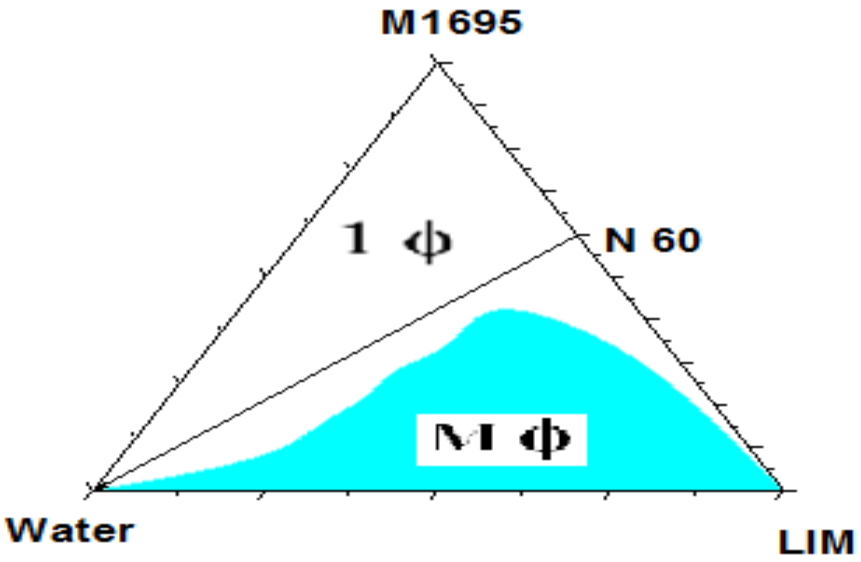

Figure 4.2: Phase diagram of the system: water / sucrose myristate M1695 / R (+)-limonene at 25 °C. [The one phase region is designated by 1Φ, and the multiple phase regions are designated by M Φ]. N60 is the dilution line where the weight ratio of surfactant / single oil equals 60/40.

4.1.1.c Water / sucrose myristate M1695 / caprylic/capric triglyceride oil

This section studies the phase behavior of the system: water / sucrose myristate M1695 / caprylic/capric triglyceride oil in order to determine the boundary of one phase region at different temperatures (25°C,37°C,45°C). Based on results of phase diagram, the total area of the one phase microemulsion region A_T (±2%), was determined.

Figure 4.3 presents the phase diagram of the system: water / sucrose myristate M1695 / caprylic/capric triglyceride at 25°C. The single phase appears for surfactant contents above 60% wt from the first addition of water. For surfactant contents below 60% wt, the system extends multiple phase regions.

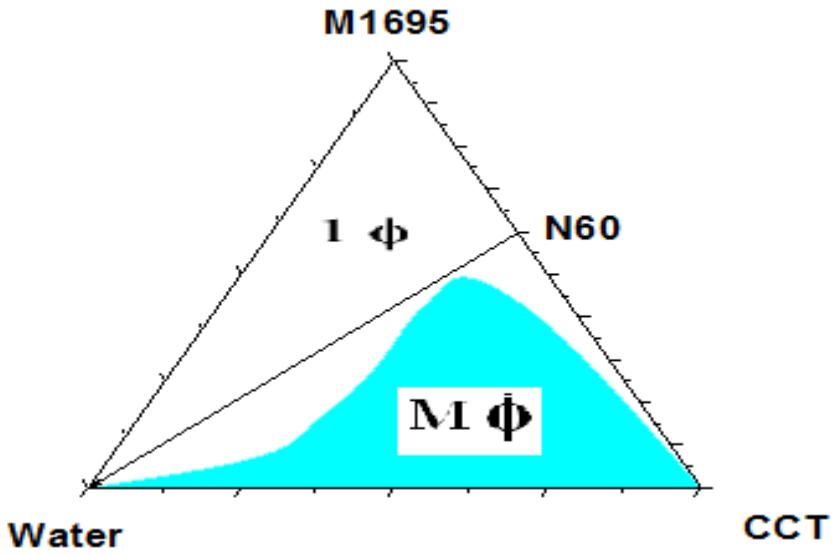

Figure 4.3: Phase diagram of the system: water / sucrose myristate M1695 / caprylic/capric triglyceride at 25 °C [The one phase region is designated by 1Φ, and the multiple phase regions are designated by M Φ]. N60 is the dilution line where the weight ratio of surfactant / single oil equals 60/40.

4.1.1.d Water / sucrose myristate M1695 / isopropylmyristate oil

This section, study the phase behavior of the system: water / sucrose myristate M1695 / isopropylmyristate oil in order to determine the boundary of one phase region at different temperatures (25°C,37°C,45°C). Based on results of phase diagram, the total area of the one phase microemulsion region A_T (±2%), was determined.

Figure 4.4 presents the phase diagram of the system: water / sucrose myristate M1695 / isopropylmyristate at 25°C. The single phase appears for surfactant contents above 60% wt from the first addition of water. For surfactant contents below 60% wt, the system extends multiple phase regions.

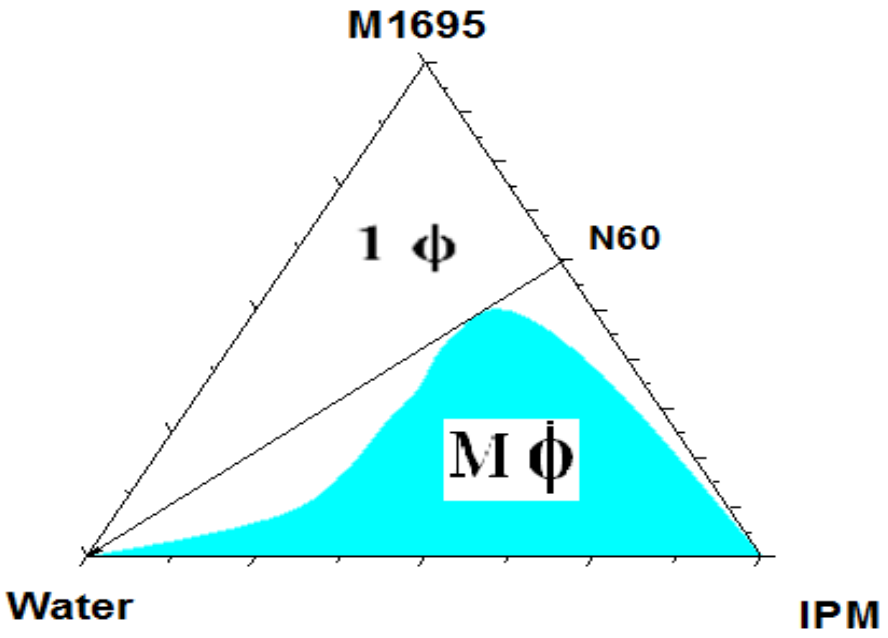

Figure 4.4: Phase diagram of the system: water / sucrose myristate M1695 / isopropylmyristate at 25 °C [The one phase region is designated by 1Φ, and the multiple phase regions are designated by M Φ]. N60 is the dilution line where the weight ratio of surfactant / single oil equals 60/40.

In this part of this research, the values of the total monophasic area A_T (±2%), for the system: water / sucrose myristate M1695 / single oil at different oil types and different temperatures. In Table 4.1, the surfactant sucrose myristate M1695 used with different oils were used without mixing with cosurfactant. In this table, a comparison between different types of oils was conducted to determine the total area of the one phase microemulsion region A_T (±2%).

Table 4.1: The total monophasic area A_T (±2%), for the system: water / sucrose myristate M1695 / single oil, different oil type at different temperatures.

	A_T (±2%)		
Oil type	**25°C**	**37°C**	**45°C**
MNT	58	58	58
LIM	59	59	59
CCT	58	58	58
IPM	57	57	57

Figure 4.5 and 4.6, show the difference on the total monophasic region A_T (%) in the system: water / sucrose myristate M1695 / oil in different oil types and different temperatures (25,37,45 ˚C) as a histogram and line chart.

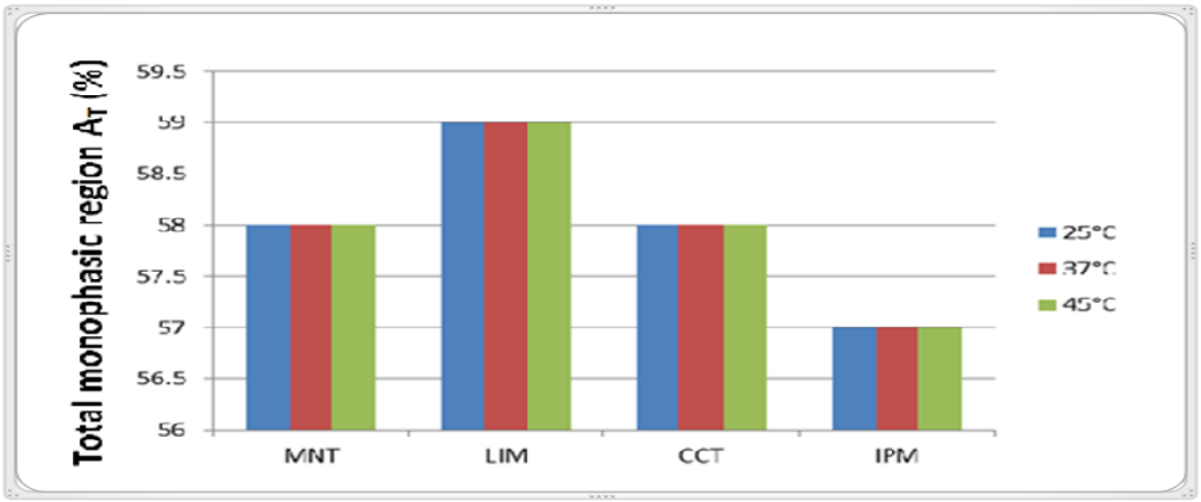

Figure 4.5**:** Variation of the total monophasic region A_T (±2%), (for the system: water / sucrose myristate M1695 / single oil, different oil type and different temperatures (25,37,45˚C).

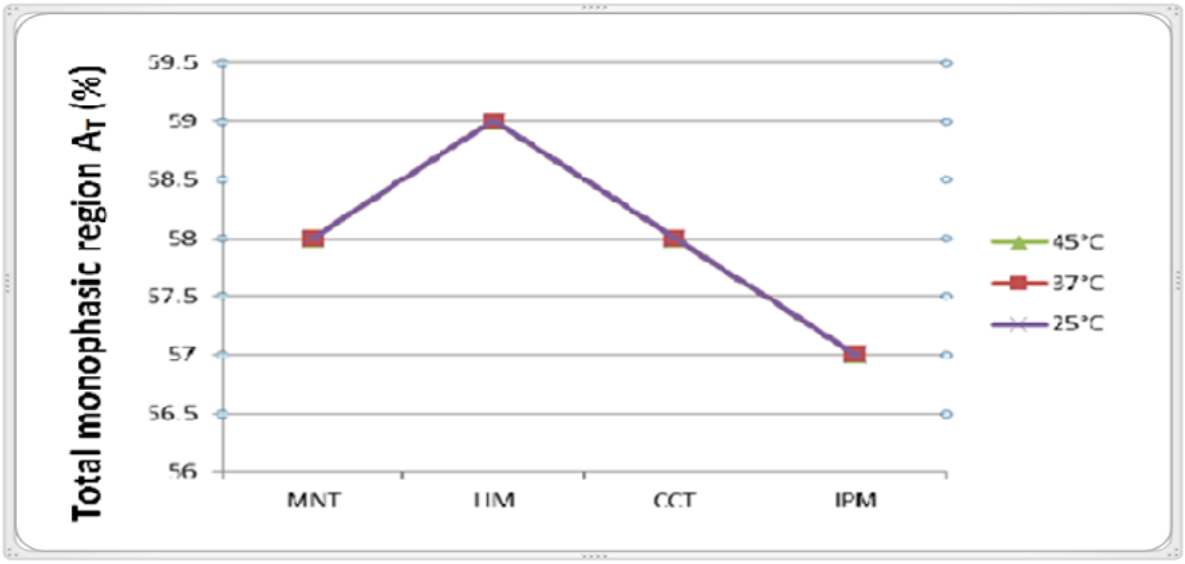

Figure 4.6**:** Variation of the total monophasic region A_T (±2%), for the system: water / sucrose myristate M1695 / single oil, different oil type, and different temperatures (25,37,45 °C).The chemical structure of the oil affects its penetration in the surfactants layer and determines the extent of water solubilization.

From the results presented in Table 4.1 and Figure 4.5 and 4.6, it is observed that for microemulsion systems based on sucrose myristate M1695; only R (+)-limonene oil has the higher total monophasic area values followed by peppermint and caprylic/capric. This refers to the cyclic structure of R (+)-limonene oil that tends to penetrate in the surfactant layer and widen the effective cross-sectional area per surfactant.

Triglyceride oil caprylic/capric triglyceride and linear oil isopropylmyristate has low total monophasic area because of its high molecular volume, and so the ability to penetrate the interfacial film is very low and does not assist to obtain the optimum curvature of surfactants. When temperature changed from 25°C to 45°C, the total monophasic region A_T was not affected because the surfactant nonionic and microemulsion thermodynamic staple. Increasing temperature from 25°C to 45°C induces small changes in the monophasic area indicating temperature insensitive microemulsions formation, so when surfactants are sucrose esters temperature insensitive microemulsions were observed.

4.1.2 Water / sucrose myristate M1695 / oil + ethanol (1/1)

4.1.2.a Water / sucrose myristate M1695 / peppermint + ethanol (1/1)

The phase behavior of the system: water / sucrose myristate M1695 / peppermint + ethanol (1/1), where the surfactant sucrose myristate M1695 and the peppermint oil mixed with short chain alcohol, cosurfactant in order to determine the boundary of one phase region at different temperatures (25°C,37°C,45°C). The results from phase diagram, allowed to determination the total area of the one phase microemulsion region A_T (±2%).

Figure 4.7 presents the phase diagram of the system: water / sucrose myristate M1695 / peppermint + ethanol as cosurfactant at 25°C. The single phase appears for surfactant contents above 60% wt from the first addition of water. For surfactant contents below 60% wt, the system extends multiple phase regions.

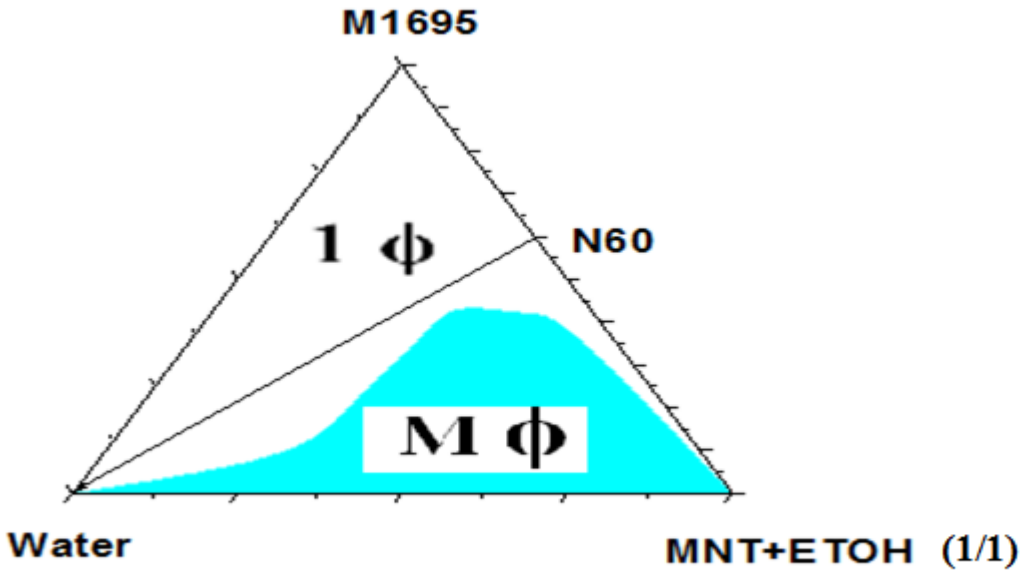

Figure 4.7: Phase diagram of the system: water / sucrose myristate M1695 / peppermint + ethanol as a cosurfactant at 25 °C. [The one phase region is designated by 1Φ, and the multiple phase regions are designated by M Φ]. N60 is the dilution line where the weight ratio of surfactant / mixed oils with cosurfactant equals 60/40.

4.1.2.b Water / sucrose myristate M1695 / R (+)-limonene oil + ethanol

The phase behavior of the system: water / sucrose myristate M1695 / R (+)-limonene oil + ethanol (1/1), where the surfactant sucrose myristate M1695 and the peppermint oil mixed with short chain alcohol, cosurfactant in order to determine the boundary of one phase region at different temperatures (25°C,37°C,45°C). The results from phase diagram, allowed to determination the total area of the one phase microemulsion region A_T (±2%).

Figure 4.8 presents the phase diagram of the system: water / sucrose myristate M1695 / R (+)-limonene + ethanol as cosurfactant at 25°C. The single phase appears for surfactant contents above 60% wt from the first addition of water. For surfactant contents below 60% wt, the system extends multiple phase regions.

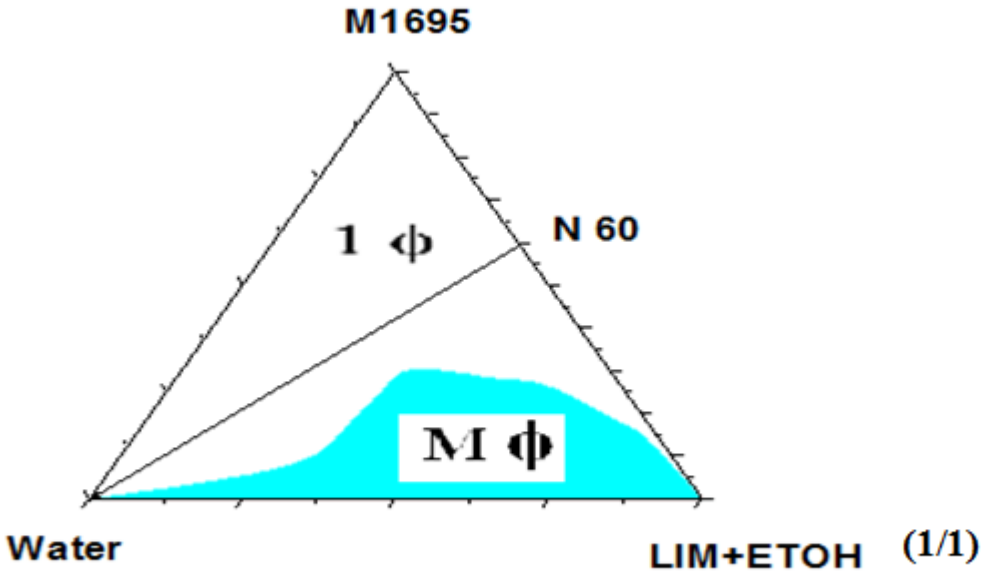

Figure 4.8: Phase diagram of the system: water / sucrose myristate M1695 / R (+)-limonene + ethanol as a cosurfactant at 25 °C. [The one phase region is designated by 1Φ, and the multiple phase regions are designated by M Φ]. N60 is the dilution line where the weight ratio of surfactant/ mixed oils with cosurfactant equals 60/40.

4.1.2.c Water / sucrose myristate M1695 / caprylic/capric triglyceride + ethanol

The phase behavior of the system: water / sucrose myristate M1695 / caprylic/capric triglyceride oil + ethanol (1/1), where the surfactant sucrose myristate M1695 and the peppermint oil mixed with short chain alcohol, cosurfactant in order to determine the boundary of one phase region at different temperatures (25°C,37°C,45°C). The results from phase diagram, allowed to determination the total area of the one phase microemulsion region A_T (±2%).

Figure 4.9 presents the phase diagram of the system: water / sucrose myristate M1695 / caprylic/capric triglyceride + ethanol as cosurfactant at 25°C. The single phase appears for surfactant contents above 60% wt, from the first addition of water. For surfactant contents below 60% wt, the system extends multiple phase regions.

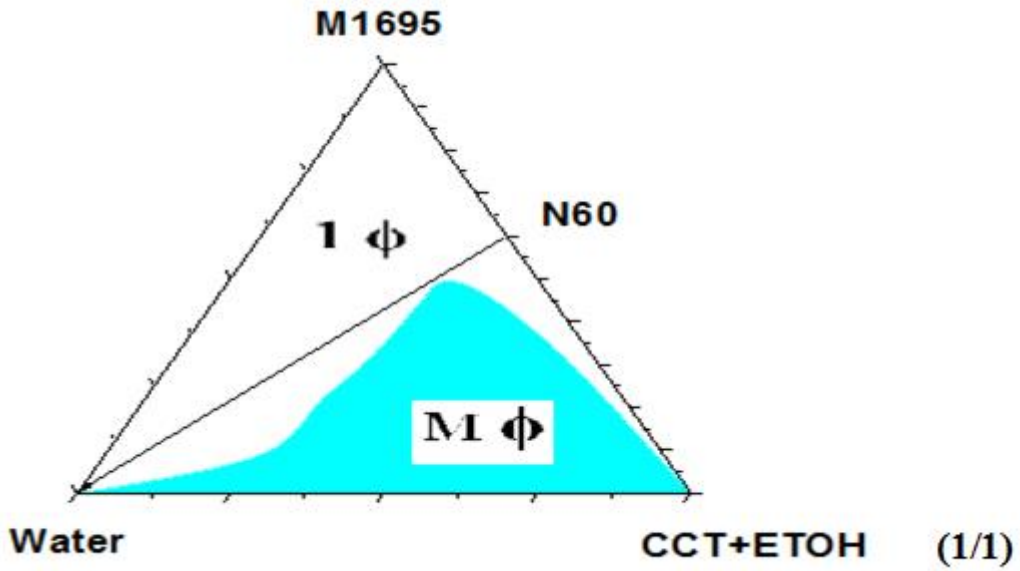

Figure 4.9: Phase diagram of the system: water / sucrose myristate M1695 / caprylic/capric triglyceride + ethanol as a cosurfactant at 25 °C. [The one phase region is designated by 1Φ, and the multiple phase regions are designated by M Φ]. N60 is the dilution line where the weight ratio of surfactant / mixed oils with cosurfactant equals 60/40.

4.1.2.d Water / sucrose myristate M1695 / isopropylmyristate + ethanol

The phase behavior of the system: water / sucrose myristate M1695 / isopropylmyristate oil + ethanol (1/1), where the surfactant sucrose myristate M1695 and the peppermint oil mixed with short chain alcohol, cosurfactant in order to determine the boundary of one phase region at different temperatures (25°C,37°C,45°C). The results from phase diagram, allowed to determination the total area of the one phase microemulsion region A_T (±2%).

Figure 4.10 presents the phase diagram of the system: water / sucrose myristate M1695 / isopropyl myristate + ethanol as cosurfactant at 25°C. The single phase appears for surfactant contents above 60% wt, from the first addition of water. For surfactant contents below 60% wt, the system extends multiple phase regions.

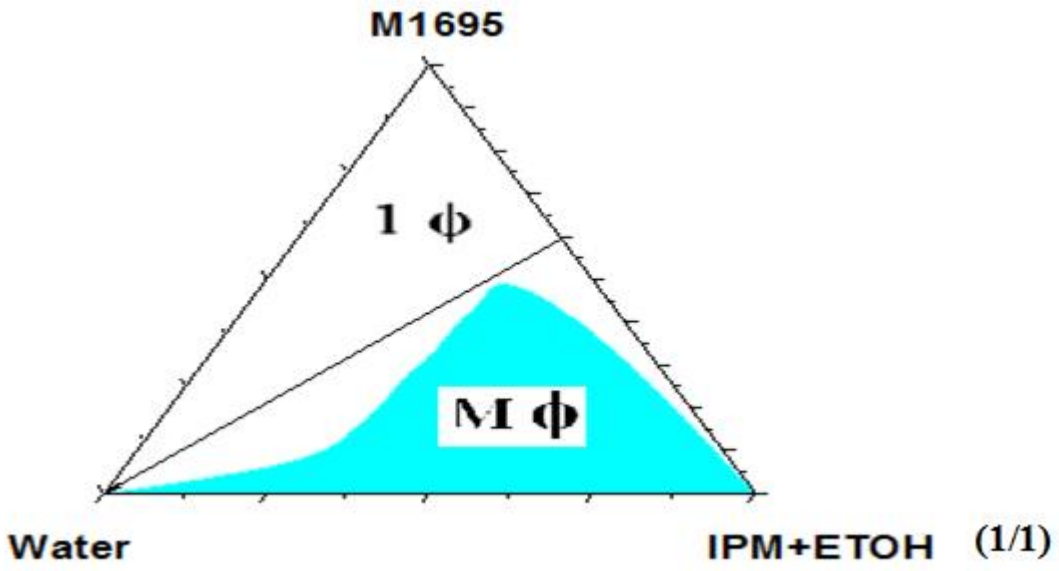

Figure 4.10: Phase diagram of the system: water / sucrose myristate M1695 / isopropyl myristate + ethanol as a cosurfactant at 25 °C. [The one phase region is designated by 1Φ, and the multiple phase regions are designated by M Φ]. N60 is the dilution line where the weight ratio of surfactant / mixed oils with cosurfactant equals 60/40.

In this part, we studied the effect of adding cosurfactant that is ethanol on the microemulsion region A_T, values of the total monophasic area A_T (±2%), for the system water / sucrose myristate M1695 / single oil mixed with cosurfactant, ethanol, at different oil types and different temperatures. In Table 4.2, the surfactant is sucrose myristate M1695 and different oils are used pure mixed with cosurfactant, ethanol.

Table 4.2: The total monophasic area A_T (±2%), for the system: water / sucrose myristate M1695 / single oil+ ethanol at different oil types and different temperatures.

	A_T (±2%)		
Oil type	**25°C**	**37°C**	**45°C**
MNT+ETOH	60	60	60
LIM+ETOH	70	70	70
CCT+ETOH	57	57	57
IPM+ETOH	59	59	60

In Figures 4.11 and 4.12, we will show the difference on the total monophasic region A_T (%) in the system: water / sucrose myristate M1695 / oil in different oil types and different temperatures (25,37,45°C) as a histogram and line chart when the oil mixed with cosurfactant, ethanol.

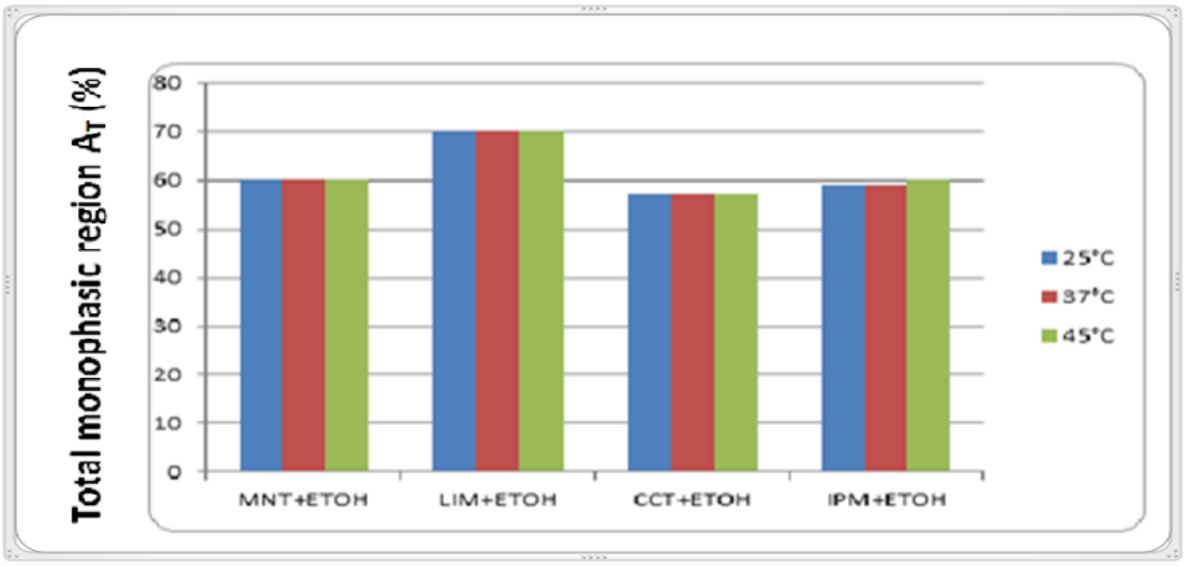

Figure 4.11**:** Variation of the total monophasic region A_T (±2%), for the system: water / sucrose myristate M1695 / single oil + ethanol at different oil types and different temperatures (25,37,45 °C).

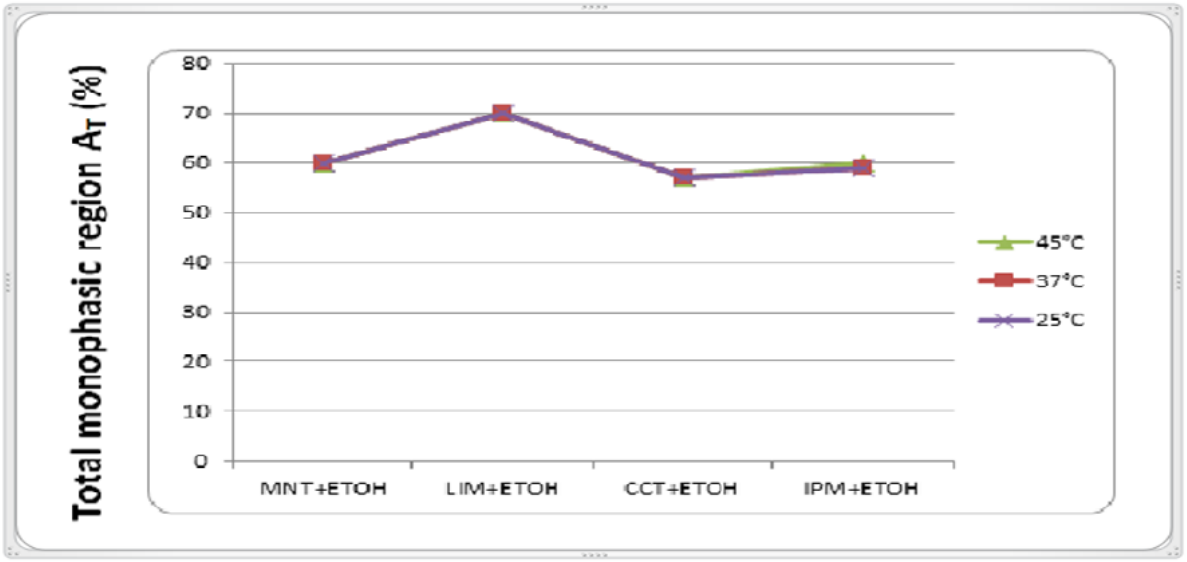

Figure 4.12: Variation of the total monophasic region A_T (±2%), for the system: water / sucrose myristate M1695 / single oil + ethanol at different oil types and different temperatures (25,37,45 °C).

From the results presented in the Table 4.2 and Figures 4.11 and 4.12, we observe that the systems containing cyclic oils peppermint and R (+)-limonene, linear oil isopropyl myristate and triglyceride oil caprylic/capric triglyceride, we observe that the total monophasic area A_T (±2%) in the microemulsion systems triglyceride oil was less than other oils used in this study; cyclic and linear oils. This is due to the fact that caprylic/capric triglyceride oil is triglyceride with high molecular volume and so the ability to penetrate the interfacial film is low when compared with e.g. cyclic oils which are non-triglycerides oils. Formation of microemulsion depends on the oil structure and oil penetration which was infected by molecular volume. Triglycerides have bulky shape and high molecular volume which increases the difficulty to penetrate the interfacial film to assist the optimum curvature [Hou. M.j, Shah. D.O, Langmuir 1987].

The result shows that the total monophasic area A_T (%) in the microemulsion systems decreases when the molecular volume of oil increase. There is a rapid decrease in the solubilization with the increase in the molecular volume of the linear hydrocarbons. After adding cosurfactant, ethanol, it is clear that the total monophasic area A_T has increased.

The ethanol cosurfactant contains one hydroxyl group (OH). When ethanol is added to the system, the results increase. The presence of hydroxyl group (OH) cause hydration of both the phospholipid head groups and hydroxyl groups of cosurfactant associated with droplet, this gives an increase in the total amount of alcohol associated with droplet, so this gives an increase in the total monophasic area A_T (%), because microemulsion were more stable when alcohol cosurfactant was added. When adding ethanol to the system, it improves the water solubilization capacity of the microemulsions and made the system more organized.

4.1.3 Water / sucrose myristate M1695 / oil + propylene glycol (1/1)

4.1.3.a Water / sucrose myristate M1695 / peppermint + propylene glycol (1/1)

We study the phase behavior of the system: water / sucrose myristate M1695 / peppermint + propylene glycol, where the surfactant sucrose myristate M1695 and the peppermint oil mixed with short chain alcohol cosurfactant that is propylene glycol in order to determine the boundary of one phase region at different temperatures (25°C,37°C,45°C). The results from phase diagram, allowed to determination the total area of the one phase microemulsion region A_T (±2%).

Figure 4.13 presents the phase diagram of the system: water / sucrose myristate M1695 / peppermint + propylene glycol as cosurfactant at 25°C. The single phase appears for surfactant contents above 60% wt from the first addition of water. For surfactant contents below 60% wt, the system extends multiple phase regions.

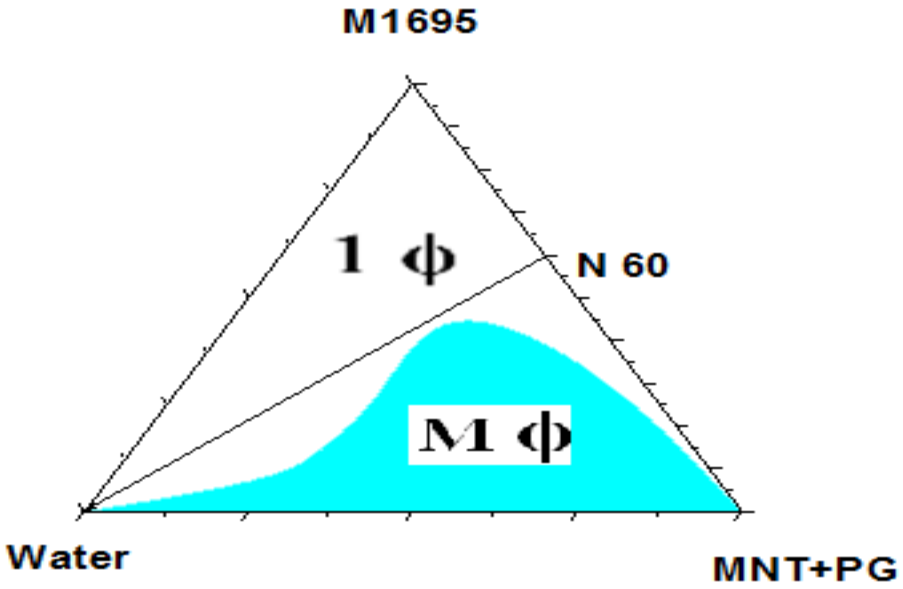

Figure 4.13: Phase diagram of the system: water / sucrose myristate M1695 / peppermint + propylene glycol as cosurfactant at 25 °C. [The one phase region is designated by 1Φ, and the multiple phase regions are designated by M Φ]. N60 is the dilution line where the weight ratio of surfactant / mixed oils with cosurfactant equals 60/40.

4.1.3.b Water / sucrose myristate M1695 / R (+)-limonene + propylene glycol (1/1)

We study the phase behavior of the system: water / sucrose myristate M1695 / R (+)-limonene + propylene glycol(1/1), where the surfactant sucrose myristate M1695 and the R (+)-limonene mixed with short chain alcohol, cosurfactant that is propylene glycol, in order to determine the boundary of one phase region at different temperatures (25°C,37°C,45°C). The results from phase diagram, allowed to determination the total area of the one phase microemulsion region A_T (±2%).

Figure 4.14 presents the phase diagram of the system: water / sucrose myristate M1695 / R (+)-limonene + propylene glycol as cosurfactant at 25°C. The single phase appears for surfactant contents above 60% wt from the first addition of water. For surfactant contents below 60% wt, the system extends multiple phase regions.

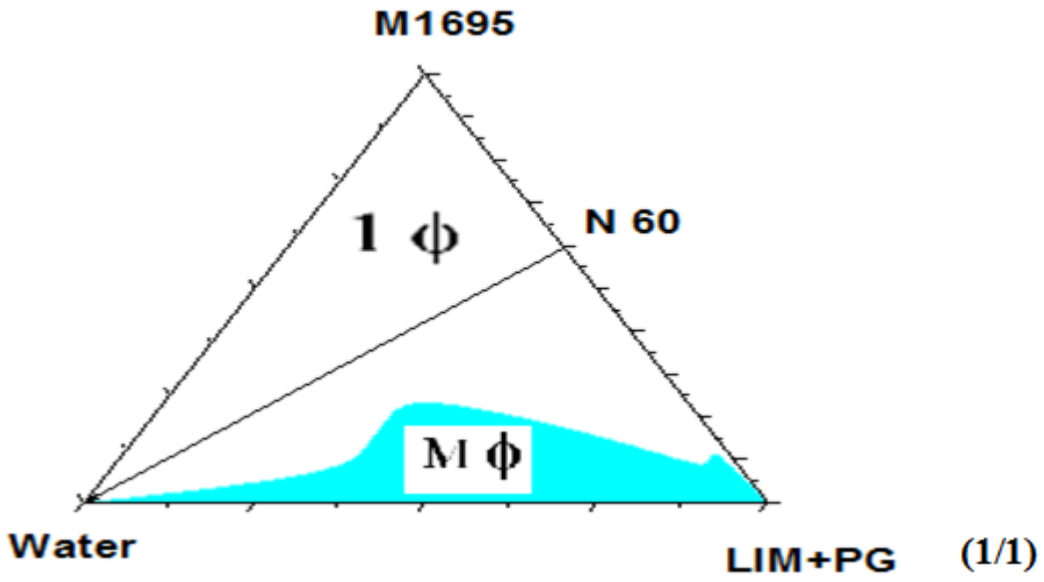

Figure 4.14: Phase diagram of the system: water / sucrose myristate M1695 / R (+)-limonene + propylene glycol as cosurfactant at 25 °C. [The one phase region is designated by 1Φ, and the multiple phase regions are designated by M Φ]. N60 is the dilution line where the weight ratio of surfactant / mixed oils with cosurfactant equals 60/40.

4.1.3.c Water / sucrose myristate M1695 / caprylic/capric triglyceride+ propylene glycol

We study the phase behavior of the system: water / sucrose myristate M1695 / caprylic/capric triglyceride + propylene glycol, where the surfactant sucrose myristate M1695 and the caprylic/capric triglyceride oil mixed with short chain alcohol, cosurfactant that is propylene glycol, in order to determine the boundary of one phase region at different temperatures (25°C,37°C,45°C). The results from phase diagram, allowed to determination the total area of the one phase microemulsion region A_T (±2%).

Figure 4.15 presents the phase diagram of the system: water / sucrose myristate M1695 / caprylic/capric triglyceride + propylene glycol as a cosurfactant at 25°C. The single phase appears for surfactant contents above 60% wt from the first addition of water. For surfactant contents below 60% wt, the system extends multiple phase regions.

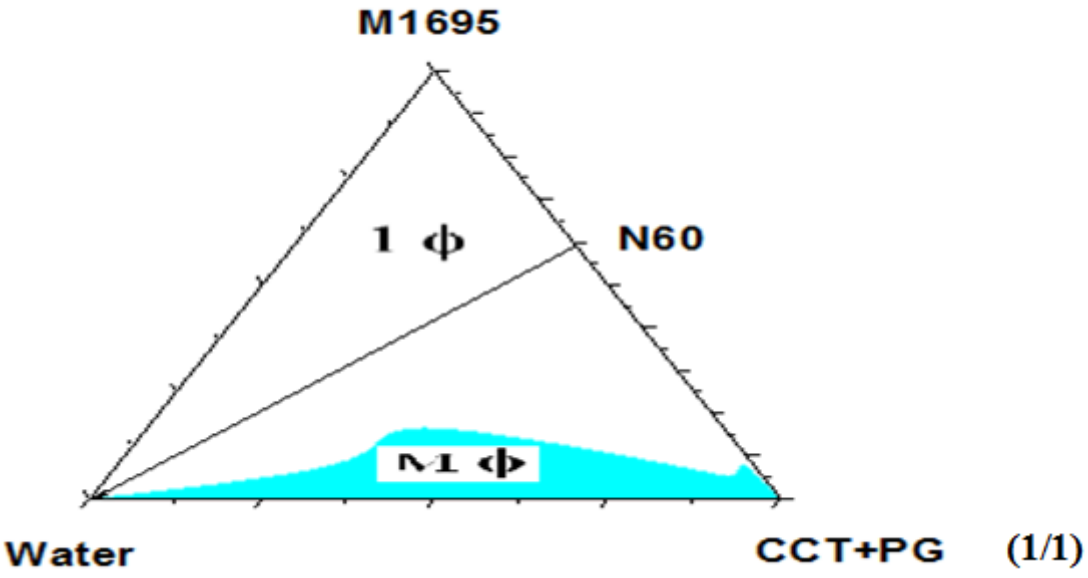

Figure 4.15: Phase diagram of the system: water / sucrose myristate M1695 / caprylic/capric triglyceride + propylene glycol as cosurfactant at 25 °C. [The one phase region is designated by 1Φ, and the multiple phase regions are designated by M Φ]. N60 is the dilution line where the weight ratio of surfactant / mixed oils with cosurfactant equals 60/40.

4.1.3.d Water/ sucrose myristate M1695 / isopropyl myristate + propylene glycol

We study the phase behavior of the system: water / sucrose myristate M1695 / isopropyl myristate + propylene glycol, where the surfactant sucrose myristate M1695 and the isopropyl myristate oil mixed with short chain alcohol, cosurfactant that is propylene glycol, in order to determine the boundary of one phase region at different temperatures (25°C,37°C,45°C). The results from phase diagram, allowed to determination the total area of the one phase microemulsion region A_T (±2%).

Figure 4.16 presents the phase diagram of the system: water / sucrose myristate M1695 / isopropyl myristate + propylene glycol as cosurfactant at 25°C. The single phase appears for surfactant contents above 60% wt from the first addition of water. For surfactant contents below 60% wt, the system extends multiple phase regions.

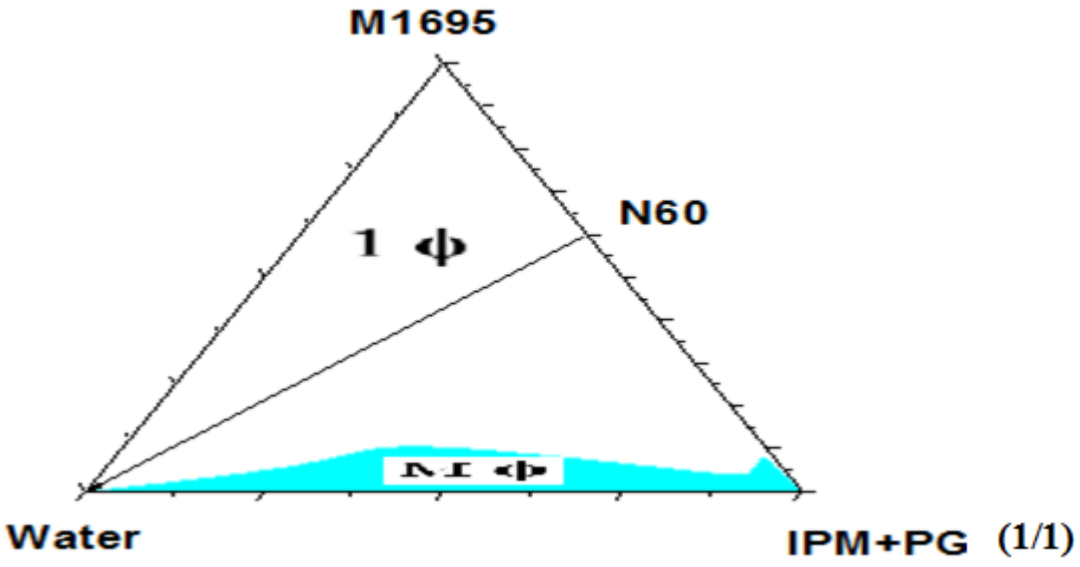

Figure 4.16: Phase diagram of the system: water / sucrose myristate M1695 / isopropyl myristate + propylene glycol as a cosurfactant at 25 °C. [The one phase region is designated by 1Φ, and the multiple phase regions are designated by M Φ]. N60 is the dilution line where the weight ratio of surfactant / mixed oils with cosurfactant equals 60/40.

We study the effect of adding cosurfactant, propylene glycol, on the microemulsion region A_T, values of the total monophasic area A_T (±2%), for the system: water / sucrose myristate M1695 / single oil mixed with cosurfactant, propylene glycol, at different oil types and different temperatures. In Table 4.3, the surfactant is sucrose myristate M1695 and different oils are used pure mix with cosurfactant, propylene glycol.

Table 4.3: The total monophasic area A_T (±2%), for the system: water / sucrose myristate M1695 / oil + propylene glycol at different oil types and different temperatures.

	A_T (±2%)		
Oil type	**25°C**	**37°C**	**45°C**
MNT+PG	57	57	59
LIM+ PG	78	78	78
CCT+ PG	83	83	83
IPM+ PG	88	88	88

Figures 4.17 and 4.18, show the difference on the total monophasic region A_T (±2%), in the system: water / sucrose myristate M1695 / oil in different oil types and different temperature (25,37,45 $^{\circ}$C) as a histogram and line chart when oils are mixed with a cosurfactant, propylene glycol.

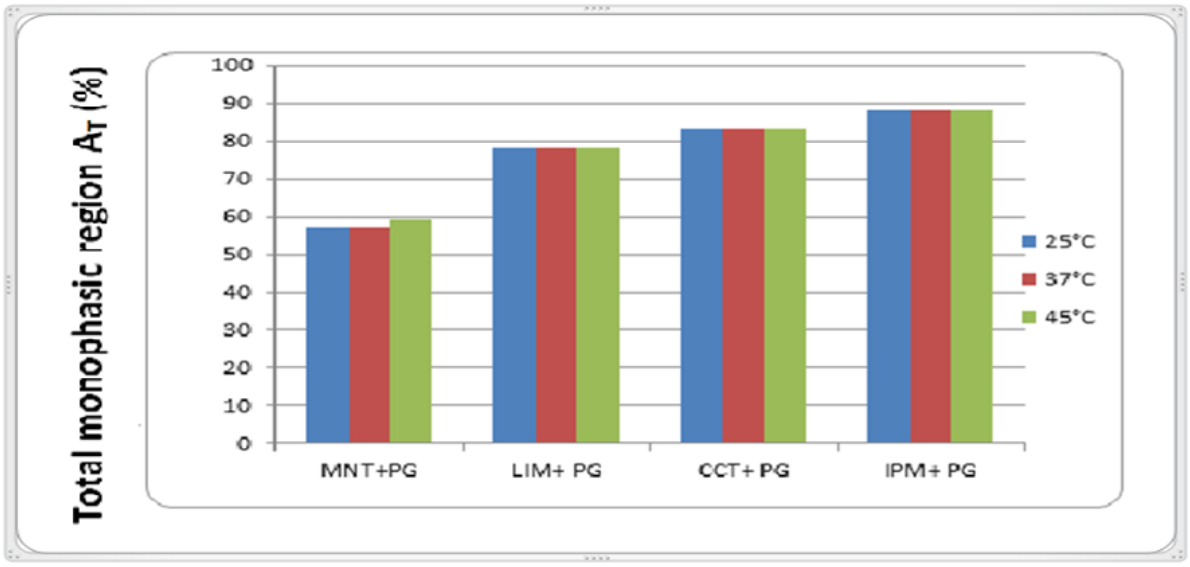

Figure 4.17: Variation of the total monophasic region A_T (±2%), for the system: water / sucrose myristate M1695 / oil + propylene glycol at different oil types and different temperatures (25,37,45 °C).

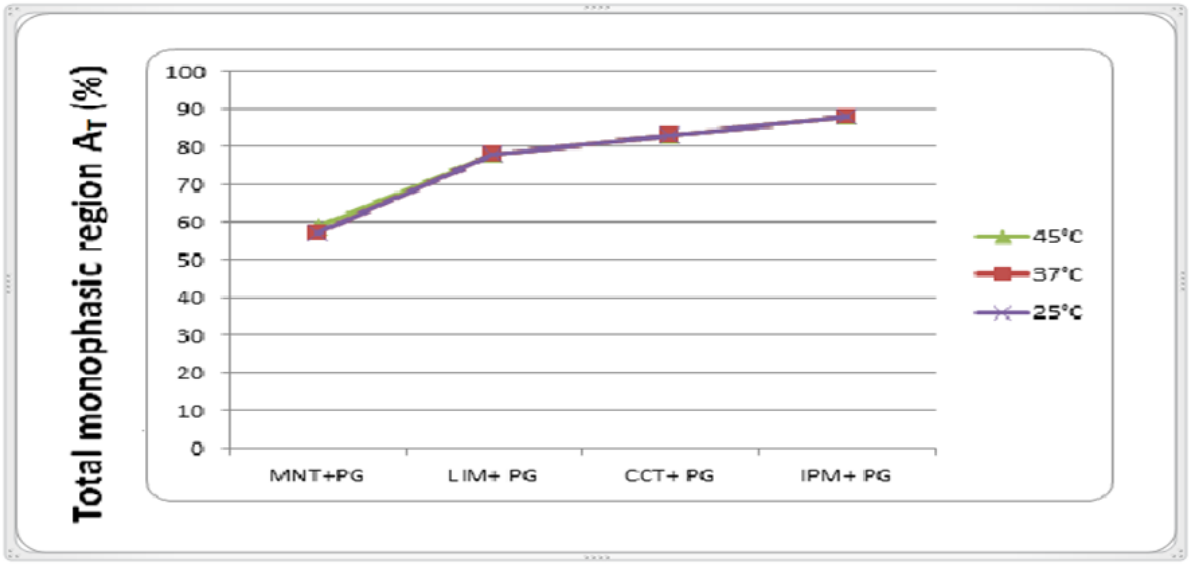

Figure 4.18: Variation of the total monophasic region A_T (±2%), for the system: water / sucrose myristate M1695 / oil + propylene glycol at different oil types and different temperatures (25,37,45 °C).

From the results presented in Table 4.3, Figure 4.17 and 4.18, we observe that the systems containing cyclic oils peppermint and R (+)-limonene and linear oil isopropyl myristate and triglyceride oil caprylic/capric triglyceride, we observed that the total monophasic area A_T (%) in the microemulsion systems the isopropylmyristate oil have the highest A_T (%) value due to its carbon number (17) and its linear structure, it is like surfactant chain length and structure, each carbon on oil bond to carbon on surfactant, this increases the stability, compatibility and the monophasic area A_T (%).

When propylene glycol was added to isopropyl myristate, this gives the maximum monophasic area A_T because propylene glycol increases the viscosity of micro emulsion due to the presence of hydroxyl group (OH), that causes to enhance stability of microemulsion.

4.1.4 Water / sucrose myristate M1695 / oil+ glycerol (1/1)

4.1.4.a Water / sucrose myristate M1695 / peppermint+ glycerol(1/1)

We study the phase behavior of the system: water / sucrose myristate M1695 / peppermint + glycerol, where the surfactant sucrose myristate M1695 and the peppermint oil mixed with short chain alcohol cosurfactant, that is glycerol, in order to determine the boundary of one phase region at different temperatures (25°C,37°C,45°C). The results from phase diagram, allowed to determination the total area of the one phase microemulsion region A_T (±2%).

Figure 4.19 presents the phase diagram of the system: water / sucrose myristate M1695 / peppermint + glycerol as cosurfactant at 25°C. The single phase appears for surfactant contents above 60% wt from the first addition of water. For surfactant contents below 60% wt, the system extends multiple phase regions.

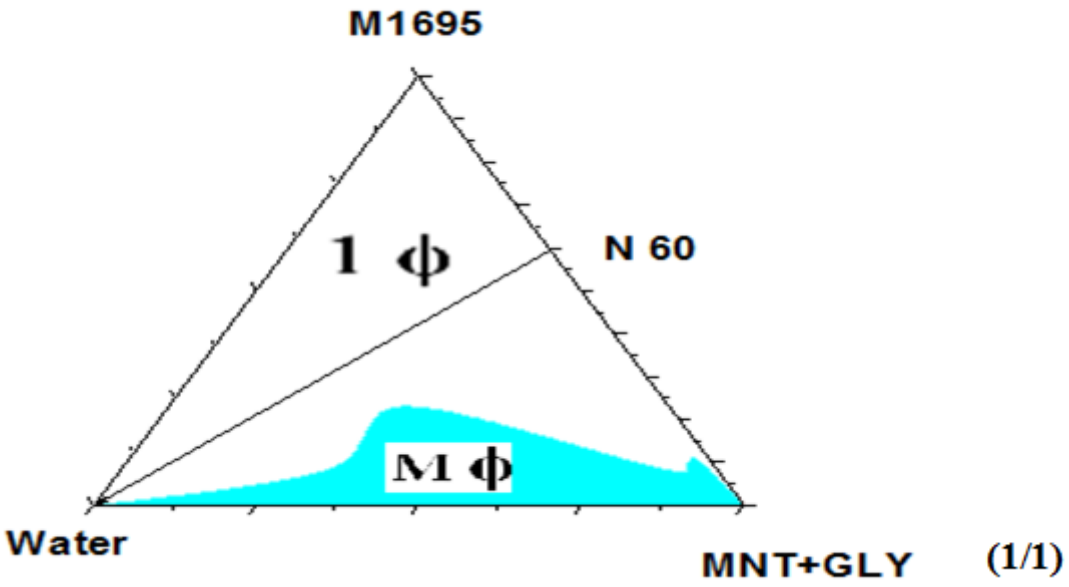

Figure 4.19: Phase diagram of the system: water / sucrose myristate M1695 / peppermint + glycerol as cosurfactant at 25 °C. [The one phase region is designated by 1Φ, and the multiple phase regions are designated by M Φ]. N60 is the dilution line where the weight ratio of surfactant / mixed oils with cosurfactant equals 60/40.

4.1.4.b Water / sucrose myristate M1695 / R (+)-limonene + glycerol(1/1)

We study the phase behavior of the system: water / sucrose myristate M1695 / R (+)-limonene + glycerol(1/1), where the surfactant sucrose myristate M1695 and the R (+)-limonene oil mixed with short chain alcohol cosurfactant, that is glycerol, in order to determine the boundary of one phase region at different temperatures (25°C,37°C,45°C). The results from phase diagram, allowed to determination the total area of the one phase microemulsion region A_T (±2%).

Figure 4.20 presents the phase diagram of the system: water / sucrose myristate M1695 R (+)-limonene + glycerol as cosurfactant at 25°C. The single phase appears for surfactant contents above 60% wt from the first addition of water. For surfactant contents below 60% wt, the system extends multiple phase regions.

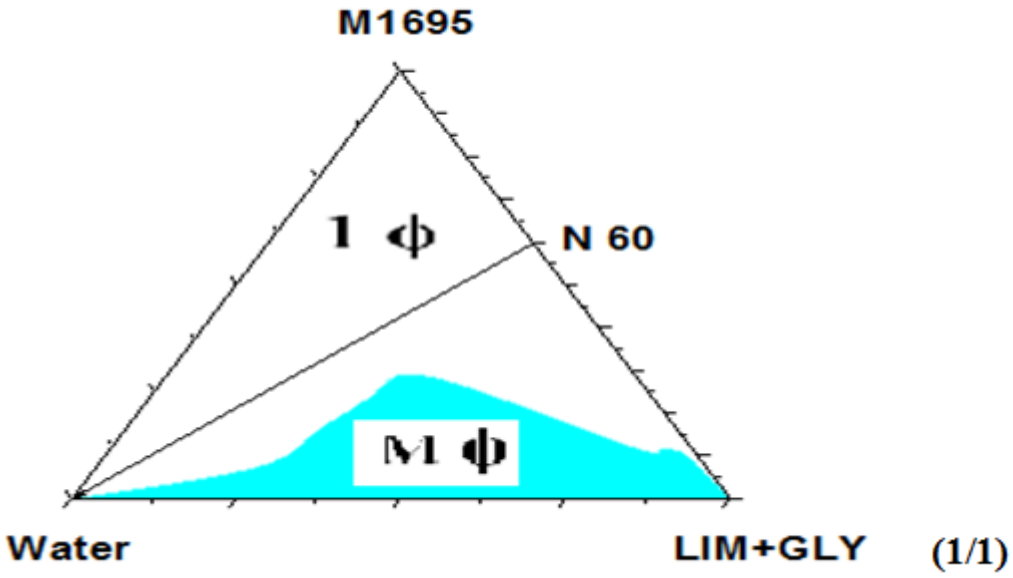

Figure 4.20: Phase diagram of the system: water / sucrose myristate M1695 / R (+)-limonene + glycerol as cosurfactant at 25 °C. [The one phase region is designated by 1Φ, and the multiple phase regions are designated by M Φ]. N60 is the dilution line where the weight ratio of surfactant / mixed oils with cosurfactant equals 60/40.

4.1.4.c Water / sucrose myristate M1695 / caprylic/capric triglyceride+ glycerol

We study the phase behavior of the system: water / sucrose myristate M1695 / caprylic/capric triglyceride + glycerol, where the surfactant sucrose myristate M1695 and the caprylic/capric triglyceride mixed with short chain alcohol cosurfactant, that is glycerol, in order to determine the boundary of one phase region at different temperatures (25°C,37°C,45°C). The results from phase diagram, we will be able to determine the total area of the one phase microemulsion region A_T (±2%).

Figure 4.21 presents the phase diagram of the system: water / sucrose myristate M1695 / caprylic/capric triglyceride + glycerol as a cosurfactant at 25°C. The single phase appears for surfactant contents above 60% wt from the first addition of water. For surfactant contents below 60% wt, the system extends multiple phase regions.

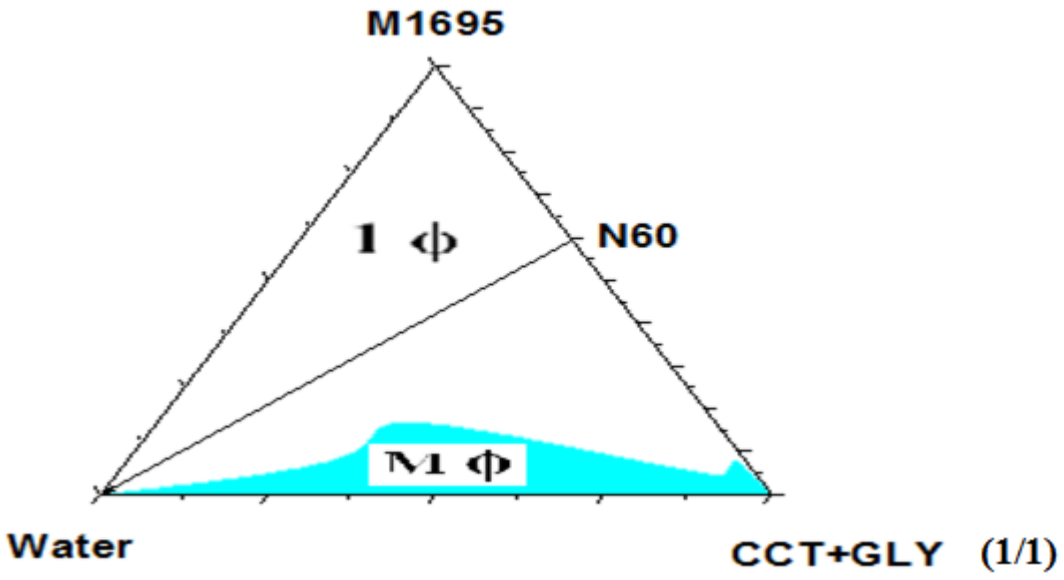

Figure 4.21: Phase diagram of the system: water / sucrose myristate M1695 / caprylic/capric triglyceride + glycerol as a cosurfactant at 25 °C. [The one phase region is designated by 1Φ, and the multiple phase regions are designated by M Φ]. N60 is the dilution line where the weight ratio of surfactant / mixed oils with cosurfactant equals 60/40.

4.1.4.d Water / sucrose myristate M1695 / isopropyl myristate + glycerol

We study the phase behavior of the system: water / sucrose myristate M1695 / isopropyl myristate + glycerol, where the surfactant sucrose myristate M1695 and the isopropyl myristate oil mixed with short chain alcohol cosurfactant, that is glycerol, in order to determine the boundary of one phase region at different temperatures (25°C,37°C,45°C). The results from phase diagram, allowed to determination the total area of the one phase microemulsion region A_T (±2%).

Figure 4.22 presents the phase diagram of the system: water / sucrose myristate M1695 / isopropyl myristate + glycerol as cosurfactant at 25°C, The single phase appears for surfactant contents above 60% wt from the first addition of water. For surfactant contents below 60% wt the system extend multiple phase regions.

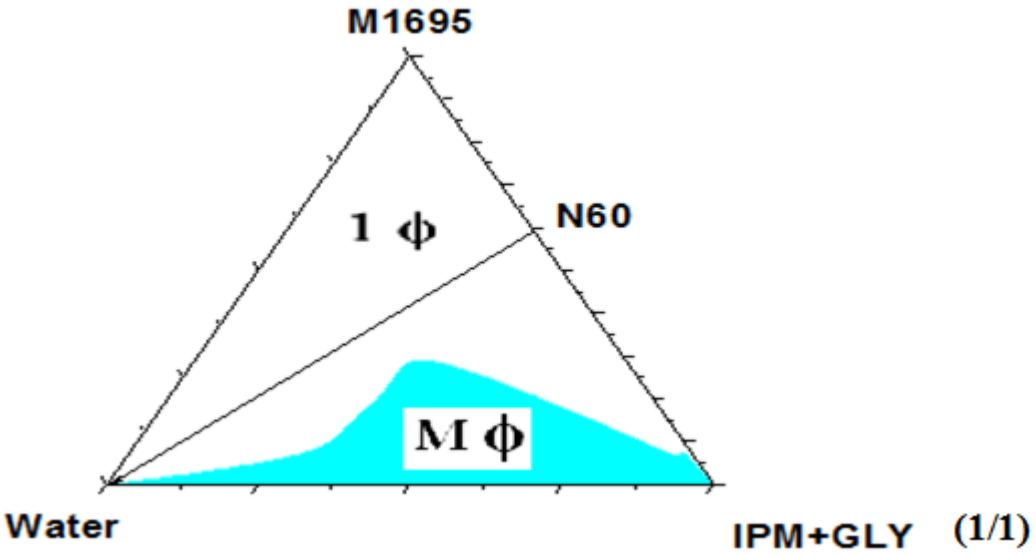

Figure 4.22: Phase diagram of the system: water / sucrose myristate M1695 / isopropyl myristate + glycerol as a cosurfactant at 25 °C. [The one phase region is designated by 1Φ, and the multiple phase regions are designated by M Φ]. N60 is the dilution line where the weight ratio of surfactant / mixed oils with cosurfactant equals 60/40.

we studied the effect of adding cosurfactant, glycerol, on the microemulsion region A_T, values of the total monophasic area A_T (±2%), for the system water / sucrose myristate M1695 /single oil mixed with cosurfactant, glycerol, at different oil types and different temperatures. In Table 4.4, the surfactant is sucrose myristate M1695 and different oils are used pure mixed with cosurfactant, glycerol.

Table 4.4: The total monophasic area A_T (±2%), for the system: water / sucrose myristate M1695 / oil + glycerol at different oil types and different temperatures.

	A_T (±2%)		
Oil type	**25°C**	**37°C**	**45°C**
MNT+GLY	79	79	79
LIM+ GLY	73	73	73
CCT+ GLY	84	84	84
IPM+ GLY	74	75	75

Figures 4.23 and 4.24**,** show the difference on the total monophasic region A_T (%) in the system: water / sucrose myristate M1695 / oil in different oil types and different temperatures (25,37,45 ˚C) as a histogram and line chart when the oil mixed with cosurfactant, glycerol.

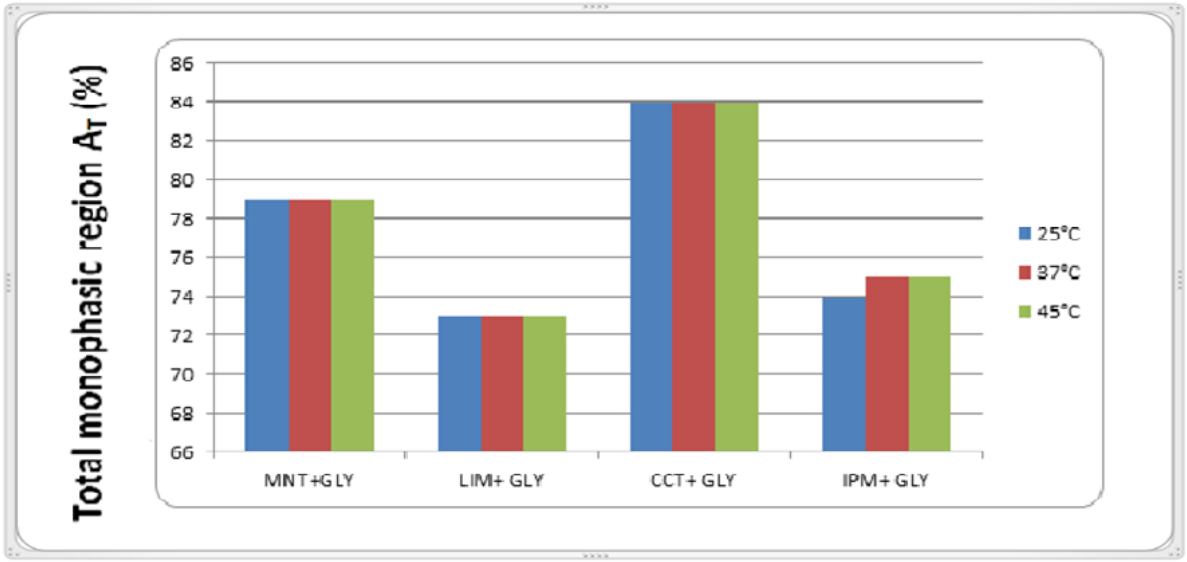

Figure 4.23**:** Variation of the total monophasic region A_T (±2%), in the system: water / sucrose myristate M1695 / oil+ glycerol in different oil types and different temperatures (25,37,45 ˚C).

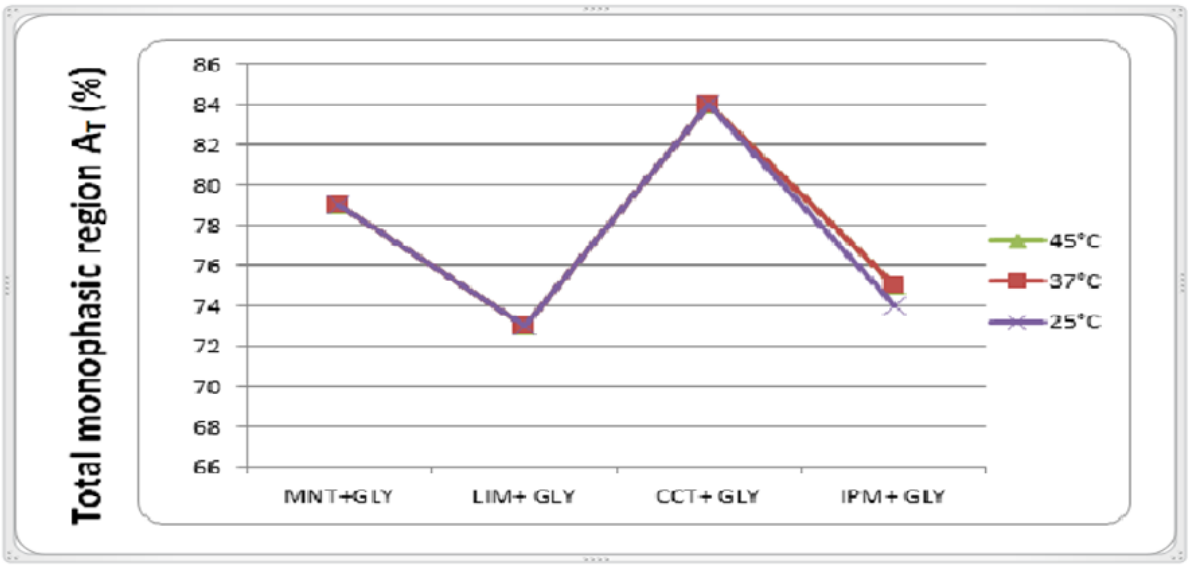

Figure 4.24**:** Variation of the total monophasic region A_T (±2%), in the system: water / sucrose myristate M1695 / oil + glycerol in different oil types and different temperatures (25,37,45 ˚C).

From the results presented in Table 4.4, Figures 4.23 and 4.24, we observed that the systems containing cyclic oils peppermint, R (+)-limonene oil, linear oil isopropyl myristate and triglyceride oil caprylic/capric triglyceride, we observed that the total monophasic area A_T (%) in the microemulsion systems the caprylic/capric triglyceride oil with glycerol have the highest A_T (%) value due to its high molecular volume (530) with higher molecular volume glycerol. This gives low viscous, low motion and high homogenized microemulsion. This also gives better water solubilization. So that mixing glycerol with caprylic/capric triglyceride oil gives us the best result, when any type of oil mixed with glycerol.

4.1.5 Water / sucrose myristate M1695 /oil + propionic acid (1/1)

4.1.5.a Water/ sucrose myristate M1695 / peppermint + propionic acid(1/1)

We study the phase behavior of the system: water / sucrose myristate M1695 / peppermint + propionic acid, where the surfactant sucrose myristate M1695 and the peppermint oil mixed with short chain alcohol cosurfactant, that is propionic acid, in order to determine the boundary of one phase region at different temperatures (25°C,37°C,45°C). The results from phase diagram, allowed to determination the total area of the one phase microemulsion region A_T (±2%).

Figure 4.25 presents the phase diagram of the system: water / sucrose myristate M1695 / peppermint + propionic acid as a cosurfactant at 25°C. The single phase appears for surfactant contents above 60% wt from the first addition of water. For surfactant contents below 60% wt, the system extends multiple phase regions.

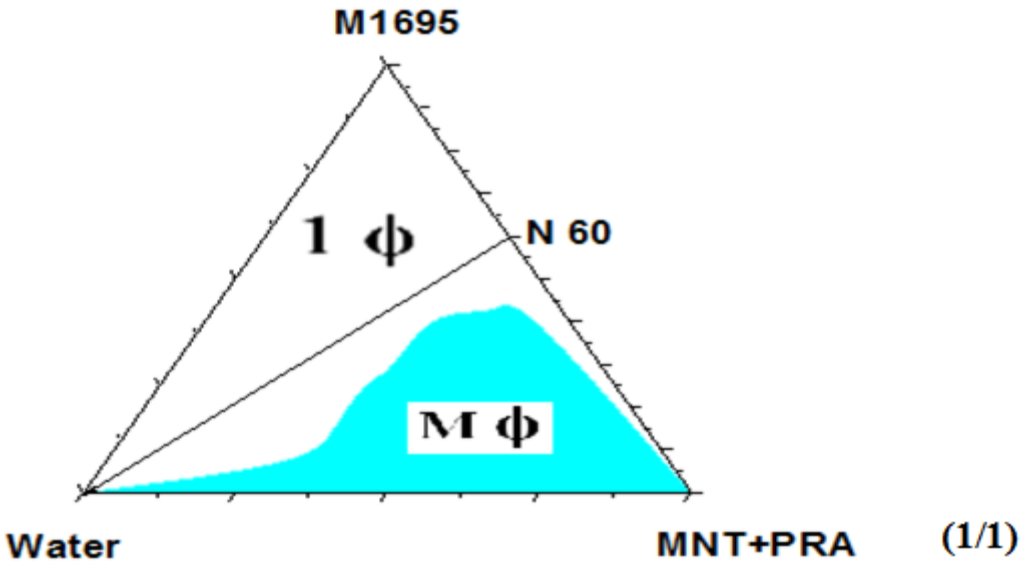

Figure 4.25: Phase diagram of the system: water / sucrose myristate M1695 / peppermint + propionic acid as cosurfactant at 25 °C. [The one phase region is designated by 1Φ, and the multiple phase regions are designated by M Φ]. N60 is the dilution line where the weight ratio of surfactant / mixed oils with cosurfactant equals 60/40.

4.1.5.b Water / sucrose myristate M1695 / R (+)-limonene + propionic acid (1/1)

We study the phase behavior the system: water / sucrose myristate M1695 / R (+)-limonene + propionic acid, where the surfactant sucrose myristate M1695 and the R (+)-limonene oil mixed with short chain alcohol cosurfactant, that is propionic acid, in order to determine the boundary of one phase region at different temperatures (25°C,37°C,45°C). The results from phase diagram, we will be able to determine the total area of the one phase microemulsion region A_T (±2%).

Figure 4.26 presents the phase diagram of the system: water / sucrose myristate M1695 / R (+)-limonene + propionic acid as a cosurfactant at 25°C. The single phase appears for surfactant contents above 60% wt from the first addition of water. For surfactant contents below 60% wt, the system extends multiple phase regions.

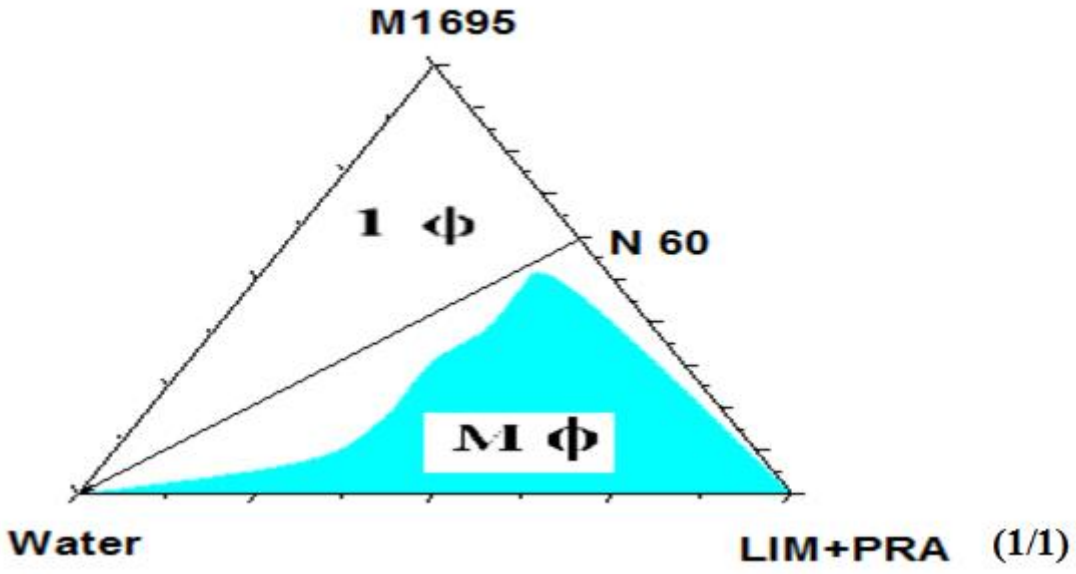

Figure 4.26: Phase diagram of the system: water / sucrose myristate M1695 / R (+)-limonene + propionic acid as a cosurfactant at 25 °C. [The one phase region is designated by 1Φ, and the multiple phase regions are designated by M Φ]. N60 is the dilution line where the weight ratio of surfactant / mixed oils with cosurfactant equals 60/40.

4.1.5.c Water / sucrose myristate M1695 / caprylic/capric triglyceride+ propionic acid

We study the phase behavior of the system: water / sucrose myristate M1695 / caprylic/capric triglyceride + propionic acid, where the surfactant sucrose myristate M1695 and the caprylic/capric triglyceride oil mixed with short chain alcohol cosurfactant, that is propionic acid, in order to determine the boundary of one phase region at different temperatures (25°C,37°C,45°C). The results from phase diagram, allowed to determination the total area of the one phase microemulsion region A_T (±2%).

Figure 4.27 presents the phase diagram of the system: water / sucrose myristate M1695 / caprylic/capric triglyceride + propionic acid as a cosurfactant at 25°C. The single phase appears for surfactant contents above 60% wt from the first addition of water. For surfactant contents below 60% wt, the system extends multiple phase regions.

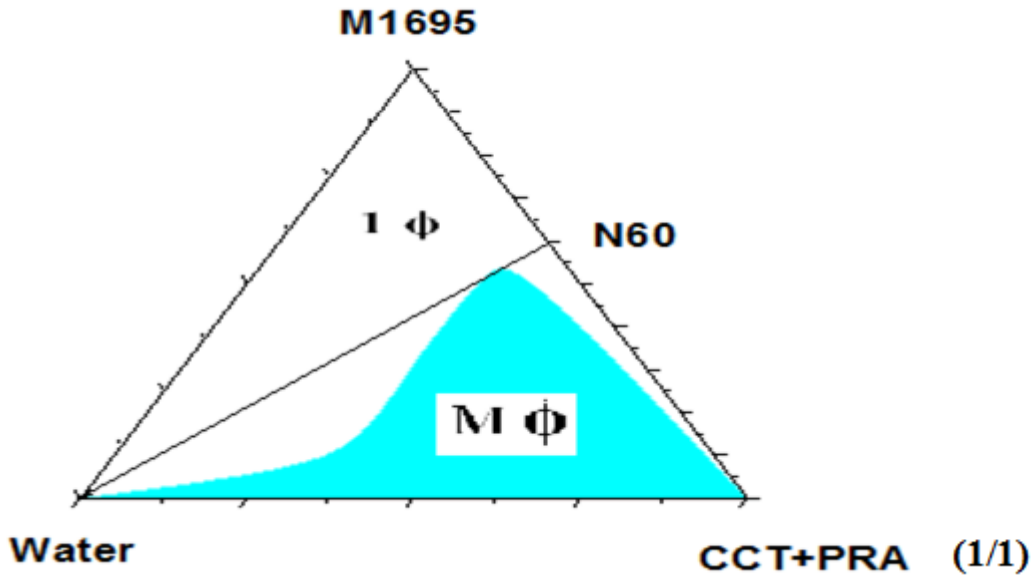

Figure 4.27: Phase diagram of the system: water / sucrose myristate M1695 / caprylic/capric triglyceride + propionic acid as a cosurfactant at 25 °C. [The one phase region is designated by 1Φ, and the multiple phase regions are designated by M Φ]. N60 is the dilution line where the weight ratio of surfactant / mixed oils with cosurfactant equals 60/40.

4.1.5.d Water / sucrose myristate M1695 / isopropyl myristate + propionic acid

We study the phase behavior of the system: water / sucrose myristate M1695 / isopropyl myristate + propionic acid, where the surfactant sucrose myristate M1695 and the isopropyl myristate oil mixed with short chain alcohol cosurfactant, that is propionic acid, in order to determine the boundary of one phase region at different temperatures (25°C,37°C,45°C). The results from phase diagram, allowed to determination the total area of the one phase microemulsion region A_T (±2%).

Figure 4.28 presents the phase diagram of the system: water / sucrose myristate M1695 / isopropyl myristate + propionic acid as a cosurfactant at 25°C. The single phase appears for surfactant contents above 60 wt% from the first addition of water. For surfactant contents below 60 wt%, the system extends multiple phase regions.

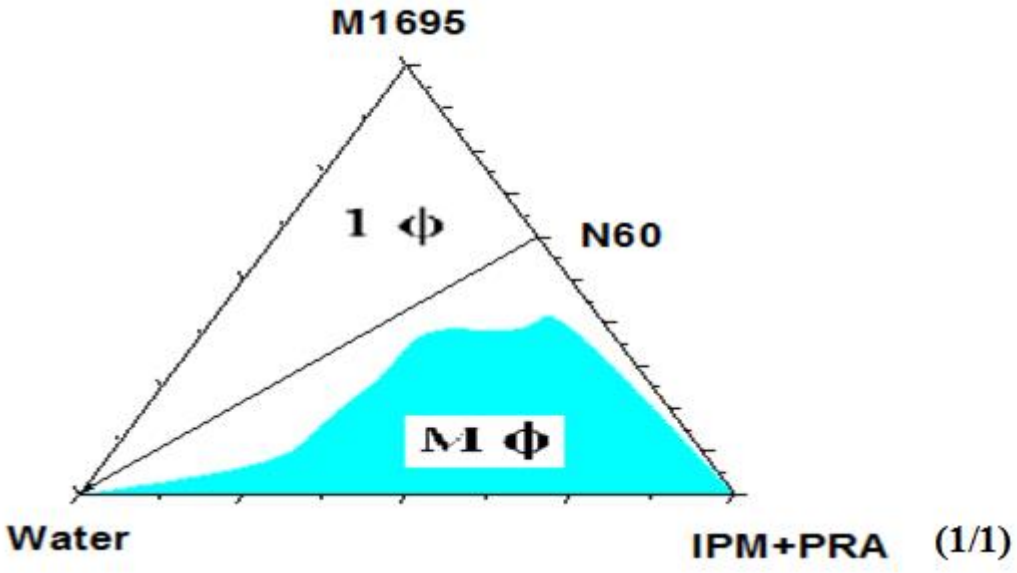

Figure 4.28: Phase diagram of the system: water / sucrose myristate M1695 / isopropyl myristate + propionic acid as a cosurfactant at 25 °C. [The one phase region is designated by 1Φ, and the multiple phase regions are designated by M Φ]. N60 is the dilution line where the weight ratio of surfactant / mixed oils with cosurfactant equals 60/40.

We studied the effect of adding cosurfactant, propionic acid, on the microemulsion region A_T, values of the total monophasic area A_T (±2%), for the system water / sucrose myristate M1695 /single oil mixed with cosurfactant, propionic acid, at different oil types and different temperatures. In Table 4.5, the surfactant is sucrose myristate M1695 and different oils are used pure mixed with cosurfactant, propionic acid.

Table 4.5: The total monophasic area A_T (±2%), for the system: water / sucrose myristate M1695 / oil + propionic acid at different oil types and different temperatures.

	A_T (±2%)		
Oil type	**25°C**	**37°C**	**45°C**
MNT+PRA	62	62	62
LIM+ PRA	60	60	60
CCT+ PRA	60	60	59
IPM+ PRA	60	60	60

In Figures 4.29 and 4.30, show the difference on the total monophasic region A_T (%) in the system: water / sucrose myristate M1695 / oil in different oil types and different temperature (25,37,45 ˚C) as a histogram and line chart when oils are mixed with a cosurfactant, propionic acid.

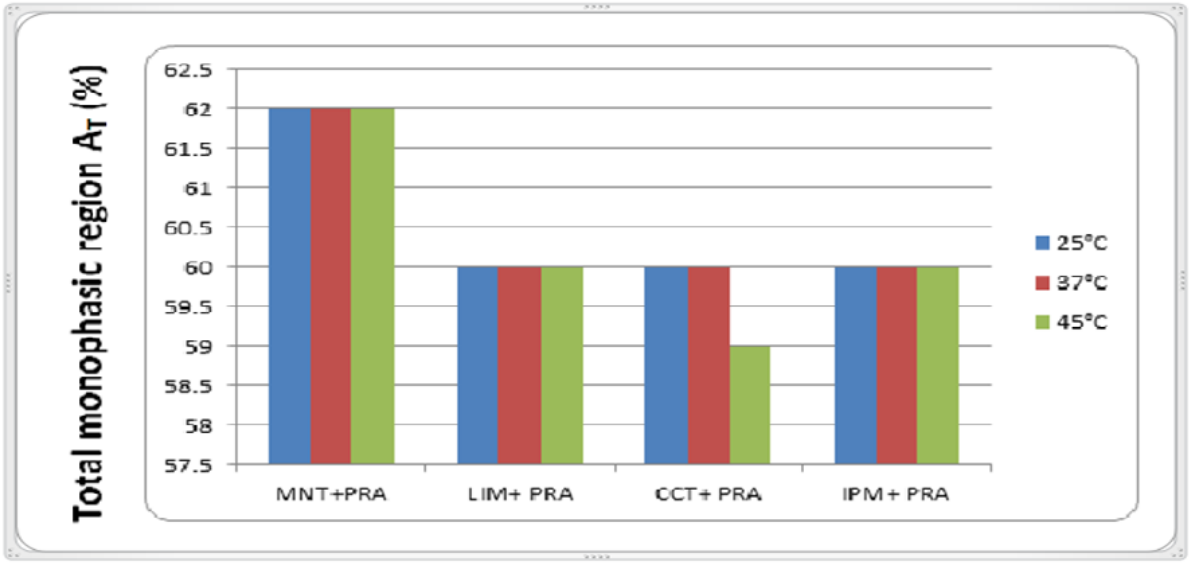

Figure 4.29**:** Variation of the total monophasic region A_T (±2%), in the system: water / sucrose myristate M1695 / oil + propionic acid, in different oil types and different temperature (25,37,45 ˚C).

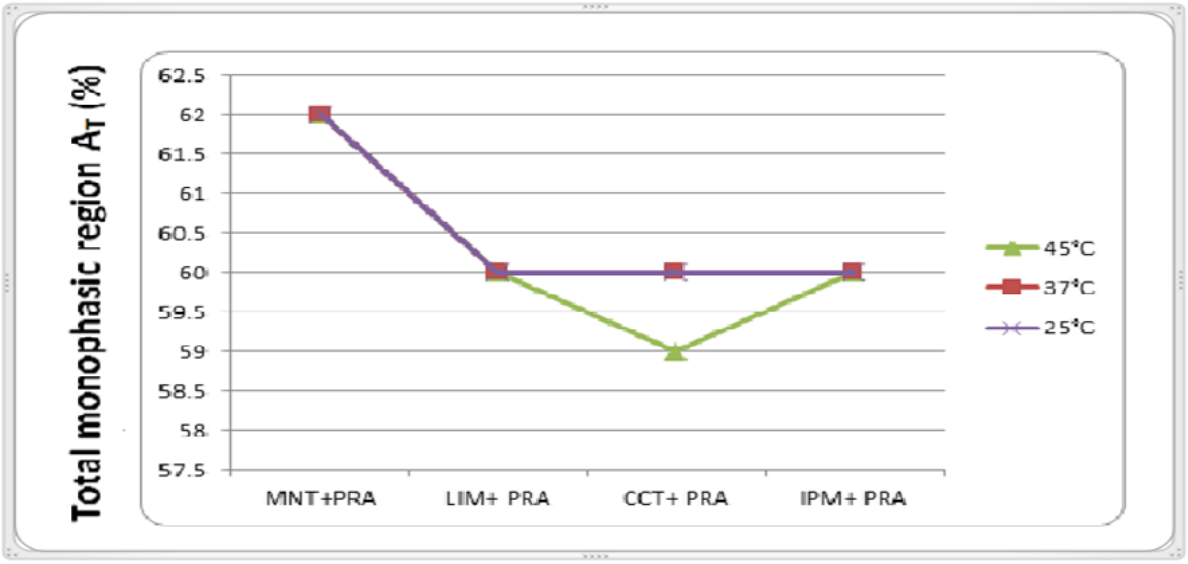

Figure 4.30**:** Variation of the total monophasic region A_T (±2%), in the system: water / sucrose myristate M1695 / oil+ propionic acid, in different oil types and different temperature (25,37,45 ˚C).

From the results presented in Table 4.5, Figures 4.29 and 4.30, we observed that the systems containing cyclic oils peppermint, R (+)-limonene, linear oil isopropyl myristate and triglyceride oil caprylic/capric triglyceride, we observed that when we start the system, propionic acid gives the very clear microemulsion and low viscosity, and after water content reached (50 %). The systems convert to two phase (emulsion), propionic acid reacts with surfactant, then hydrolization happen to surfactant, this stop the surfactant work and break down the system. Propionic acid is an acid cause burn to the surfactant and this damages the system.

Formation of microemulsion depends on the oil structure and penetration infected by molecular volume and effective carbon number. From the result presented in this study, we conclude that when effective carbon number and molecular volume increase the total monophasic region A_T decreases because when the molecular volume increase the ability to penetrate the interfacial film is very low and does not assist to obtain the optimum curvature of surfactants.

Different factors affected water solubilization, phase diagram and the total monophasic region A_T, these factor were:

- Effective carbon number.

- Molecular volume.

- Atom available for lipophilic interaction.

- Atom available for hydrophilic interaction.

The effective carbon number, molecular volume and atom available for lipophilic interaction of oils used in this research are presented in Table 4.6.

Table 4.6: The total effective carbon number, molecular volume and atom available for lipophilic interaction of oils used in this study.

Oil type	**Molecular volume**	**Effective carbon number**	**Atom available for lipophilic interaction**
Peppermint	170	6	10
R (+)-limonene	181	6	10
Caprylic/capric triglyceride	530	21	30
Isopropyl myristate	317	17	18

The effective carbon number, atom available for lipophilic interaction and atom available for hydrophilic interaction of cosurfactants used in this research presented in Table 4.7.

Table 4.7: The total effective carbon number, atom available for lipophilic interaction and atom available for hydrophilic interaction of cosurfactant used in this study.

Cosurfactant	**Effective carbon number**	**Atom available for lipophilic interaction**	**Atom available for hydrophilic interaction**
Ethanol	3	2	1
Propylene glycol	4	3	2
Propionic acid	4	3	2
Glycerol	5	3	3

The empirical BSO [Bansal .V.K, Shah.D.O, O'Connell .J.P, 1980] equation which was derived as an empirical condition for maximum water solubilization in microemulsions stabilized by anionic surfactants, in relation to the cosurfactant, alcohol, and oil chain lengths, i.e. $N_S = N_O + N_A$, where N_S, N_O, N_A are the surfactant chain lengths, oil and alcohol, respectively, was re-examined for this type of surfactants. This study demonstrates that a maximum water solubilization is obtained when the $N_S = (N_O \pm 3) + N_A$ for N_S is greater than 14; when N_S is less than 14, this equation cannot predict the maximum water solubilization.

They concluded that the maximum amount of water which may be solubilized in such a microemulsion is reached when the oil chain length (carbon number), N_O, added to that of the cosurfactant (alcohol) chain length, N_A, is equal to the surfactant chain length, N_S, i.e. $N_S = N_O + N_A$. In the following, this known as the BSO equation [Garti .N, Aserin .A, et al 1995]. We have shown for the first time that for the ethoxylated nonionic surfactants the BSO equation and the concept of chain length compatibility [Kahlweit. R, Strey. R, et al 1991], [Garti. N, Aserin. A, 1994] can predict, within some limits, conditions for maximum water solubilization.

The surfactant chain lengths, oil and alcohol (cosurfactant) respectively, BSO equation, the difference between BSO equation and surfactant chain lengths (N_S – BSO) for the system used in this study present in Tables 4.8, 4.9, 4.19 and 4.11.

The surfactant chain lengths, oil and alcohol (cosurfactant) respectively, BSO equation, the difference between BSO equation and surfactant chain lengths (N_S – BSO) for the system: water / sucrose myristate M1695/ peppermint, R (+)-limonene, caprylic/capric triglyceride, isopropyl myristate + ethanol presented in Table 4.8.

Table 4.8: The surfactant chain lengths, oil and alcohol (cosurfactant) respectively, BSO equation, and the difference between BSO equation and surfactant chain lengths for the system: water / sucrose myristate M1695/ peppermint, R (+)-limonene, caprylic/capric triglyceride, isopropyl myristate + ethanol.

System	N_S	N_O	N_A	N_S - N_A	BSO(N_O + N_A)	N_S – BSO
W/M1695/MNT+EtoH	14	6	3	11	9	5
W/M1695/LIM+ EtoH	14	6	3	11	9	5
W/M1695/CCT+ EtoH	14	21	3	11	24	10
W/M1695/IPM+ EtoH	14	17	3	11	20	6

The surfactant chain lengths, oil and alcohol (cosurfactant) respectively, BSO equation, the difference between BSO equation and surfactant chain lengths (N_S – BSO) for the system: water / sucrose myristate M1695/ peppermint, R (+)-limonene, caprylic/capric triglyceride, isopropyl myristate + propylene glycol presented in Table 4.9.

Table 4.9: The surfactant chain lengths, oil and alcohol (cosurfactant) respectively, BSO equation, and the difference between BSO equation and surfactant chain lengths for the system: water / sucrose myristate M1695 / peppermint, R (+)-limonene, caprylic/capric triglyceride, isopropyl myristate + propylene glycol.

System	N_S	N_O	N_A	$N_S - N_A$	BSO(N_O+N_A)	N_S- BSO
W/M1695/MNT+ PG	14	6	4	10	10	4
W/M1695/LIM+ PG	14	6	4	10	10	4
W/M1695/CCT+ PG	14	21	4	10	25	11
W/M1695/IPM+ PG	14	17	4	10	21	7

The surfactant chain lengths, oil and alcohol (cosurfactant) respectively, BSO equation, the difference between BSO equation and surfactant chain lengths (N_S – BSO) for the system: water / sucrose myristate M1695 / peppermint, R (+)-limonene, caprylic/capric triglyceride, isopropyl myristate + propionic acid presented in Table 4.10.

Table 4.10: The surfactant chain lengths, oil, alcohol and cosurfactant, respectively, BSO equation, and the difference between BSO equation and surfactant chain lengths for the system: water / sucrose myristate M1695 / peppermint, R (+)-limonene, caprylic/capric triglyceride, isopropyl myristate + propionic acid.

System	N_S	N_O	N_A	$N_S - N_A$	BSO(N_O + N_A)	N_S – BSO
W/M1695/MNT+ PRA	14	6	4	10	10	4
W/M1695/LIM+ PRA	14	6	4	10	10	4
W/M1695/CCT+ PRA	14	21	4	10	25	11
W/M1695/IPM+ PRA	14	17	4	10	21	7

The surfactant chain lengths, oil and alcohol (cosurfactant) respectively, BSO equation, the difference between BSO equation and surfactant chain lengths (N_S – BSO) for the system: water / sucrose myrstate M1695 / peppermint, R (+)-limonene, caprylic/capric triglyceride, isopropyl myristate + glycerol presented in Table 4.11.

Table 4.11: The surfactant chain lengths, oil and alcohol (cosurfactant) respectively, BSO equation, and the difference between BSO equation and surfactant chain lengths for the system: water / sucrose myrstate M1695/ peppermint, R (+)-limonene, caprylic/capric triglyceride, isopropyl myristate + glycerol.

System	N_S	N_O	N_A	N_S - N_A	BSO(N_O + N_A)	N_S – BSO
W/M1695/MNT+ GLY	14	6	5	9	11	3
W/M1695/LIM+ GLY	14	6	5	9	11	3
W/M1695/CCT+ GLY	14	21	5	9	26	12
W/M1695/IPM+ GLY	14	17	5	9	22	8

In Figure 4.31, we will show pseudo-ternary phase diagram where the line separating the inverse micellar (or W:O) microemulsion) region L_2 from other regions passes through a point P at which the water content reaches the maximum Wm. Solubilization parameters for a schematic phase diagram.

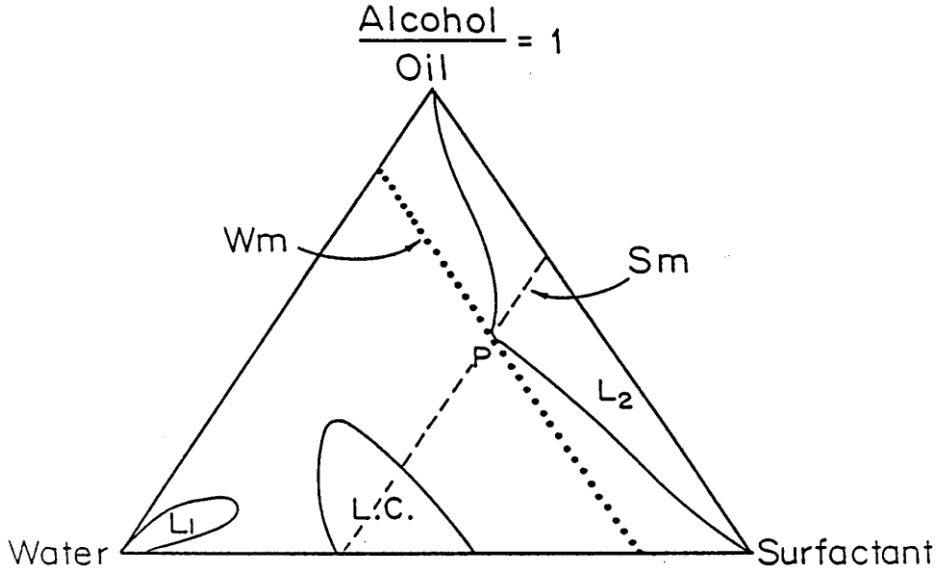

Figure 4.31: Solubilization parameters for a schematic phase diagram. The weight ratio alcohol: oil is varied from 1:1, L_1 is the area of the O: W microemulsion, L_2 is the area of the W: O microemulsion, Wm is the maximum amount of solubilized water, Sm is the amount of surfactant needed to obtain maximum solubilization, P is a point on the boundary of the monophasic area at which the water content reaches the maximum.

The solubilization and phase equilibria of water in oil microemulsions depends on two phenomenological parameters, namely the spontaneous curvature and elasticity of the interfacial film when the interfacial tension is very low. The spontaneous curvature of an interface is basically determined by the geometric packing of surfactant and cosurfactant molecules at the interface, whereas the interfacial elasticity is related to the energy required to bend the interface (attractive interactions between droplets in the system). The growth of droplets during solubilization of water is limited by either of two factors: the natural (or spontaneous) radius, Ro, of the water–oil interface and the critical radius, Rc, which limits the increase of droplet size due to inter droplet attractive interactions. A

microemulsion becomes unstable when its droplet radius is larger than Ro or Rc. These two radius depend, in opposite ways, on variables which determine the water solubilization such as molecular volume of the oil, oil chain length N_O, polar head group and concentrations of surfactant, length of the cosurfactant chain N_A, the length of the lipophilic tail of the surfactant N_S, the surfactant head group size, etc. For example, increasing the chain length of the alcohol N_A when the molar volume of the oil in the system is small will increase the oil penetration into the alkyl chains of the surfactant and the penetration of cosurfactant into the palisade layers. This will cause the interface to become more curved, thereby favoring decrease of Ro and the formation of small water in oil microemulsion droplets. On the other hand, decreased oil penetration decreases the attractive interaction potential, thereby increasing Rc. These competing effects lead to maximum solubilization, as observed experimentally.

As a tentative explanation for the problem of existence of two solubilization maxima, we suggest considering the connection between the chain length compatibility principle and the cohesive hydrophilic interfacial interactions. These interactions are included in the denominator of a modified form of the R-ratio.

$$R = \frac{(A_{C10} + A_{C20}) - A_{OO} - (A_{L1L1} + A_{L1L2} + A_{L2L2})}{(A_{C1W} + A_{C2W}) - A_{WW} - (A_{H1H1} + A_{H1H2} + A_{H2H2})}$$

Where C_1 is the surfactant and C_2 is the alcohol. The parameters A stands for cohesive energies per unit area of interface. H and L denote hydrophilic and lipophilic interactions, respectively. Thus, A_{C1O} (or A_{C1W}) is the cohesive energy between the lipophilic (or hydrophilic) portions of surfactant molecules and oil (or water); A_{C2O} (or A_{C2W}) is a similar term for the interaction between alcohol and oil (or water) molecules; A_{OO} (or A_{WW}) is the cohesive energy between oil (or water) molecules; A_{L1L1} (or A_{H1L1}) and A_{L2L2} (or A_{H2H2}) are the cohesive energies between the lipophilic (or hydrophilic) moieties of the surfactant and alcohol molecules, respectively; A_{L1L2} (or A_{H1H2}) denotes the hydrophobic (or the hydrophilic) interaction between the surfactant and alcohol. All negative terms promote segregation of the components as separate phases [Abuin. E.B, Rubio. M.A, Lissi.E.A, (1993)].

In Figure 4.32, we will show interaction energies in the amphiphilic membrane at the water: oil interface.

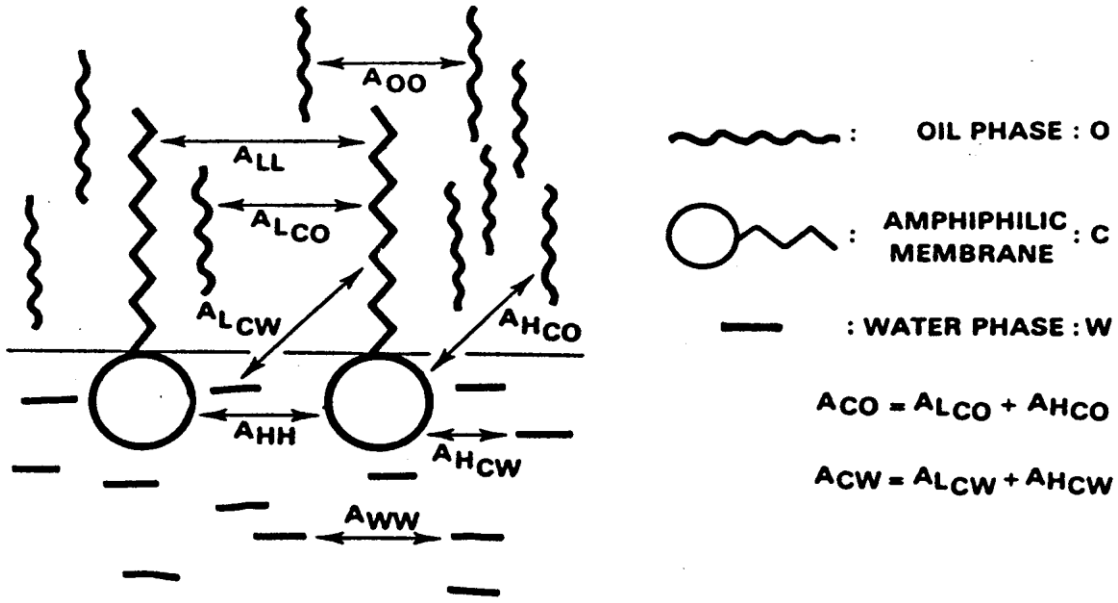

Figure 4.32: Interaction energies in the amphiphilic membrane at the water: oil interface.

By definition, A_{C2O} increases with N_A, tending to increase the R-ratio and to decrease the natural radius of curvature, Ro. Thus, when the system is in the region where the droplet size is controlled by Ro, the water solubilization diminishes as N_A increases. However, according to the chain length compatibility principle, as briefly discussed in Section 1, more head-groups can pack at the interface when $N_A+N_O = N_S$ than when $N_A+N_O = N_S$. Thus, in the case of chain length match, one would expect an increase in ($A_{C1W}+A_{C2W}$) with a corresponding decrease of R, thereby increasing water solubilization, all other interactions assumed unchanged. This assumption of similar hydrophobic interaction in the two cases seems plausible as may be judged from the following considerations.

The more vigorous thermal motion when N_A+N_O not equal N_S expands the volume available for the tails of the fewer molecules condensed into the interface so that it is presumably comparable to the volume occupied by the more crowded interfacial molecules when $N_A+N_O = N_S$. Therefore, whether the chain lengths match or mismatch, there would be roughly the same lateral pressure and interfacial curvature as a result of the

hydro-phobic interactions. Thus, it is the hydrophilic interaction (A_{C1W}+A_{C2W}) that determines the extent of the interfacial bending at the specific N_A for the corrected BSO equation is satisfied. The maximum at N_A=7 which we observed can then be regarded as a deviation from the behavior generally dominated by increased hydrophobicity, which tends to decrease the radius of curvature of the interface.

The changes of water solubilization in the systems studied, all other parameters remaining unchanged, should be the same as with the alcohol chain length. For the N_S effect, the chain length of the lipophilic tail of the surfactant, which increases the molar volume of the lipophilic tail of the surfactant with a short cosurfactant, results in an increase in oil penetration into the alkyl chains of the surfactant. This increases the attractive interaction potential, thereby suppressing the elasticity leading to smaller water droplets and lowering water solubilization. On the other hand, decreasing the length of the surfactant tail will result in a decrease in oil penetration into the alkyl chains of the surfactant, which causes the interface to become less curved, thereby favoring the growth of spontaneous curvature and the formation of larger water in oil microemulsion droplets.

4.1.6 A comparative approach to phase behavior

4.1.6.a Water / sucrose myristate M1695 / peppermint oil / cosurfactant

In this section, we will study the phase behavior of the system: water / sucrose myristate M1695 / peppermint + cosurfactant, where the surfactant sucrose myristate M1695 and the peppermint oil mixed with short chain alcohol cosurfactant, different cosurfactants are used, in order to determine the boundary of one phase region. The results from phase diagram, we will be able to determine the total area of the one phase microemulsion region A_T (%) (The total monophasic area A_T (%)).

Values of the total monophasic area A_T (±2%), for the system: water / sucrose myristate M1695 / peppermint at different cosurfactant types presented in Table 4.12. The surfactant is sucrose myristate M1695 and different cosurfactants are mixed with peppermint oil. In Table 4.12, we compared different types of cosurfactants to determine the total area of the one phase microemulsion region A_T.

Table 4.12: The total monophasic area A_T (±2%), for the system: water / sucrose myristate M1695 / peppermint+(ethanol , propylene glycol, glycerol , propionic acid).

Peppermint+ cosurfactant	**A_T (%)**
MNT+ETOH	60
MNT+PG	57
MNT+GLY	79
MNT+PRA	62

Figure 4.33 and 4.34, show the difference on the total monophasic region A_T (%) in the system: water / sucrose myristate M1695 / peppermint+ different cosurfactants as a histogram and line chart.

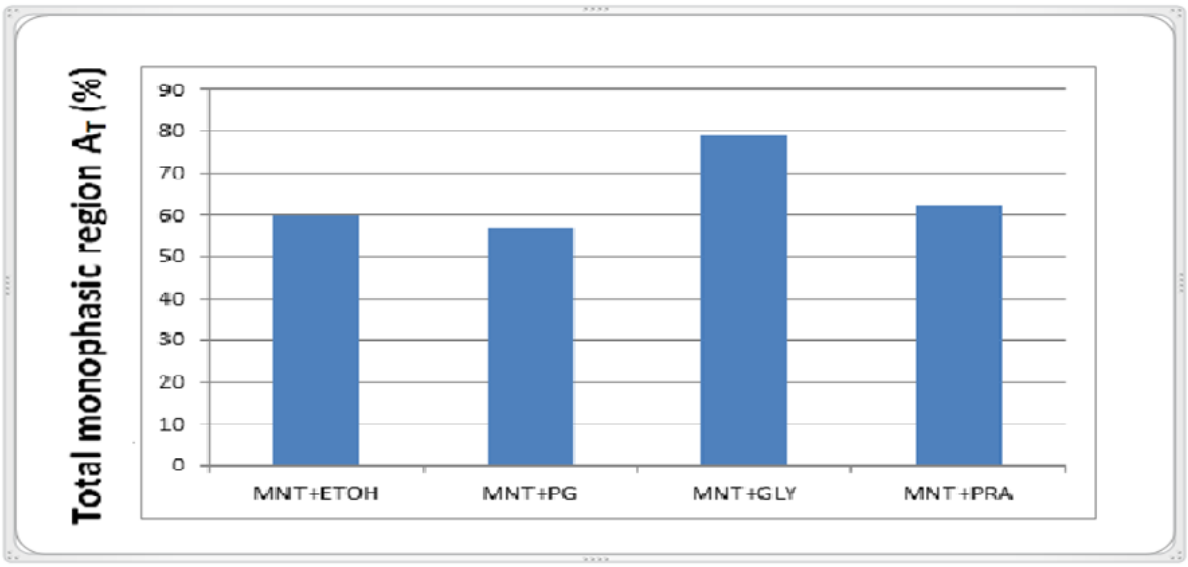

Figure 4.33**:** Variation of the total monophasic region A_T (±2%), for the system: water / sucrose myristate M1695 / peppermint+ (ethanol , propylene glycol, glycerol , propionic acid).

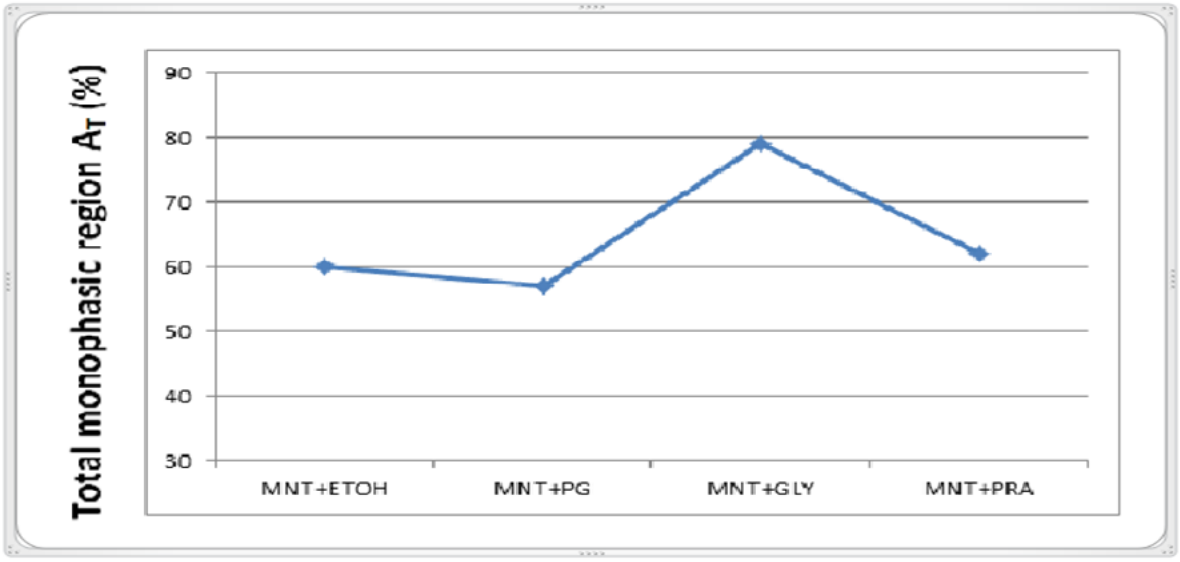

Figure 4.34**:** Variation of the total monophasic region A_T (±2%), for the system: water / sucrose myristate M1695 / peppermint+ (ethanol , propylene glycol, glycerol , propionic acid).

From the results printed in Table 4.12 and Figures 4.33 and 4.34, we observed that the systems containing cyclic oils peppermint with (ethanol , propylene glycol, glycerol , propionic acid) as a cosurfactant, we observed that peppermint + glycerol have a higher monophasic region A_T because glycerol has three hydroxyl groups that react with water

and because of peppermint cyclic oil that increases the penetrate in the surfactant layer and this improves solubility and causes an increase in monophasic region A_T.

As shown in Tables 4.8, 4.9, 4.10 and 4,11, the system: water / sucrose myristate M1695 / peppermint + glycerol has the lowest value of N_S – BSO where N_S the surfactant chain length and N_S – BSO. The difference between surfactant chain length and (oil chain length + alcohol chain length) as empirical Bansal, Shah, O'Connell (BSO). They concluded that the maximum amount of water which may be solubilized in such a microemulsion is reached when the oil chain length (carbon number), N_O, added to the cosurfactant (alcohol) chain length, N_A, is equal to the surfactant chain length, N_S, i.e. $N_S = N_O + N_A$ then when this value increases the water solubilization decreases, and chain length compatibility decreases.

Increasing the chain length of the alcohol N_A (glycerol 5), this value is the highest chain length of alcohol used in this study, and when the molar volume of the oil (peppermint 170) is small, this is the lowest molar volume of oils used in this study this causes an increase in the oil penetration into the alkyl chains of the surfactant and the penetration of cosurfactant into the palisade layers, and cause the interface to become more curved, thereby favoring decrease of Ro and the formation of small water in oil microemulsion droplets. On the other hand, decreased oil penetration decreases the attractive interaction potential, thereby increasing Rc. These competing effects lead to maximum solubilization, as observed experimentally.

4.1.6.b Water / sucrose myristate M1695 / R (+)-limonene oil + (ethanol , propylene glycol, glycerol , propionic acid)

In this section, we will study the phase behavior of the system: water / sucrose myristate M1695 / R (+)-limonene + cosurfactant, where the surfactant sucrose myristate M1695 and the R (+)-limonene oil mixed with short chain alcohol cosurfactant, different cosurfactant are used, in order to determine the boundary of one phase region. The results from phase diagram, we will be able to determine the total area of the one phase microemulsion region A_T (%) (The total monophasic area A_T (%)). In this part, we

compared between R (+)-limonene oil and different types of cosurfactant to see which is the best cosurfactant gives the maximum total monophasic area A_T and whose the worst.

Values of the total monophasic area A_T (±2%), for the system: water / sucrose myristate M1695 / R (+)-limonene at different cosurfactant types present in Table 4.13, the surfactant is sucrose myristate M1695 and different cosurfactants are mixed with R (+)-limonene oil. In Table 4.13, we compared between different types of cosurfactant to determine the total area of the one phase microemulsion region A_T(±2%)

Table 4.13: The total monophasic area A_T (±2%), for the system: water / sucrose myristate M1695 / R (+)-limonene oil + (ethanol , propylene glycol, glycerol , propionic acid).

R (+)-limonene + cosurfactant	**A_T (%)**
LIM+ETOH	70
LIM+PG	78
LIM+GLY	73
LIM+PRA	60

In Figures 4.35 and 4.36**,** we will show the difference on the total monophasic region A_T (±2%), in the system: water / sucrose myristate M1695 / R (+)-limonene + different cosurfactants as a histogram and line chart.

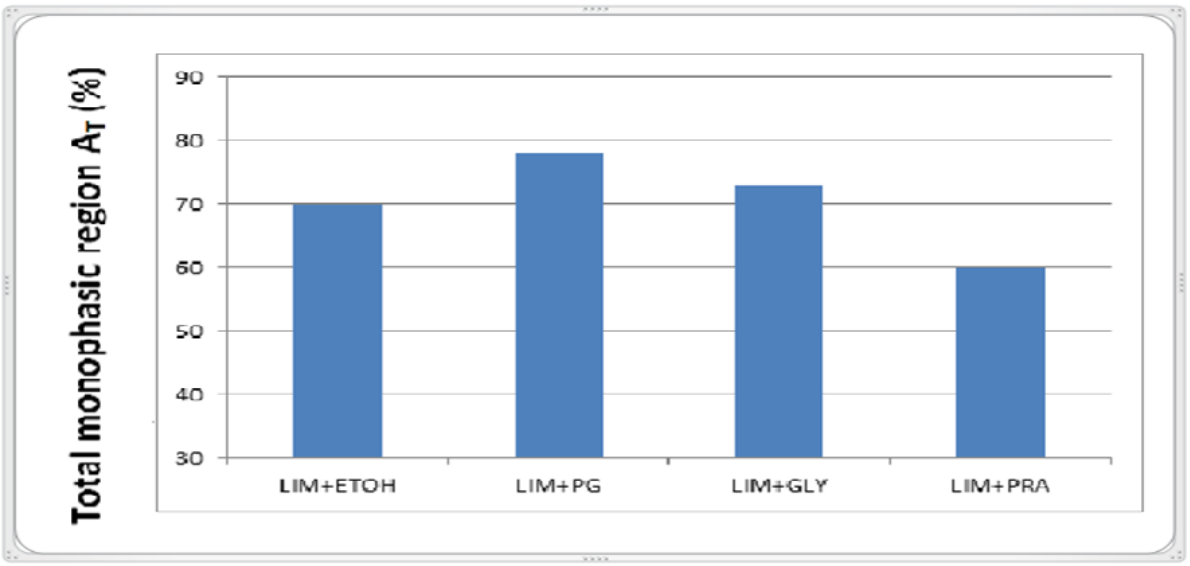

Figure 4.35**:** Variation of the total monophasic region A_T (±2%), for the system: water / sucrose myristate M1695 / R (+)-limonene oil+(ethanol , propylene glycol, glycerol , propionic acid).

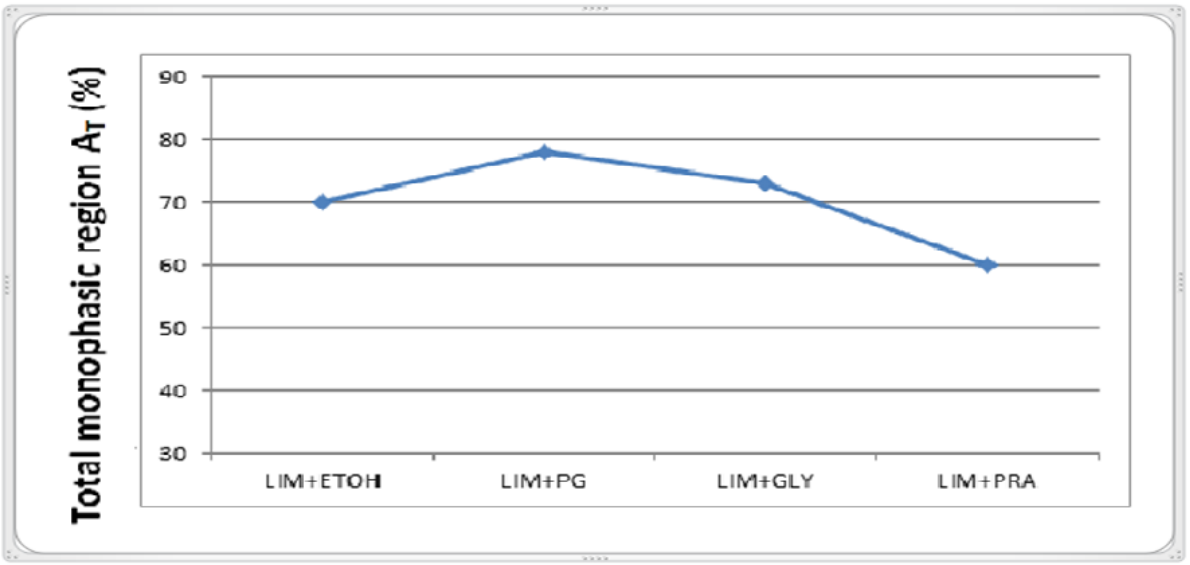

Figure 4.36**:** Variation of the total monophasic region A_T (±2%), for the system: water / sucrose myristate M1695 / R (+)-limonene oil+(ethanol , propylene glycol, glycerol , propionic acid).

From the results printed in Table 4.13 and Figures 4.35 and 4.36, we observed that the systems containing cyclic oils R (+)-limonene with (ethanol , propylene glycol, glycerol , propionic acid) as a cosurfactant ,we observed that in all types, except propionic acid, we have a very good results because R (+)-limonene is cyclic oil and has a low molecular volume, a low effective carbon number, when effective carbon number and molecular volume decrease this gives an increase in monophasic area $A_T(\pm 2\%)$,.

R (+)-limonene oil has a higher total monophasic area values. This refers to the cyclic structure of R (+)-limonene oil which tends to penetrate in the surfactant layer and widen the effective cross- sectional area per surfactant.

As shown in Tables 4.8, 4.9, 4.10 and 4,11, the system: water / sucrose myristate M1695 / R (+)-limonene + glycerol, and propylene glycol has the lowest value of $N_S - BSO$ where N_S the surfactant chain length and $N_S - BSO$. The difference between surfactant chain and (oil chain length + alcohol chain length) as empirical Bansal, Shah, O'Connell (BSO), they concluded that the maximum amount of water which may be solubilized in such a microemulsion is reached when the oil chain length (carbon number), N_O, added to the cosurfactant (alcohol) chain length, N_A, is equal to the surfactant chain length, N_S, i.e. $N_S = N_O + N_A$ then when this value increases the water solubilization decreases and chain length compatibility decreases.

Increasing the chain length of the alcohol N_A (propylene glycol 4), and when the molar volume of the oil (R (+)-limonene 181) in the system is small, this causes an increase the oil penetration into the alkyl chains of the surfactant and the penetration of cosurfactant into the palisade layers, and causes the interface to become more curved, thereby favoring decrease of Ro and the formation of small water in oil microemulsion droplets. On the other hand, decreased oil penetration decreases the attractive interaction potential, thereby increasing Rc. These competing effects lead to maximum solubilization, as observed experimentally.

4.1.6.c Water / sucrose myristate M1695 / isopropyl myristate oil+ (ethanol , propylene glycol, glycerol , propionic acid)

In this section, we will study the phase behavior of the system: water / sucrose myristate M1695 / isopropyl myristate + cosurfactant, where the surfactant sucrose myristate M1695 and the isopropyl myristate oil mixed with short chain alcohol cosurfactant, different cosurfactants are used, in order to determine the boundary of one phase region. The results from phase diagram, we will be able to determine the total area of the one phase microemulsion region A_T (%) (The total monophasic area A_T (%)). In this part, we compared between isopropyl myristate oil and different types of cosurfactants to see which is the best cosurfactant gives the maximum total monophasic area A_T and whose the worst.

Values of the total monophasic area A_T (±2%), for the system: water / sucrose myristate M1695 / isopropyl myristate at different cosurfactant types presented in Table 4.14, the surfactant is sucrose myristate M1695 and different cosurfactants are mixed with isopropyl myristate oil. In Table 4.14, we compared between different types of cosurfactants to determine the total area of the one phase microemulsion region A_T(±2%),.

Table 4.14: The total monophasic area A_T (±2%), for the system: water / sucrose myristate M1695 / isopropyl myristate oil+ (ethanol , propylene glycol, glycerol , propionic acid).

Isopropyl myristate + cosurfactant	**A_T (%)**
IPM+ETOH	59
IPM+PG	88
IPM+GLY	74
IPM+PRA	60

In Figures 4.37 and 4.38, we will show the difference on the total monophasic region A_T (%) in the system: water / sucrose myristate M1695 / isopropyl myristate + different cosurfactants as a histogram and line chart.

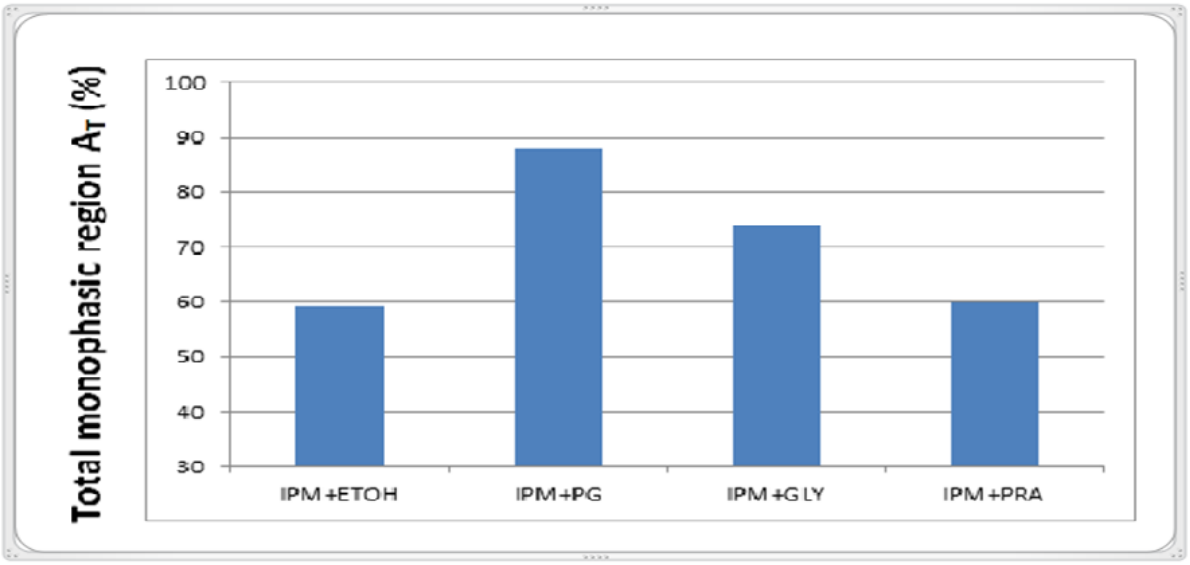

Figure 4.37: The total monophasic area A_T (±2%), for the system: water / sucrose myristate M1695 / isopropyl myristate oil+ (ethanol , propylene glycol, glycerol , propionic acid).

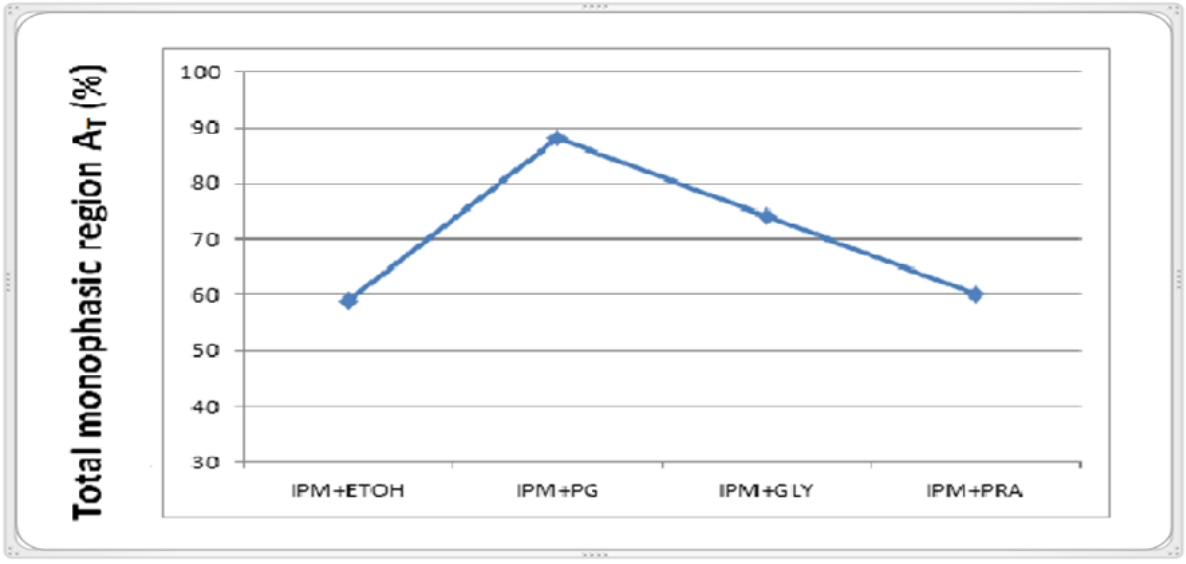

Figure 4.38**:** The total monophasic area A_T (±2%), for the system: water / sucrose myristate M1695 / isopropyl myristate oil+ (ethanol , propylene glycol, glycerol , propionic acid).

From the results printed in Table 4.14 and Figures 4.37 and 4.38, we observed that the systems containing linear oil isopropyl myristate with (ethanol , propylene glycol, glycerol , propionic acid) as a cosurfactant, the isopropyl myristate with propylene glycol and glycerol have the higher monophasic area A_T (±2%), because they have more than one hydroxyl group on cosurfactant.

Isopropyl myristate + propylene glycol have maximum A_T % because propylene glycol contains two hydroxyl group and low molecular volume than glycerol that gives optimal curvature.

Increasing the chain length of the alcohol N_A (propylene glycol 4, glycerol 5), these two values are the highest chain length of alcohol used in this study, and when the molar volume of the oil (isopropyl myristate 317) is small, this causes an increase in the oil penetration into the alkyl chains of the surfactant and the penetration of cosurfactant into the palisade layers, and causes the interface to become more curved, thereby favoring decrease of Ro and the formation of small water in oil microemulsion droplets. On the other hand, decreased oil penetration decreases the attractive interaction potential, thereby increasing Rc. These competing effects lead to maximum solubilization, as observed experimentally.

4.1.6.d Water / sucrose myristate M1695 / caprylic/capric triglyceride oil+ (ethanol , propylene glycol, glycerol , propionic acid)

In this section, we will study the phase behavior of water / sucrose myristate M1695 / caprylic/capric triglyceride + cosurfactant, where the surfactant sucrose myristate M1695 and the caprylic/capric triglyceride oil mixed with short chain alcohol cosurfactant, different cosurfactants are used, in order to determine the boundary of one phase region. The results from phase diagram, we will be able to determine the total area of the one

phase microemulsion region A_T (%) (The total monophasic area A_T (%)). In this part, we compared between caprylic/capric triglyceride oil and different types of cosurfactant to see which is the best cosurfactant that gives the maximum total monophasic area A_T and whose the worst.

Values of the total monophasic area A_T (±2%), for the system: water / sucrose myristate M1695 / caprylic/capric triglyceride at different cosurfactant types presented in Table 4.15, the surfactant is sucrose myristate M1695 and different cosurfactants are mixed with caprylic/capric triglyceride oil. In this Table, we compared between different types of cosurfactant to determine the total area of the one phase microemulsion region A_T.

Table 4.15**:** The total monophasic area A_T (±2%), for the system: water / sucrose myristate M1695 / caprylic/capric triglyceride oil+ (ethanol , propylene glycol, glycerol , propionic acid).

Caprylic/capric triglyceride + cosurfactant	**A_T (%)**
CCT+ETOH	57
CCT+PG	83
CCT+GLY	84
CCT+PRA	60

Figures 4.39 and 4.40**,** show the difference on the total monophasic region A_T (%) in the system: water / sucrose myristate M1695 / caprylic/capric triglyceride + different cosurfactant as a histogram and line chart.

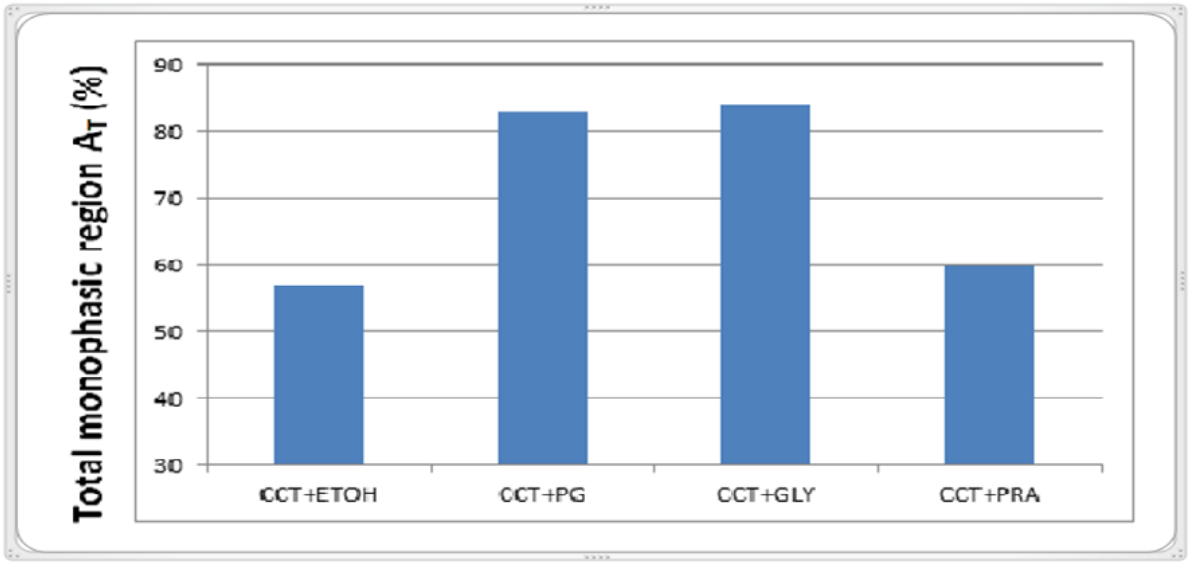

Figure 4.39: The total monophasic area A_T (±2%), for the system: water / sucrose myristate M1695 / caprylic/capric triglyceride oil+ (ethanol , propylene glycol, glycerol , propionic acid).

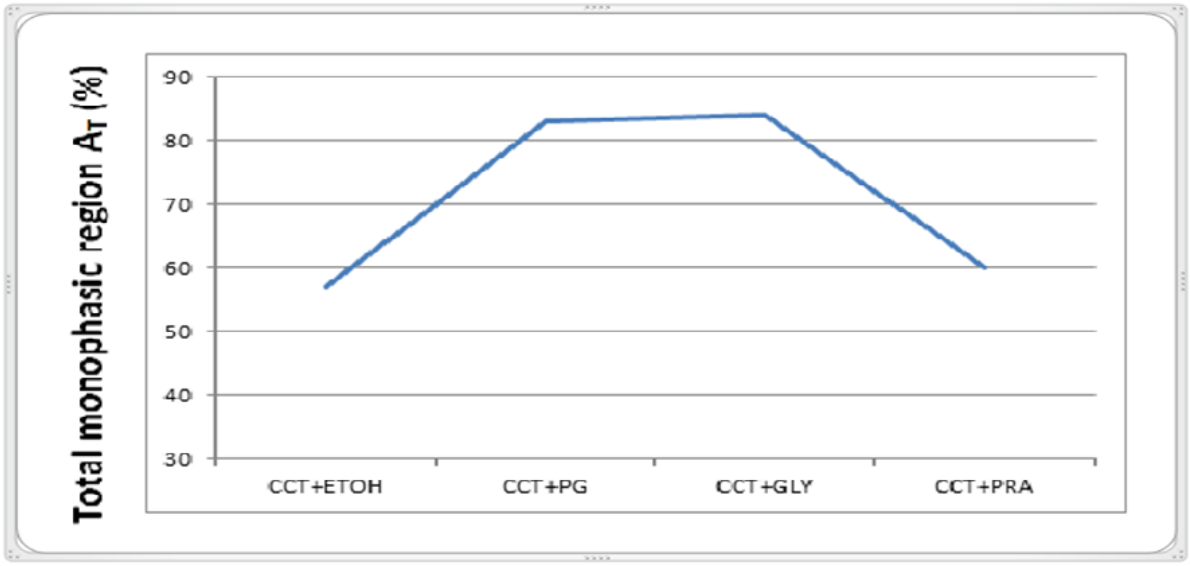

Figure 4.40**:** The total monophasic area A_T (±2%), for the system: water / sucrose myristate M1695 / caprylic/capric triglyceride oil+ (ethanol , propylene glycol, glycerol , propionic acid).

From the results printed in Table 4.15 and Figures 4.39 and 4.40, we observed that the systems containing triglyceride oil caprylic/capric triglyceride with (ethanol , propylene glycol, glycerol , propionic acid) as a cosurfactant, the caprylic/capric triglyceride with propylene glycol and glycerol have the higher monophasic area A_T %.

Hydroxyl group found in cosurfactant (glycerol, propylene glycol , ethanol) (3,2,1) that causes an increase in interaction with water, this gives enhance curvature of droplets size, decreases interfacial tension and gives an increase in monophasic area $A_{T\,\%}$.

Increasing the chain length of the alcohol N_A, when the molar volume of the oil in the system is small, will increase the oil penetration into the alkyl chains of the surfactant and the penetration of cosurfactant into the palisade layers. This will cause the interface to become more curved, thereby favoring decrease of Ro and the formation of small water in oil microemulsion droplets. On the other hand, decreased oil penetration decreases the attractive interaction potential, thereby increasing Rc. These competing effects lead to maximum solubilization, as observed experimentally.

The system: water / sucrose myristate M1695 / caprylic/capric triglyceride oil+ ethanol has the lowest monophasic area A_T % because that contains alcohol (ethanol) with small chain length and oil (caprylic/capric triglyceride) with high molar volume that cases decreasing the oil penetration into the alkyl chains of the surfactant and the penetration of cosurfactant into the palisade layers. This will cause the interface to become less curved, thereby favoring increase of Ro and the formation of big water in oil microemulsion droplets. These competing effects lead to minimum solubilization, as observed experimentally.

In general, the increase in molecular volume and carbon number cases a decrease in monophasic area A_T. Cyclic oil peppermint, R (+)-limonene oil have higher total monophasic area because cyclic structure of R (+)-limonene and oil peppermint oil which tends to penetrate in the surfactant layer and widen the effective cross-sectional area per surfactant, and the presence of cosurfactant improves the solubilization of water , this gives an increase in monophasic area A_T.

Triglyceride oil, caprylic/capric triglyceride and linear oil isopropyl myristate, has low total monophasic area because they have high molecular volume than cyclic oil peppermint, R (+)-limonene and so the ability to penetrate the interfacial film is very low and does not assist to obtain the optimum curvature of surfactants, decreasing the length of the surfactant tail will result in a decrease in oil penetration into the alkyl chains of the surfactant, which causes the interface to become less curved, thereby favoring the growth of spontaneous curvature and the formation of larger water in oil microemulsion droplets.

4.2 Electrical conductivity

Understanding of the microemulsions properties is needed for any scientific or industrial application of these systems; thus much work has been done over the last decades in this particular area [De Campo. L, Yaghmur. A, et al 2004], [Yaghmur. A, De Campo. L, and et al 2004], [Glatter. O, Orthaber. D, Stradner. A, Scherf. G, Fanun. M and et al 2001] , [Papadimitriou. V, Sotiroudis. T.G, and Xenakis. A, 2007], and [Salazar-Alvarez. G, Björkman. E, et 2007]. Microemulsion domain structures are often characterized as water in oil (W/O) oil-continuous or bicontinuous or oil in water (O/W) water-continuous. These structures are influenced both by the water to oil ratio and by the preferred curvature of the surfactant, which results from the interactions of the surfactant layer with the oil and water phases, [Biais.J, Clin. B, Laolanne. P,1987]. Properties of microemulsions can be determined using various techniques such as electrical conductivity, [Bumajdad, A. and Eastoe, J, 2004] and [Kahlweit. M, Busse. G, and Winkler. J, 1993], to study the effects of changing the relative amounts of microemulsion components on the transport, diffusion and structural properties of these self-assemblies were investigated using electrical conductivity, [MacKay .R.A, R. Agarwal .R, 1978], [Bordi. F, Cametti. C, 1996] and [Bumajdad. A, Eastoe.J, 2004].

[Fanun. M, 2009] studied the unity and studied the properties of water + propylene glycol l/ sugar surfactant/ peppermint oil + ethanol using electrical conductivity. It was found in all studies the same result; the electrical conductivity increases as the water volume fraction increases, [Fanun. M, 2009] studied the systems water / sucrose laurate/ ethoxylated mono-di glyceride/ isopropylmyristate/ peppermint oil. The solubilization capacity of water in the oils is dependent on the surfactants and oils mixing ratios (w/w). The transport properties (electrical conductivity and dynamic viscosity) were studied as function of water volume fraction. It was found that increasing the weight ratio of peppermint oil in the mixed oils improved the water solubilization capacity in the microemulsions. The molar ratios of mixed surfactants play an important role in determining the maximum water solubilization, this study reveals that the electrical conductivities increase with the increase water volume fraction.

The high values of electrical conductivity at high-water volume fractions are explained by the fact that the sodium chloride ions are present in the external phase, which is the water. These results permit to distinguish between w/o and o/w microemulsions, [Fanun. M, 2007], [Fanun. M, and Salah Al-Diyn. W, 2007], [Fanun. M, and Salah Al-Diyn. W, 2006] and [Kahlweit. M, Busse. G, and Winkler. J, 1993]. The electrical conductivity and periodicity of the microemulsions increases with the aqueous phase content while the dynamic viscosity decreases. The variations in the values of the correlation length with the aqueous phase contents indicate the onset of structural transitions. Structural transitions from the water-in-oil to a bicontinuous phase then inversion to oil-in-water occurs in the system, [Fanun. M, 2010].

In this section, we will study the properties of microemulsions by electrical conductivity, we studied the effects of changing the relative amounts of microemulsion components on the transport, diffusion and structural properties of these self-assemblies. In this part of this study, we will determine the type of microemulsion droplets formed (i.e. water-in-oil (W/O), bicontinues, or oil-in-water (O/W) by electrical conductivity measurements.

Water / sucrose myristate M1695 / R (+)-limonene oil+ propylene glycol, water/ sucrose myristate M1695 / caprylic/capric triglyceride + propylene glycol and water/ sucrose myristate M1695 / isopropyl myristate + propylene glycol are studied in this research because they have the highest monophasic region A_T. In this section of this study, we did a comparative study between different types of oil and propylene glycol as a cosurfactant, we chose these three systems because they have better comparable results of monophasic region A_T.

4.2.1 Water / sucrose myristate M1695 / R (+)-limonene oil + propylene glycol

In this section, we will study the electrical conductivity for the system: water / sucrose myristate M1695 / R (+)-limonene oil+ propylene glycol where the dilution line N60, the phase diagrams is presented in Figure 4.14. Figure 4.41 and Table 4.16 display the influence of water content and temperature on the electrical conductivity (σ), values of the electrical conductivity (σ) for the system: water / sucrose myristate M1695 / R (+)-limonene oil + propylene glycol at different water contents and different temperatures presented in Table 4.16. In this Table, the surfactant is sucrose myristate M1695 and the

oil is R (+)-limonene + propylene glycol as a cosurfactant, where the temperature changed from 25-45°C and water content increased from 0-92% water content.

Table 4.16**:** The electrical conductivity (σ) for the system: water / sucrose myristate M1695 / R (+)-limonene oil + propylene glycol at different water contents and different temperatures, measured along the dilution line N60 presented in Figure 4.14.

	σ (µS/cm)		
Water content (wt.%)	**25°C**	**37°C**	**45°C**
0%	8	16	57
1%	8	19	66
2%	9	35	69
4%	37	67	76
6%	63	116	78
8%	69	159	85
10%	78	180	130
15%	88	220	183
20%	121	258	326
25%	171	301	439
30%	262	313	634
35%	308	360	726
40%	366	403	774
45%	401	458	868
50%	415	446	888
55%	423	468	926
60%	453	489	945
65%	426	438	831
70%	356	405	750
75%	338	390	711
80%	287	281	565
85%	211	207	409
90%	148	153	301
92%	126	105	201

In Figure 4.41, we will show the difference on the electrical conductivity (σ) for the system: water / sucrose myristate M1695 / R (+)-limonene oil+ propylene glycol at different water contents and different temperatures

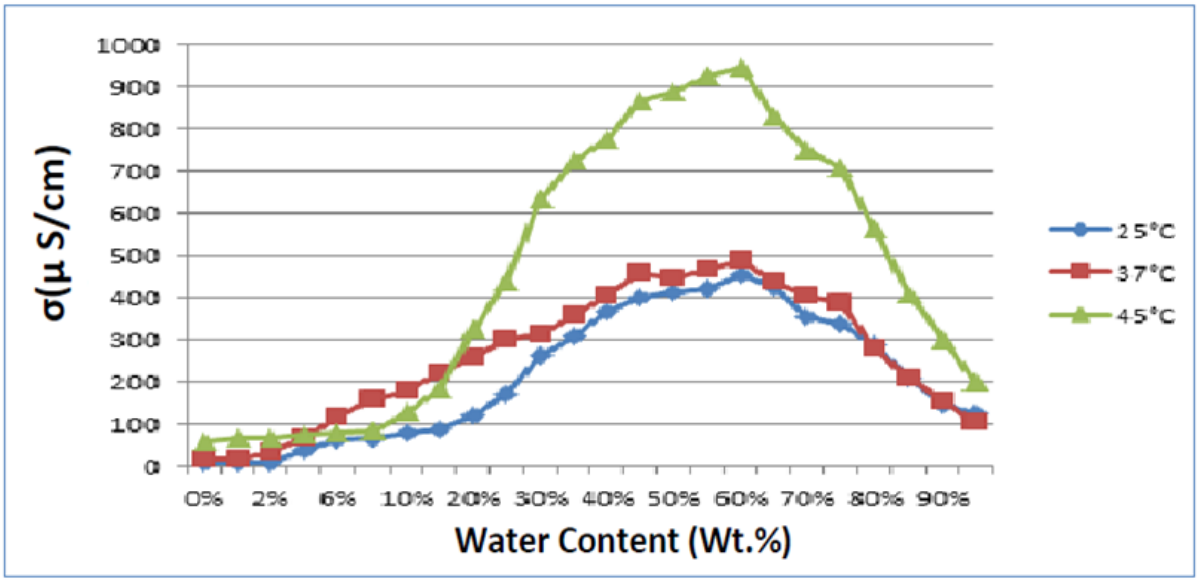

Figure 4.41**:** Variation of the electrical conductivity (σ) for the system: water / sucrose myristate M1695 / R (+)-limonene oil + propylene glycol as function of water content along the dilution line N60. The phase diagrams is presented in Figure 4.14, at different temperatures (25°C, 37°C and 45°C).

At water content less than 4%, samples along the dilution line N60 were tested. The system: water / sucrose myristate M1695 / R (+)-limonene oil + propylene glycol as shown in Figure 4.41, has low values of electrical conductivity; the low conductivity in this region indicates restricted water mobility, then the values of the electrical conductivity increase continuously with the increase in the water content. High electrical conductivity 55-65% water content on the N60 line suggests that the system undergoes a structural inversion to bicontinues microemulsion. Water content less than 55-65% is water in oil microemulsion, decreased the electrical conductivity above 65% suggests that the system undergoes a structural inversion to oil in water.

As shown in the result presented in Figure 4.41, the electrical conductivity increases continuously with the increase in the water content to reach 55-65% water content, then electrical conductivity starts decreasing from 4-55% water content, water in oil microemulsion, 55-65 % water content phase inversion bicontinues then from 65-92% water content oil in water microemulsion.

4.2.2 Water / sucrose myristate M1695 / caprylic/capric triglyceride + propylene glycol

In this section, we will study the electrical conductivity for the system: water / sucrose myristate M1695 / caprylic/capric triglyceride + propylene glycol where the dilution line N60 the phase diagrams is presented in Figure 4.15. Figure 4.42 and Table 4.17 display the influence of water content and temperature on the electrical conductivity (σ).

Values of the electrical conductivity (σ) for the system: water / sucrose myristate M1695 / caprylic/capric triglyceride oil + propylene glycol at different water contents and different temperatures presented in Table 4.17. In this Table, the surfactant is sucrose myristate M1695 and the oil is caprylic/capric triglyceride + propylene glycol as a cosurfactant, where the temperature changed from 25-45°C and water content increased from 0-85% water content.

Table 4.17: The electrical conductivity (σ) for the system: water / sucrose myristate M1695 / caprylic/capric triglyceride oil+ propylene glycol at different water contents and different temperatures, measured along the dilution line N60 presented in Figure 4.15.

	σ (µS/cm)		
Water content (wt.%)	**25°C**	**37°C**	**45°C**
0%	0	0	0
1%	1.6	4	2
2%	1.8	4	8
4%	2	5	9
6%	6	11	24
8%	9	18	35
10%	11	19	47
15%	31	47	124
20%	64	82	182
25%	87	105	229
30%	123	133	281
35%	161	191	376
40%	202	232	449
45%	241	253	486
50%	243	255	471
55%	203	227	434
60%	142	189	375
65%	123	151	353
70%	121	142	335
75%	84	141	299
80%	66	139	275
85%	55	121	235

In Figure 4.42**,** we will show the difference on the electrical conductivity (σ) for the system: water / sucrose myristate M1695 / caprylic/capric triglyceride oil + propylene glycol at different water contents and different temperatures.

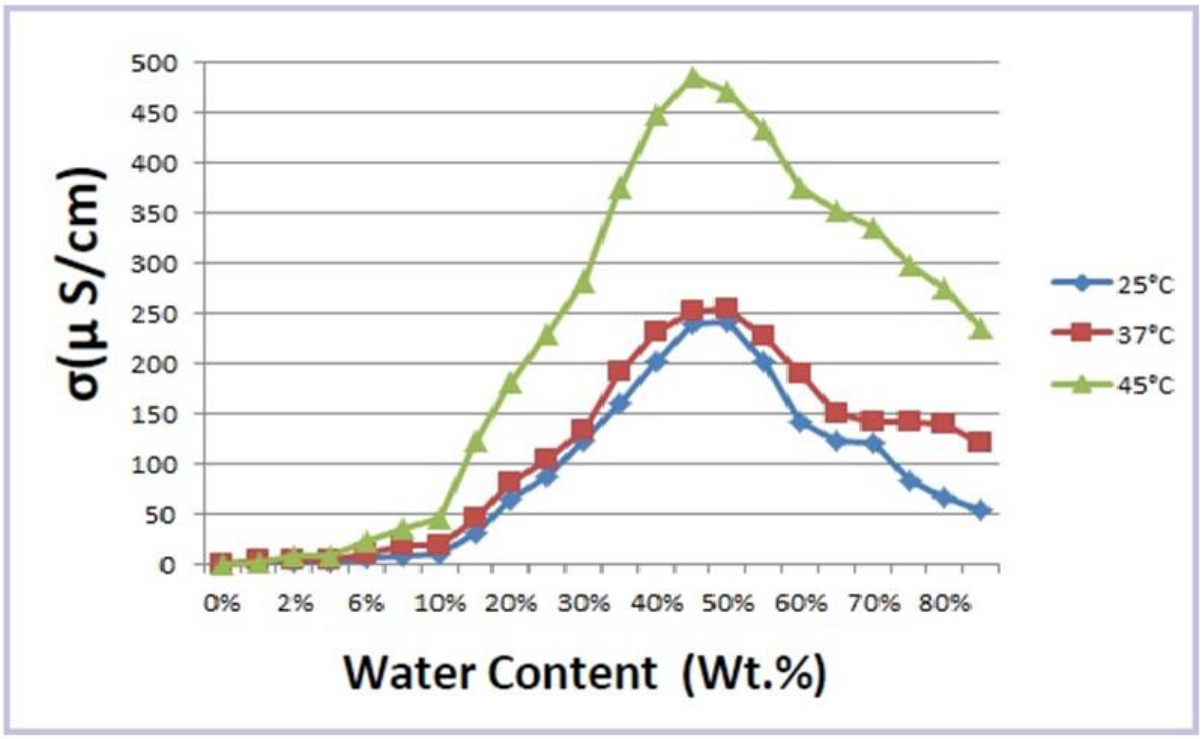

Figure 4.42**:** Variation of the electrical conductivity (σ) for the system: water / sucrose myristate M1695 / caprylic/capric triglyceride oil + propylene glycol as function of water content along the dilution line N60. The phase diagrams is presented in Figure 4.15 at different temperatures (25°C, 37°C and 45°C).

The electrical conductivity at water content equals 0 wt% is very low, and when the water content increased from 0 wt% to 15 wt%, the electrical conductivity has been slightly increased in steadily fashion due to formation reverse micelles (water-in-oil microemulsion). A sudden increase in the electrical conductivity happens at water content above 15 wt% due to formation bicontinuous structure in which the electrical current passes through internal channels. Conductivity was increased as temperature increases in steadily fashion at water content higher than 15 wt %, but it decreases the electrical

conductivity happens at water content above 55 wt % due to formation oil in water microemulsion.

At water content less than 15%, samples along the dilution line N60 were tested. The system: water / sucrose myristate M1695 / caprylic/capric triglyceride oil + propylene glycol, shown in Figure 4.42, have low values of electrical conductivity. The low conductivity in this region indicates restricted water mobility, then the values of the electrical conductivity increase continuously with the increase in the water content. High electrical conductivity 45-55% water content on the N60 line suggests that the system undergoes a structural inversion to bicontinues microemulsion. At water content less than 45-55 % water content, it is water in oil microemulsion, decreased the electrical conductivity above 55% suggests that the system undergoes a structural inversion to oil in water.

As shown from results presented in Figure 4.42, the electrical conductivity increases continuously with the increase in the water content to reach 45-55% water content, then electrical conductivity starts decreasing from 55-85% water content. At water content 15-45% water in oil microemulsion. Then at 45-55% water content, the phase inversion to bicontinues. From 55-85% water content, it becomes oil in water microemulsion.

4.2.3 Water / sucrose myristate M1695 / isopropyl myristate + propylene glycol

In this section, we study the electrical conductivity for the system: water / sucrose myristate M1695 / isopropyl myristate + propylene glycol, where the dilution line N60 the phase diagrams is presented in Figure 4.16. Figures 4.43 and Table 4.18 display the influence of water content and temperature on the electrical conductivity (σ).

Values of the electrical conductivity (σ) for the system: water / sucrose myristate M1695 / isopropyl myristate oil + propylene glycol at different water contents and different temperatures presented in Table 4.18. In this Table, the surfactant is sucrose myristate

M1695 and the oil is isopropyl myristate + propylene glycol as a cosurfactant, where the temperature changed from 25-45°C and water content increased from 0-92% water content.

Table 4.18**:** The electrical conductivity (σ) for the system: water / sucrose myristate M1695 / isopropyl myristate + propylene glycol at different water contents and different temperatures, measured along the dilution line N60 presented in Figure 4.16.

	σ (μS/cm)		
Water content (wt.%)	**25°C**	**37°C**	**45°C**
0%	131	202	465
1%	135	205	471
2%	145	223	492
4%	215	266	546
6%	241	282	591
8%	251	297	607
10%	274	311	626
15%	308	346	774
20%	311	365	786
25%	359	401	802
30%	379	436	852
35%	406	448	865
40%	424	456	893
45%	434	471	903
50%	442	474	926
55%	443	472	922
60%	429	448	896
65%	391	428	884
70%	389	427	832
75%	383	401	772
80%	343	363	706
85%	297	306	592
90%	227	233	455
92%	184	191	365

In the Figure 4.43, we will show the difference on the electrical conductivity (σ) for the system: water / sucrose myristate M1695 / isopropyl myristate oil + propylene glycol at different water contents and different temperatures.

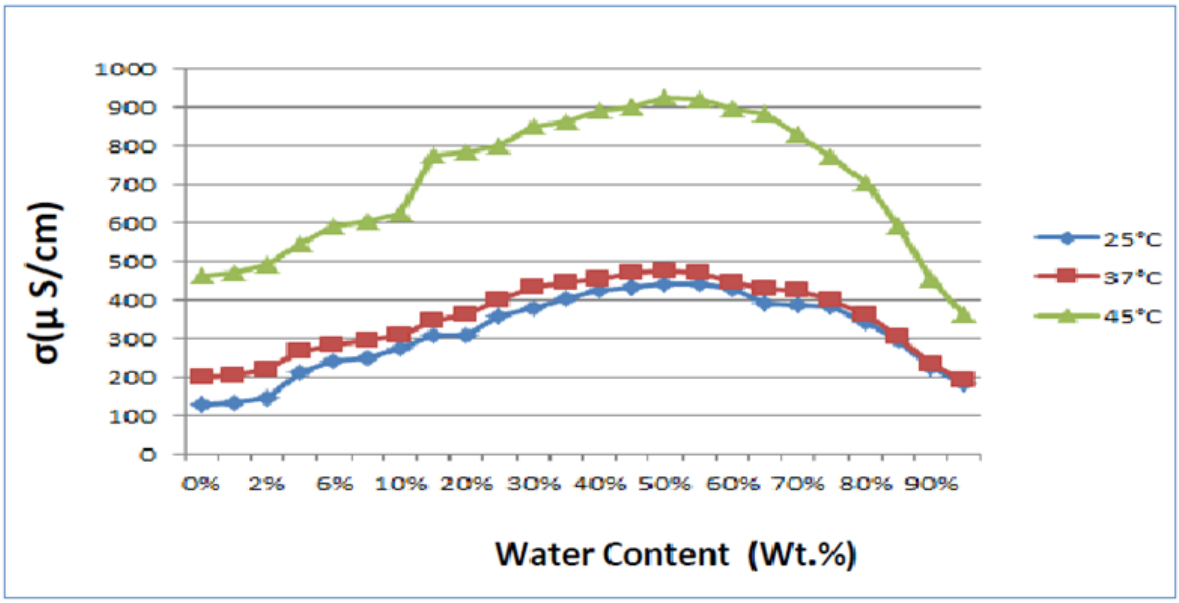

Figure 4.43**:** Variation of the electrical conductivity (σ) for the system: water / sucrose myristate M1695 / isopropyl myristate + propylene glycol as function of water content along the dilution line N60. The phase diagrams is presented in Figure 4.16 at different temperatures (25°C, 37 °C and 45°C).

The result in the previous Table and Figure shows that this system is different from other systems because at water content 0%, along the dilution line N60 tested, the system: water / sucrose myristate M1695 / isopropyl myristate + propylene glycol have high values of electrical conductivity. The high electrical conductivity in this region indicates restricted water mobility. The electrical conductivity increases continuously with the increase in the water content. High electrical conductivity 50-60 % water content on the N60 dilution line suggests that the system undergoes a structural inversion to bicontinues microemulsion, at water content less than 50-60 % water content are water in oil microemulsion, decreased the electrical conductivity above 60% water content suggests that the system undergoes a

structural inversion to oil in water. As shown in the results presented in Figure 4.43, the electrical conductivity increases continuously with the increase in the water content to reach 50-60% water content, then electrical conductivity starts decreasing. From 0-50 % water content, water in oil microemulsion, 50-60 % water content phase inversion bicontinues then from 60-92% water content oil in water microemulsion.

Clusters of droplets which, in turn, generate water networks throughout the water-in-oil phase are produced by the short-range attractive interactions. As a sequence, important changes of the transport properties, such as diffusion and electrical conductivity, occur. The phenomena have been described in terms of percolation, [Feldman. Y, Kozlovich. N, Nir. I, Garti.N, at el 1991]. According to the percolation model, the conductivity remains low up to a certain volume fraction of water at constant temperature, when the temperature reaches a value T_c at constant water volume fraction, or when the water-to-surfactant molar ratio increases. It must be emphasized that these conducting water-in-oil droplets, below volume fraction are isolated from each other embedded in nonconducting continuum oil phase and hence contribute very little to the conductance. However, as the volume fraction of water reaches the percolation threshold volume fraction, some of these conductive droplets begin to contact each other and form clusters which are sufficiently close to each other. The number of such clusters increases very rapidly above the percolation threshold volume fraction, giving rise to the observed changes of properties, in particular to the increase of electrical conductivity. The electrical conductivity r above volume fraction has been attributed to the transfer of counter ions from one droplet to another through water channels opening between droplets during sticky collisions through transient merging of droplets, [Moulik. S.P, and Paul. B.K,1998].

The existence and position of this threshold depends on the interactions between droplets which control the duration of the collision and the degree of the interface overlapping, hence the probability of merging. Building up of conductivity needs attractive interactions and volume fraction decreases when the strength of these interdroplet interactions increases as predicted by recent theoretical calculations, [Safran. S.A, Grest. G.S, and Bug. A, Webman, I, et al 1987].

In Figure 4.44, we will show schematic presentation of the structural transitions and the change in the electrical conductivity along the N60 dilution line.

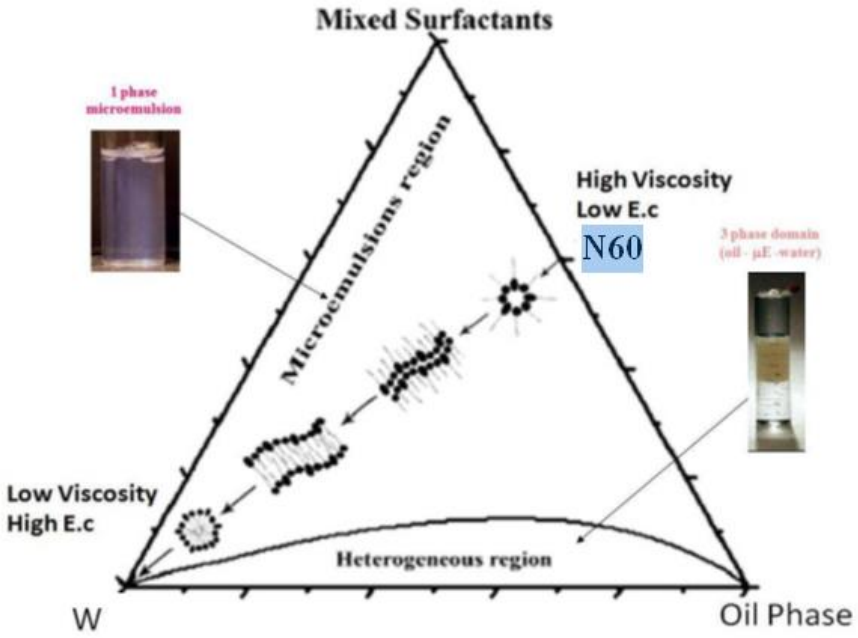

Figure 4.44: Schematic presentation of the structural transitions and the change in the electrical conductivity along the N60 dilution line.

4.2.4 A comparative approach on the electrical conductivity

In this part of this study, we did a comparative approach on the electrical conductivity. In part one, we used different types of oil at 25°C then at 37°C then at 45°C to study the effect of changing temperature at different water contents (0,10,20,40,60,80 (wt.%). In part two, we study the effect of changing tempreture on electrical conductivity for R (+)-limonene, isopropyl myristate, caprylic/capric triglyceride + propylene glycol.

Values of the electrical conductivity σ (μS/cm) for the system: water / sucrose myristate M1695 / R (+)-limonene, isopropyl myristate, caprylic/capric triglyceride oil+ propylene glycol at different water contents and a stable temperature 25°C presented in Table 4.19, the surfactant is sucrose myristate M1695 and different oils are used. In this Table, we compared between different types of oil to determine the electrical conductivity σ (μS/cm) at temperature 25°C .

Table 4.19: The electrical conductivity (σ) for the system: water / sucrose myristate M1695 / R (+)-limonene, isopropyl myristate, caprylic/capric triglyceride oil + propylene glycol at different water contents and a stable temperature 25°C, measured along the dilution line N60 presented in Figures 4.14, 4.15 and 4.16.

σ (μS/cm)			
Water content (wt.%)	**25°C**		
	LIM	**CCT**	**IPM**
0%	8	0	131
10%	78	11	274
20%	121	64	311
40%	366	202	424
60%	453	142	429
80%	287	66	343

In Figure 4.45, we will show the difference on the electrical conductivity (σ) for the system: water / sucrose myristate M1695 / R (+)-limonene, isopropyl myristate, caprylic/capric triglyceride oil + propylene glycol at different water contents and a stable temperature 25°C.

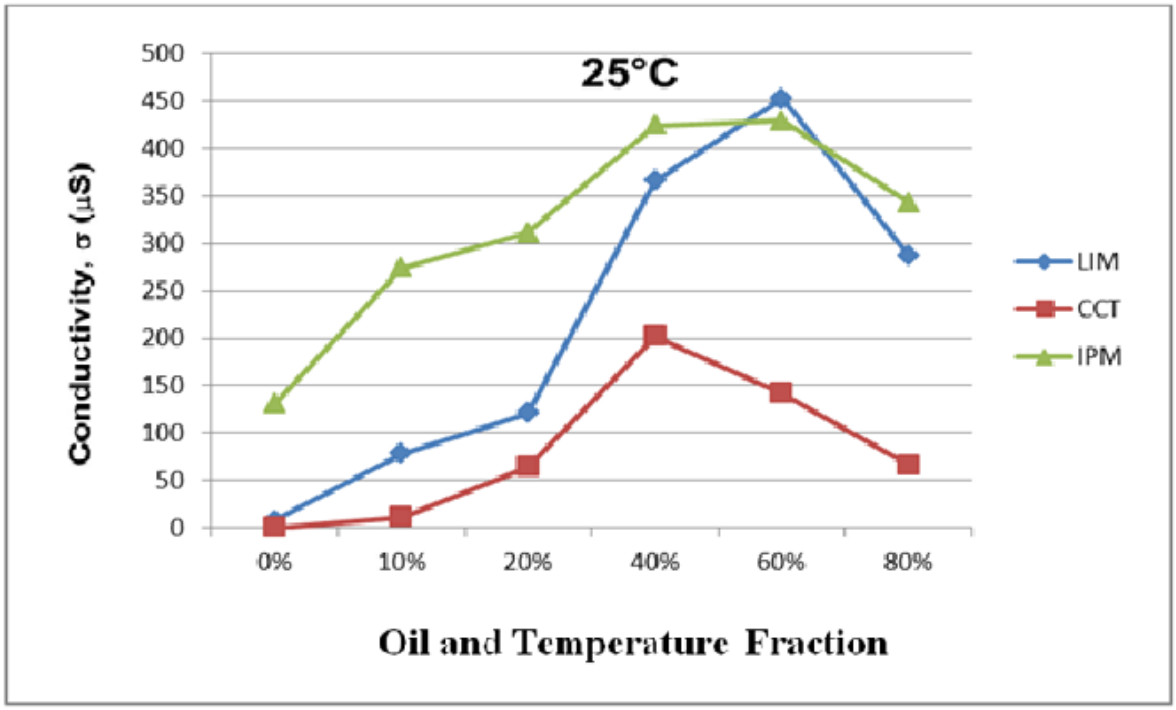

Figure 4.45: Variation of the electrical conductivity (σ) for the system: water / sucrose myristate M1695 / R (+)-limonene, isopropyl myristate, caprylic/capric triglyceride oil + propylene glycol as function of water content along the dilution line N60 presented in Figure 4.14, 4.15 and 4.16 at 25°C.

Values of the electrical conductivity σ (µS/cm) for the system: water / sucrose myristate M1695 / R (+)-limonene, isopropyl myristate, caprylic/capric triglyceride oil + propylene glycol at different water contents and a stable temperature 37°C presented in Table 4.20, the surfactant is sucrose myristate M1695 and different oils are used. In this Table, we compared between different types of oil to determine the electrical conductivity σ (µS/cm) at 37°C.

Table 4.20: The electrical conductivity (σ) for the system: water / sucrose myristate M1695 / R (+)-limonene, isopropyl myristate, caprylic/capric triglyceride oil + propylene glycol at different water contents and a stable temperature 37°C, measured along the dilution line N60 presented in Figure 4.14, 4.15 and 4.16.

σ (μS/cm)			
	37°C		
Water content (wt.%)	LIM	CCT	IPM
0%	16	0	202
10%	180	19	311
20%	258	82	365
40%	403	232	456
60%	489	189	448
80%	281	139	363

In Figure 4.46, we will show the difference on the electrical conductivity (σ) for the system: water / sucrose myristate M1695 / R (+)-limonene, isopropyl myristate, caprylic/capric triglyceride oil + propylene glycol at different water contents and a stable temperature 37°C.

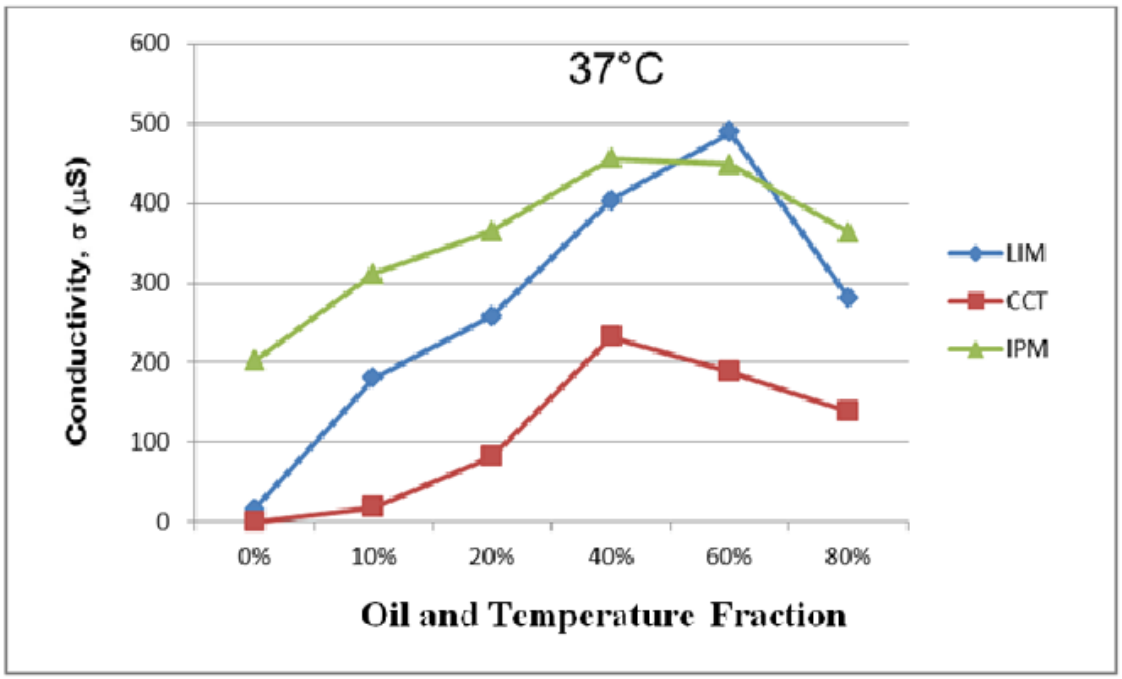

Figure 4.46: Variation of the electrical conductivity (σ) for the system: water / sucrose myristate M1695 / R (+)-limonene, isopropyl myristate, caprylic/capric triglyceride oil + propylene glycol as function of water content along the dilution line N60 presented in Figures 4.14, 4.15 and 4.16 at 37°C.

Values of the electrical conductivity σ (µS/cm) for the system: water / sucrose myristate M1695 / R (+)-limonene, isopropyl myristate, caprylic/capric triglyceride oil + propylene glycol at different water contents and a stable temperature 45°C presented in Table 4.21, the surfactant is sucrose myristate M1695 and different oils are used. In this Table, we compared between different types of oil to determine the electrical conductivity σ (µS/cm) at temperature 45°C.

Table 4.21**:** The electrical conductivity (σ) for the system: water / sucrose myristate M1695 / R (+)-limonene, isopropyl myristate, caprylic/capric triglyceride oil + propylene glycol at different water contents and a stable temperature 45°C, measured along the dilution line N60 presented in Figures 4.14, 4.15 and 4.16.

σ (μS/cm)			
	45°C		
Water content (wt.%)	**LIM**	**CCT**	**IPM**
0%	57	0	465
10%	130	47	626
20%	326	182	786
40%	774	494	893
60%	945	375	896
80%	565	275	706

In Figure 4.47, we will show the difference on the electrical conductivity (σ) for the system: water / sucrose myristate M1695 / R (+)-limonene, isopropyl myristate, caprylic/capric triglyceride oil + propylene glycol at different water contents and a stable temperature 45°C.

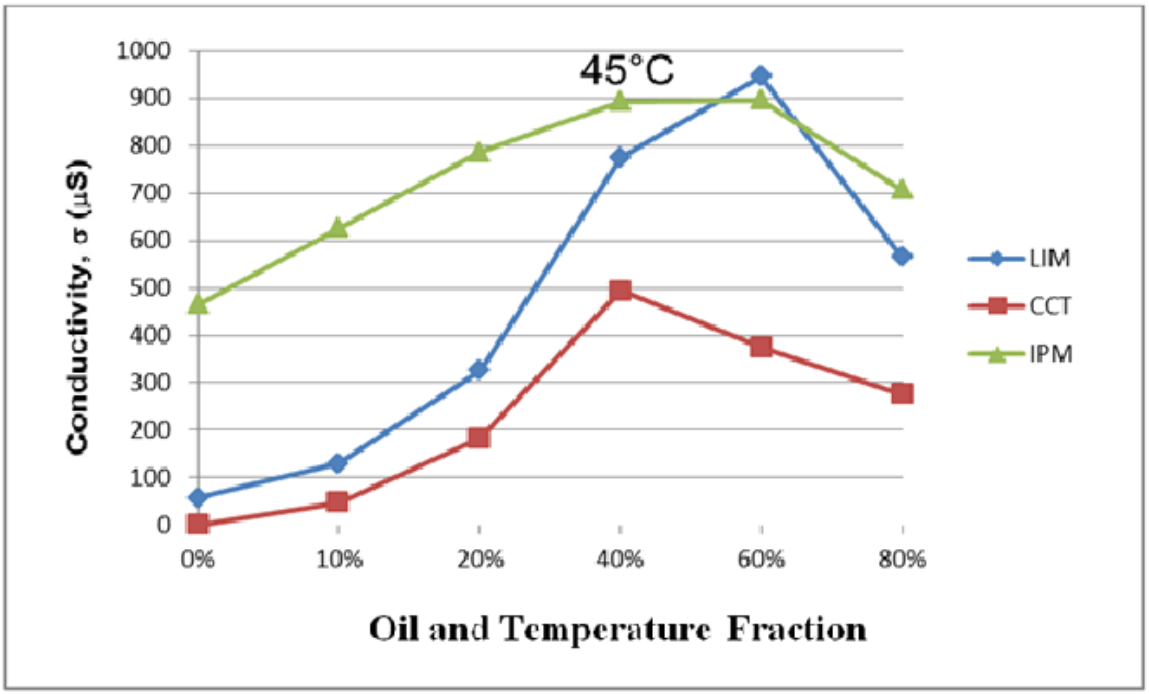

Figure 4.47: Variation of the electrical conductivity (σ) for the system: water / sucrose myristate M1695 / R (+)-limonene, isopropyl myristate, caprylic/capric triglyceride oil + propylene glycol as function of water content along the dilution line N60 presented in Figures 4.14, 4.15 and 4.16 at 45°C.

As shown in the result presented in the Figures 4.45, 4.46 and 4.47, the electrical conductivity increases continuously with the increase in the water content as water in oil microemulsion, then electrical conductivity starts decreasing when the system is oil in water microemulsion. The electrical conductivity also increases in Figure 4.47 more than in Figure 4.46 and more than in Figure 4.45 because electrical conductivity increases with an increase in the temperature (25°,37°,45° C). Figure 4.45 has low values of electrical conductivity, the low conductivity in this region indicates restricted water mobility, then the values of the electrical conductivity increases continuously with the increase in the temperature, increased temperature causes the increase in kinetic energy which causes increasing the collision between droplet and increasing movement of ions.

As shown in Table 4.9, the system: water / sucrose myristate M1695 / caprylic/capric triglyceride oil + propylene glycol has the highest value of N_S – BSO, where N_S the surfactant chain length and N_S – BSO the difference between surfactant chain and (oil chain length + alcohol chain length) as empirical Bansal, Shah, O'Connell (BSO), they concluded that the maximum amount of water which may be solubilized in such a microemulsion is reached when the oil chain length (carbon number), N_O, added to that of the cosurfactant, alcohol, chain length, N_A, is equal to the surfactant chain length, N_S, i.e. $N_S = N_O + N_A$ then when this value increases the water solubilization and electrical conductivity decreases, and the chain length compatibility decreases.

In this part, we study the effect of changing temperature on electrical conductivity at different water content (0,10,20,40,60,80) for R (+)-limonene, isopropyl myristate, caprylic/capric triglyceride oil + propylene glycol.

Values of the electrical conductivity σ (μS/cm) for the system: water / sucrose myristate M1695 / R (+)-limonene, isopropyl myristate, caprylic/capric triglyceride oil + propylene glycol at different temperatures and 0% water content presented in Table 4.22, the surfactant is sucrose myristate M1695 and different oils are used. In this Table, we compared between different types of oils to determine the electrical conductivity σ (μS/cm) at water content 0%.

Table 4.22: The electrical conductivity (σ) for the system: water / sucrose myristate M1695 / R (+)-limonene, isopropyl myristate, caprylic/capric triglyceride oil + propylene glycol at different temperatures and 0% water content, measured along the dilution line N60 presented in Figure 4.14, 4.15 and 4.16 .

σ (μS/cm)			
	Water content (wt.0%)		
System	**25°C**	**37°C**	**45°C**
LIM	8	16	57
CCT	0	0	0
IPM	131	202	465

In Figure 4.48, we will show the difference on the electrical conductivity (σ) for the system: water / sucrose myristate M1695 / R (+)-limonene, isopropyl myristate, caprylic/capric triglyceride oil + propylene glycol at different temperatures and water content 0%.

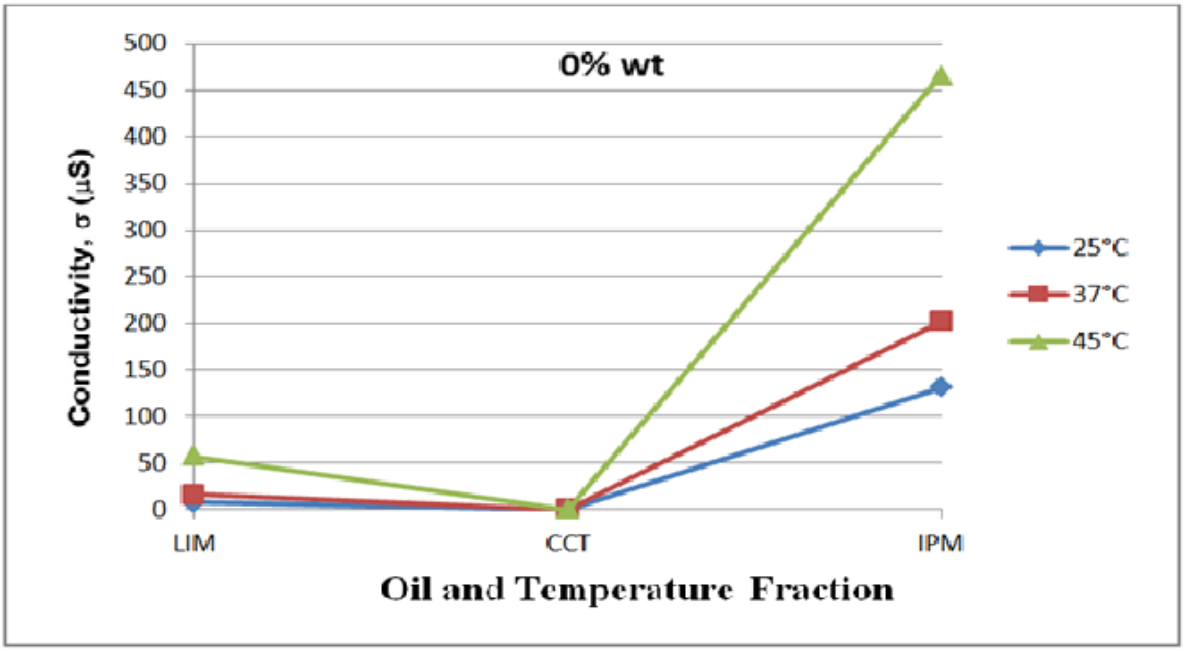

Figure 4.48: Variation of the electrical conductivity (σ) for the system: water / sucrose myristate M1695 / R (+)-limonene, isopropyl myristate, caprylic/capric triglyceride oil + propylene glycol, at water content 0%, as function of temperature along the dilution line N60 presented in Figures 4.14, 4.15 and 4.16.

Values of the electrical conductivity σ (μS/cm) for the system: water / sucrose myristate M1695 / R (+)-limonene, isopropyl myristate, caprylic/capric triglyceride oil + propylene glycol at different temperatures and 10% water content presented in Table 4.23, the surfactant is sucrose myristate M1695 and different oils are used. In this Table, we compared between different types of oils to determine the electrical conductivity σ (μS/cm) at water content 10%.

Table 4.23: The electrical conductivity (σ) for the system: water / sucrose myristate M1695 / R (+)-limonene, isopropyl myristate, caprylic/capric triglyceride oil + propylene glycol at different temperatures and 10% water content, measured along the dilution line N60 presented in Figures 4.14, 4.15 and 4.16.

σ (µS/cm)			
	Water content (wt.10%)		
System	25°C	37°C	45°C
LIM	78	180	130
CCT	11	19	47
IPM	247	311	626

In Figure 4.49, we will show the difference on the electrical conductivity (σ) for the system: water / sucrose myristate M1695 / R (+)-limonene, isopropyl myristate, caprylic/capric triglyceride oil + propylene glycol at different temperatures and water content 10%.

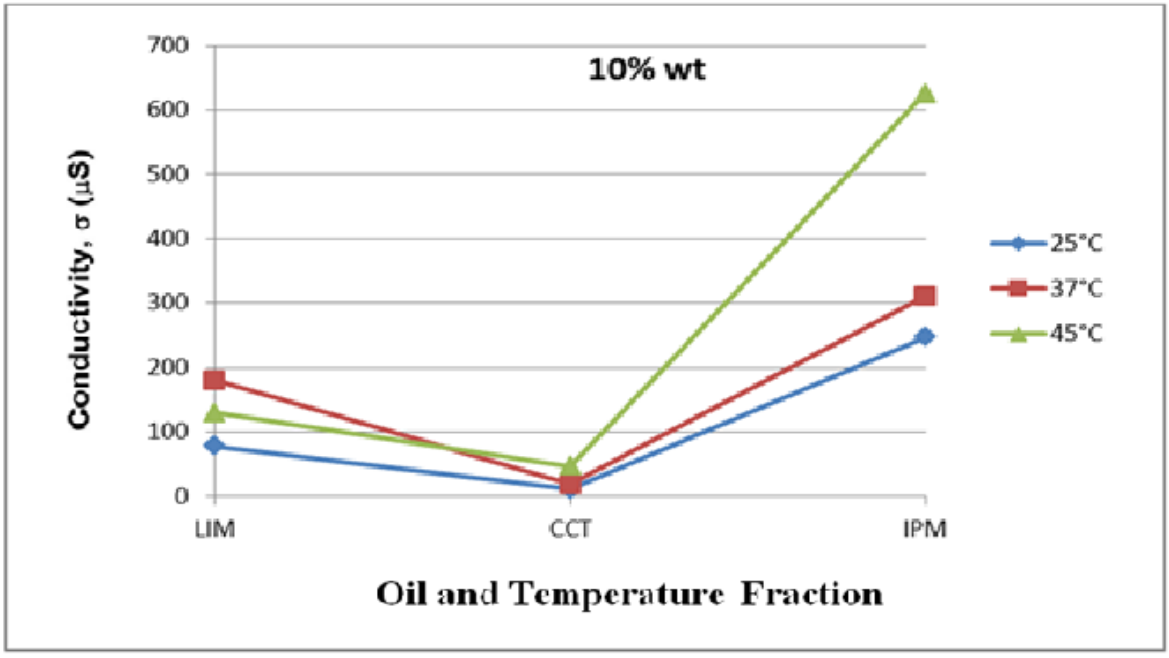

Figure 4.49: Variation of the electrical conductivity (σ) for the system: water / sucrose myristate M1695 / R (+)-limonene, isopropyl myristate, caprylic/capric triglyceride oil + propylene glycol at water content 10%, as function of temperature along the dilution line N60 presented in Figures 4.14, 4.15 and 4.16.

Values of the electrical conductivity σ (μS/cm) for the system: water / sucrose myristate M1695 / R (+)-limonene, isopropyl myristate, caprylic/capric triglyceride oil+ propylene glycol at different temperatures and 20% water content presented in Table 4.24, the surfactant is sucrose myristate M1695 and different oils are used. In this Table, we compared between different types of oils to determine the electrical conductivity σ (μS/cm) at water content 20%.

Table 4.24: The electrical conductivity (σ) for the system: water / sucrose myristate M1695 / R (+)-limonene, isopropyl myristate, caprylic/capric triglyceride oil + propylene glycol at different temperatures and 20% water content, measured along the dilution line N60 presented in Figures 4.14, 4.15 and 4.16.

σ (μS/cm)			
	Water content (wt.20%)		
System	**25°C**	**37°C**	**45°C**
LIM	121	258	326
CCT	64	82	182
IPM	311	365	786

In Figure 4.50, we will show the difference on the electrical conductivity (σ) for the system: water / sucrose myristate M1695 / R (+)-limonene, isopropyl myristate, caprylic/capric triglyceride oil + propylene glycol at different temperatures and water content 20%.

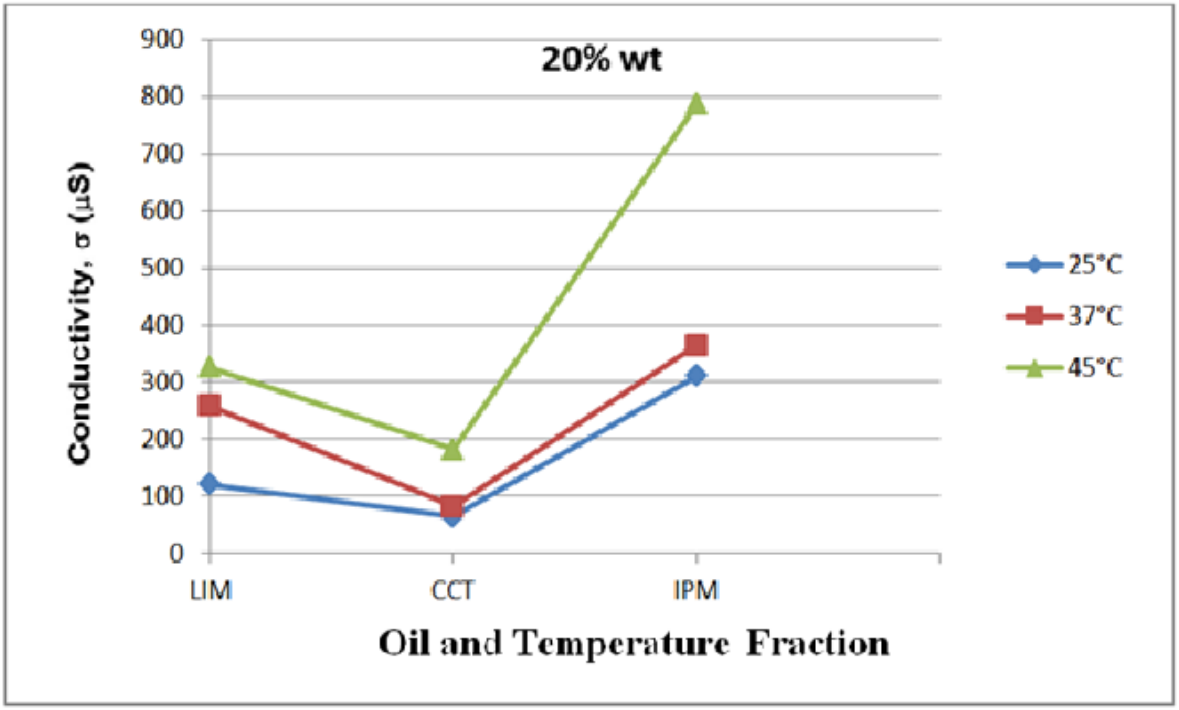

Figure 4.50**:** Variation of the electrical conductivity (σ) for the system: water / sucrose myristate M1695 / R (+)-limonene, isopropyl myristate, caprylic/capric triglyceride oil + propylene glycol, at water content 20%, as function of temperature along the dilution line N60 presented in Figures 4.14, 4.15 and 4.16.

Values of the electrical conductivity σ (μS/cm) for the system: water / sucrose myristate M1695 / R (+)-limonene, isopropyl myristate, caprylic/capric triglyceride oil+ propylene glycol at different temperatures and 40% water content presented in Table 4.25, the surfactant is sucrose myristate M1695 and different oils are used, In this Table, we compared between different types of oils to determine the electrical conductivity σ (μS/cm) at water content 40%.

Table 4.25**:** The electrical conductivity (σ) for the system: water / sucrose myristate M1695 / R (+)-limonene, isopropyl myristate, caprylic/capric triglyceride oil + propylene glycol at different temperatures and 40% water content, measured along the dilution line N60 presented in Figures 4.14, 4.15 and 4.16.

σ (µS/cm)			
	Water content (wt.40%)		
System	**25°C**	**37°C**	**45°C**
LIM	366	403	774
CCT	202	232	449
IPM	424	456	893

In Figure 4.51, we will show the difference on the electrical conductivity (σ) for the system: water / sucrose myristate M1695 / R (+)-limonene, isopropyl myristate, caprylic/capric triglyceride oil + propylene glycol at different temperatures and water content 40%.

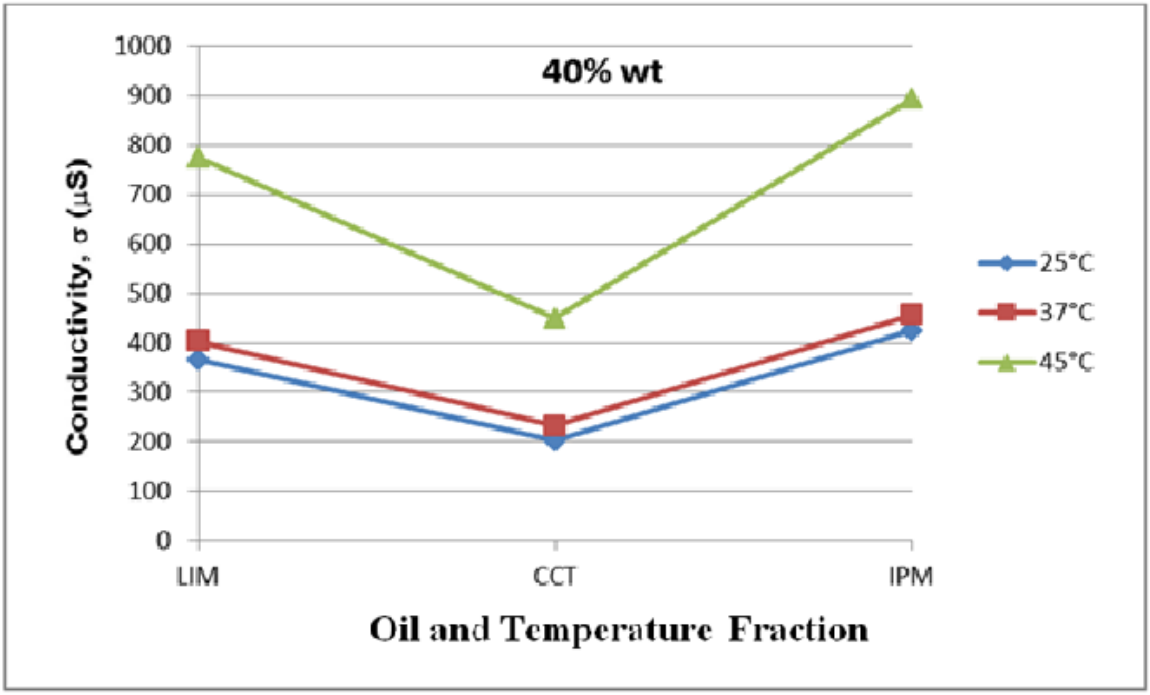

Figure 4.51: Variation of the electrical conductivity (σ) for the system: water / sucrose myristate M1695 / R (+)-limonene, isopropyl myristate, caprylic/capric triglyceride oil +

propylene glycol at water content 40%, as function of temperature along the dilution line N60 presented in Figures 4.14, 4.15 and 4.16.

Values of the electrical conductivity σ (μS/cm) for the system: water / sucrose myristate M1695 / R (+)-limonene, isopropyl myristate, caprylic/capric triglyceride oil + propylene glycol at different temperatures and 60% water content presented in Table 4.26, the surfactant is sucrose myristate M1695 and different oils are used. In this Table, we compared between different types of oils to determine the electrical conductivity σ (μS/cm) at water content 60%.

Table 4.26: The electrical conductivity (σ) for the system: water / sucrose myristate M1695 / R (+)-limonene, isopropyl myristate, caprylic/capric triglyceride oil + propylene glycol at different temperatures and 60% water content, measured along the dilution line N60 presented in Figures 4.14, 4.15 and 4.16.

σ (μS/cm)			
	Water content (wt.60%)		
System	**25°C**	**37°C**	**45°C**
LIM	453	489	945
CCT	142	189	375
IPM	429	448	896

In Figure 4.52, we will show the difference on the electrical conductivity (σ) for the system: water / sucrose myristate M1695 / R (+)-limonene, isopropyl myristate, caprylic/capric triglyceride oil + propylene glycol at different temperatures and water content 60%.

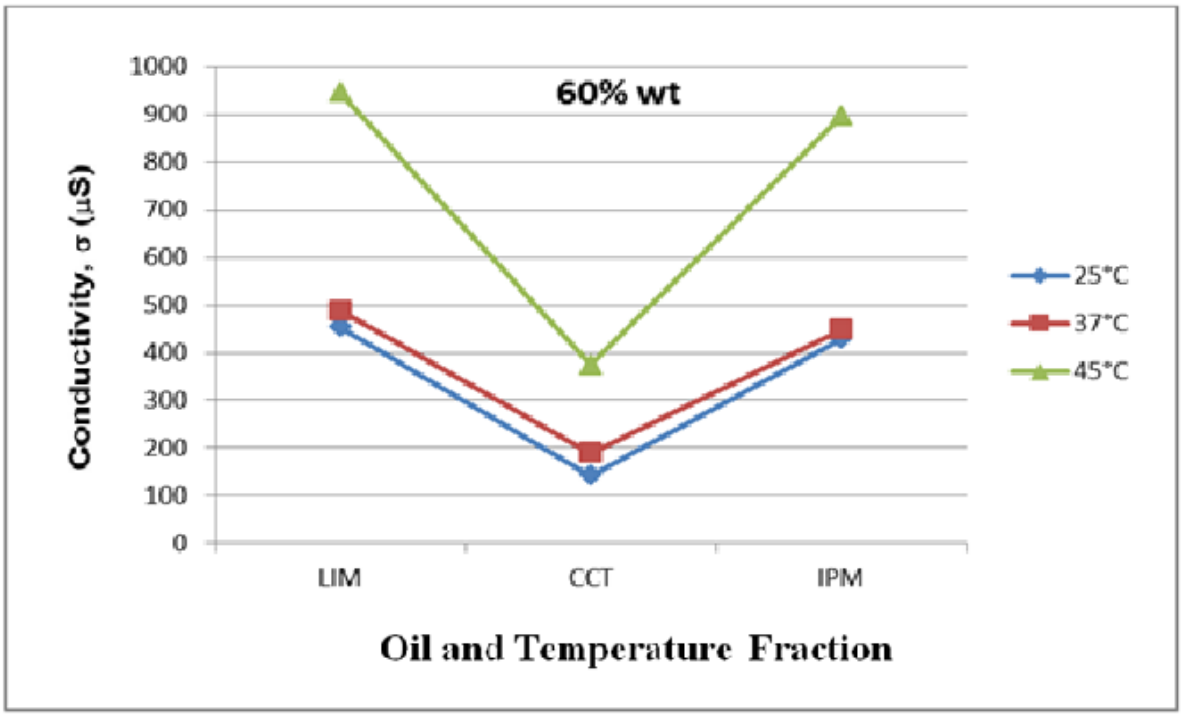

Figure 4.52**:** Variation of the electrical conductivity (σ) for the system: water / sucrose myristate M1695 / R (+)-limonene, isopropyl myristate, caprylic/capric triglyceride oil + propylene glycol, at water content 60%, as function of temperature along the dilution line N60 presented in Figures 4.14, 4.15 and 4.16.

Values of the electrical conductivity σ (μS/cm) for the system: water / sucrose myristate M1695 / R (+)-limonene, isopropyl myristate, caprylic/capric triglyceride oil + propylene glycol at different temperatures and 80% water content presented in Table 4.27, the surfactant is sucrose myristate M1695 and different oils are used. In this Table, we compared between different types of oils to determine the electrical conductivity σ (μS/cm) at water content 80%.

Table 4.27**:** The electrical conductivity (σ) for the system: water / sucrose myristate M1695 / R (+)-limonene, isopropyl myristate, caprylic/capric triglyceride oil + propylene glycol at different temperatures and 80% water content, measured along the dilution line N60 presented in Figures 4.14, 4.15 and 4.16.

σ (μS/cm)			
	Water content (wt.80%)		
System	**25°C**	**37°C**	**45°C**
LIM	287	281	565
CCT	66	139	275
IPM	343	363	706

In Figure 4.53, we will show the difference on the electrical conductivity (σ) for the system: water / sucrose myristate M1695 / R (+)-limonene, isopropyl myristate, caprylic/capric triglyceride oil + propylene glycol at different temperatures and water content 80%.

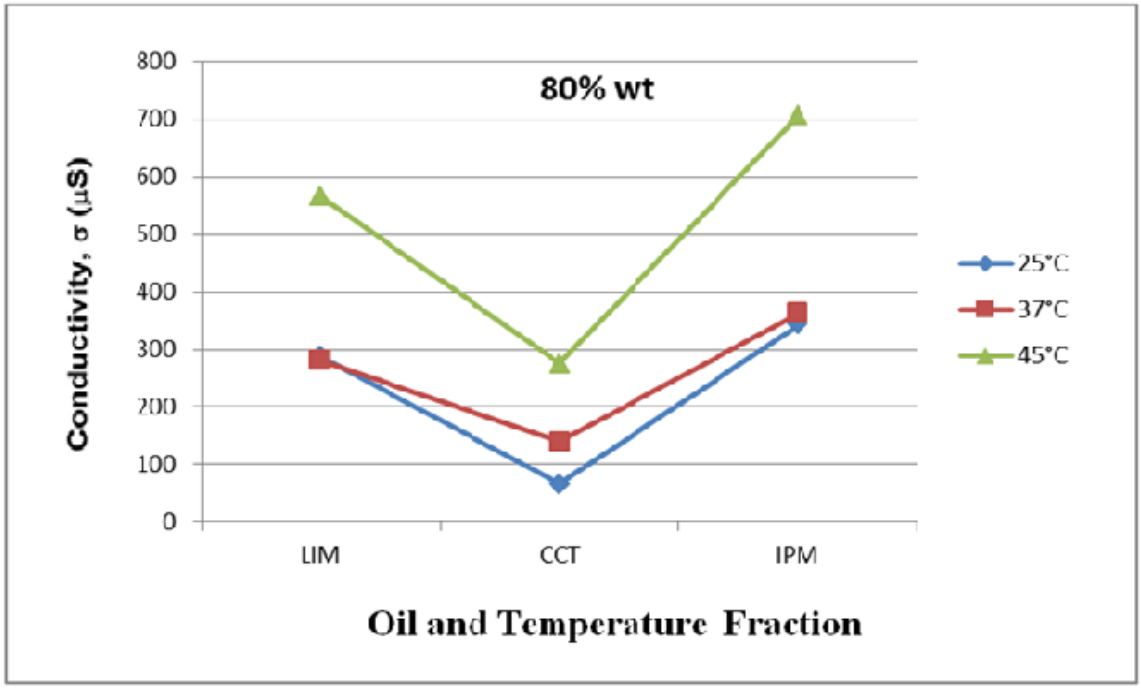

Figure 4.53**:** Variation of the electrical conductivity (σ) for the system: water / sucrose myristate M1695 / R (+)-limonene, isopropyl myristate, caprylic/capric triglyceride oil + propylene glycol, at water content 80%, as function of temperature along the dilution line N60 presented in Figures 4.14, 4.15 and 4.16.

About electrical conductivity

The effect of water content:

The previous result shows that when water content increases the electrical conductivity increases exponentially. The increase in the electrical conductivity as function of water content is due to the increase in the fraction of sodium chloride ions that are not enclosed in the core of the microemulsions. The high values of electrical conductivity at high-water volume fractions are explained by the fact that the sodium chloride ions are present in the external phase, which is the water and these results permit to distinguish between water in oil and oil in water microemulsions.

The effect of temperature:

The electrical conductivities increases with the increase in temperature at a given dispersed phase volume fraction, different percolation thresholds are observed which varies depending on the oil used in the microemulsion formulation, [Fanun. M, 2008].

The previous result shows that electrical conductivity increases when temperature increases, this is due to the increase in kinetic energy which causes increase the collision between droplet and increase movement of ions.

By raising the temperature, the collision probability between the droplets increases and the opening and reforming of droplets will increase the mobility of water and the electrical conductivity will again rises with temperature. In addition, the possibility of percolation becomes larger and the formation of water channels will also increase the electrical conductivity of the system.

The relatively high values of electrical conductivity of the microemulsions studied can be explained by the chemical structure of the oils and its capability to penetrate between the chains of surfactants to the interface. So that in this section, we compared between different chemical structures of oils used in this research, and the results can be explained as the following: increasing the molecular volume of the oils decreases the capability of the microemulsions to incorporate water, decreases the mobility of the water in the droplets and hences the electrical conductivity decreases.

For R(+)-limonene oil, the high viscosity microemulsion are observed for water content lower than 4% because that R (+)-limonene oil have lower electrical conductivity values, so that R (+)-limonene oil tends to be form gel microemulsion, so the viscous microemulsion has low electrical conductivity because the structure is more network form between water and the surfactant, the movement of water between the droplets is low.

For isopropyl myristate oil has ketones group that is soluble in water, carbonyl compounds, they can hydrogen-bond to water through the carbonyl oxygen, but ketones decrease solubility in water when the increase in molecular volume, isopropyl myristate make in microemulsion as penetration enhancer its causes to increase electrical conductivity of the system isopropyl myristate.

For caprylic/capric triglyceride oil they have the lowest electrical conductivity value because they have the highest molecular volume oil (530), more than isopropyl myristate (317), more than R (+)-limonene (181). The high value of caprylic/capric triglyceride molecular volume decreases the capability of the microemulsions to incorporate water, decreases the mobility of the water in the droplets and hences the electrical conductivity decreases as we shown in previous result.
This study reveals that the electrical conductivities increase with the increase in water volume fraction. Static percolation was observed in these systems. The diffusion data suggests that the variations in the properties of the systems, with the increase in the water volume fraction, are correlated to structural transition from water-in-oil to bicontinues to oil-in-water microemulsions, [Fanun.M, 2009]. Conductivity increases as temperature increases in steadily fashion for the systems.

As shown in the result presented about electrical conductivity, they have the highest value of $N_S - BSO$ where N_S the surfactant chain length and $N_S - BSO$ the difference between surfactant chain and (oil chain length + alcohol chain length) as empirical Bansal, Shah, O'Connell (BSO), they concluded that the maximum amount of water which may be solubilized in such a microemulsion is reached when the oil chain length (carbon number), N_O, added to that of the cosurfactant ,alcohol, chain length, N_A, is equal to the surfactant chain length, N_S, i.e. $N_S = N_O + N_A$ then when this value increases the water solublization and electrical conductivity decrease, and the chain length compatibility decreases.

Increasing the water volume fraction induces increases in the electrical conductivity exponentially in all systems. These changes have been attributed to the occurrence of a percolation transition, In this percolation model, the conductivity remains low up to a certain volume fraction of water. It must be emphasized that these conducting water-in-oil droplets, below volume fraction, are isolated from each other embedded in non conducting continuum oil phase and hence contribute very little to the conductance.

However, as the volume fraction of water reaches the percolation thresholds (Tables 4.16,4.17,4.18) some of these conductive droplets begin to contact each other and form clusters which are sufficiently close to each other.

The number of such clusters increases very rapidly above the percolation threshold, giving rise to the observed changes of properties, in particular to the increase of electrical conductivity. The water volume fraction, above water volume, has been attributed to the transfer of counter ions from one droplet to another through water channels opening between droplets during sticky collisions through transient merging of droplets.

The existence and position of this threshold depend on the interactions between droplets which depend on the components present in the microemulsion and that controls the duration of the collision, and the degree of the interface overlapping, hences the probability of merging. Building up of conductivity needs attractive interactions decreases when the strength of these inter droplet interactions increases as predicted by recent theoretical calculations.

Fairly slow decrease in the electrical conductivity could be associated with the fact that the system has been transformed into a bicontinuous phase, and the interfacial area remains almost unchanged and the rate of transport of ions decreases slowly. A sharp decrease is observed in the electrical conductivity indicating the transfer from bicontinuous to oil-in-water structure.

4.3 Drug Solubilization

Sucrose esters surfactants have unique properties (biodegradable, nontoxic and capable of forming temperature-insensitive microemulsions), which make them suitable for a variety of food-based and pharmaceutical application. Sucrose contains in its structure eight-hydroxyl groups that can be esterified. If the esterification degree increases on the hydroxyl groups by fatty acids, the hydrophobicity will increase. Partial esterification will produce sucrose ester with amphiphilic properties. Mono, di and tri ester of sucrose usually used as emulsifier in foods, cosmetic, detergent, etc, [Garti. N, Clement. V, Laser. M, Aserin. A and Fanun. M, 1999].

The main requirements of the pharmaceutical market entering drug delivery formulations are ease of preparation, physical stability, excipients that are well tolerated and accepted by regulatory authorities, and the availability of large-scale production that is sanctioned by regulatory authorities, [Muller, R. H. and Keck, C. M, 2004].

Microemulsions characteristic enable them to use as drug carriers for topical, oral, parenteral and other administration routes due to the small size of the dispersed droplets (Less than 100 nm) and their high specific surface, high percentages of surfactants are required. Skin damages then could be induced, [Thevenin. M.A, Grossiord. J.L, and Poelman. M.C,1996]. The characterization of microemulsions used as drug delivery systems is necessary to determine the locus of the drug in the loaded microemulsion.

The adsorption of drugs using microemulsion systems is influenced by the particle size, the partition coefficient of the drug between the two immiscible phases, the presence of the drug in the interface, the site or path of the absorption of the microemulsion components that can act as absorption enhancers, and the drug solubility in the microemulsion components. Microemulsions are, [Bagwe.R.P and et al, 2001, Lawrence. M.J, and Rees. G.D, 2000, Terjarla. S, 1999], effective vehicles for the solubilization of certain drugs because they provide all of the possible requirements of a liquid system including thermodynamic stability, ease of preparation, low viscosity, high surface area, and very small droplet size.

Compounds which are able to form nontoxic microemulsions and solubilize high quantity of the drug are the most suitable for application in pharmaceutical formulations. Solubilization and deposition of the drug in the microemulsion depend on the microstructure of these microemulsions.

Over the years, a variety of solubilization techniques have been studied to improve the solubility, dissolution rate and the subsequent bioavailability of drugs which induces:

I. Modifying the drug properties at the molecular level by using salt forms of drugs.

II. Using colloidal drug delivery systems.

III. By modifying the properties of drugs at the particulate level.

In this section, we investigated the solubilization capacity of cefuroxime axetil in different microemulsion systems: water / sucrose myristate M1695 / oil + cosurfactant.

4.3.1 Cefuroxime axetil solubilization capacity in pure substances

In this section, we will study the solubilization capacity (SC) of cefuroxime axetil at 25°C, in different samples, we will try to benefit from the unique properties of microemulsions that include the high mutual solubilization of water and oil to solubilize active pharmaceutical ingredients cefuroxime axetil by dissolving in microemulsion that are normally poor soluble.

Values of the solubilization capacity (SC) of cefuroxime axetil at 25°C in different samples are presented in Table 4.28 and Figure 4.54, 4.55, 4.56, and 4.57 respectively.

Table 4.28: The solubilization capacity (SC) of cefuroxime axetil (mg drug / g microemulsion) as function of compounds content at 25°C.

System Name	(SC) of the Cefuroxime Axetil (mg drug / g microemulsion)
LIM	**15**
LIM+ETOH	**10**
LIM+PG	**10**
LIM+GLY	**5**
CCT	**18**
CCT+ETOH	**10**
CCT+PG	**5**
CCT+GLY	**4.9**
IPM	**10**
IPM+ETOH	**5.5**
IPM+PG	**10**
IPM+GLY	**5**
ETOH	**20**
PG	**20**
GLY	**20**

In the Figure 4.54, we will show the solubilization capacity (SC) of cefuroxime axetil (mg drug / g microemulsion) as function of compounds content at 25°C in the system: water / sucrose myristate M1695 / oil, and pure cosurfactant.

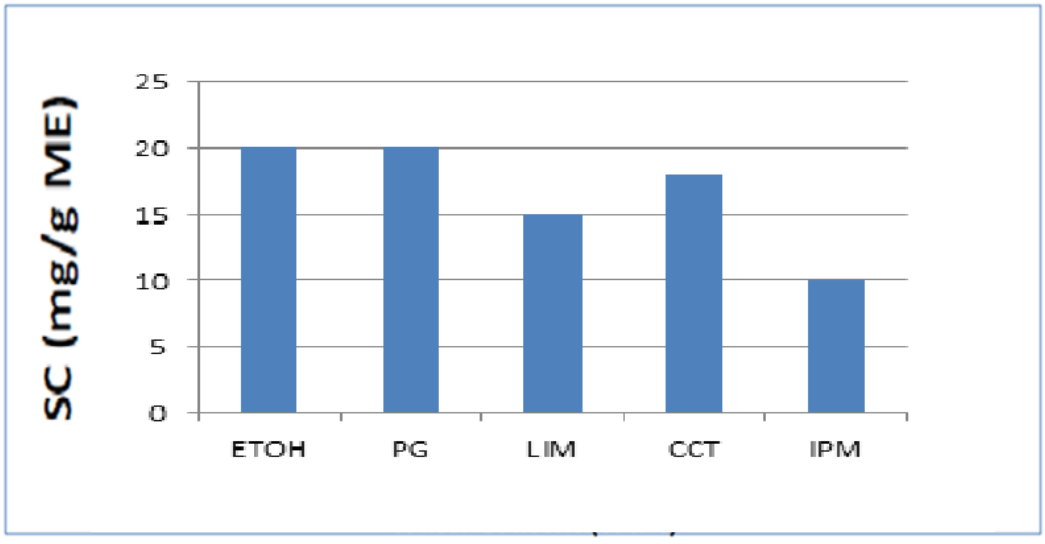

In the Figure 4.55, we will show the solubilization capacity (SC) of cefuroxime axetil (mg drug / g microemulsion) as function of compounds content at 25°C in the system: water / sucrose myristate M1695 / oil + ethanol.

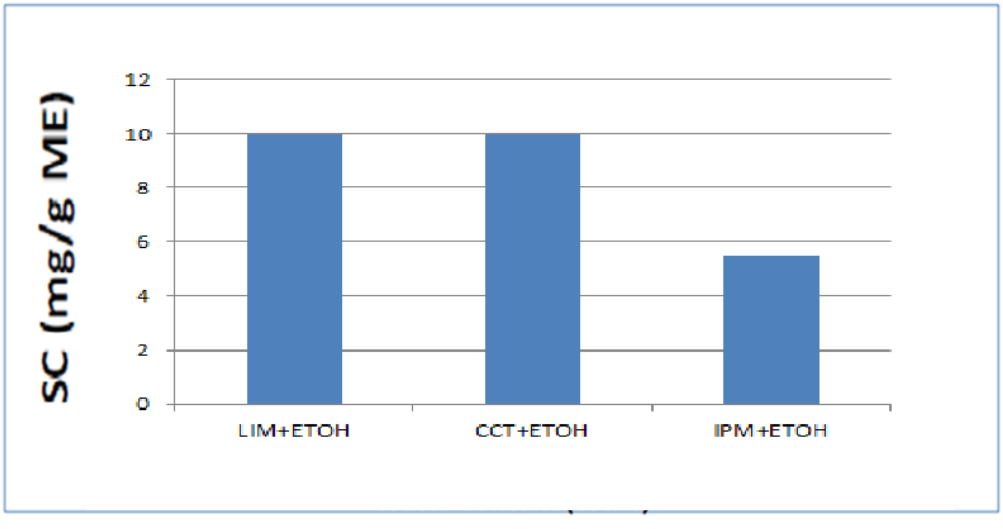

Figure 4.55: The solubilization capacity (SC) of cefuroxime axetil (mg drug / g microemulsion) as function of compounds content at 25°C.

In Figure 4.56**,** we will show the solubilization capacity (SC) of cefuroxime axetil (mg drug / g microemulsion) as function of compounds content at 25°C in the system: water / sucrose myristate M1695 / oil + propylene glycol.

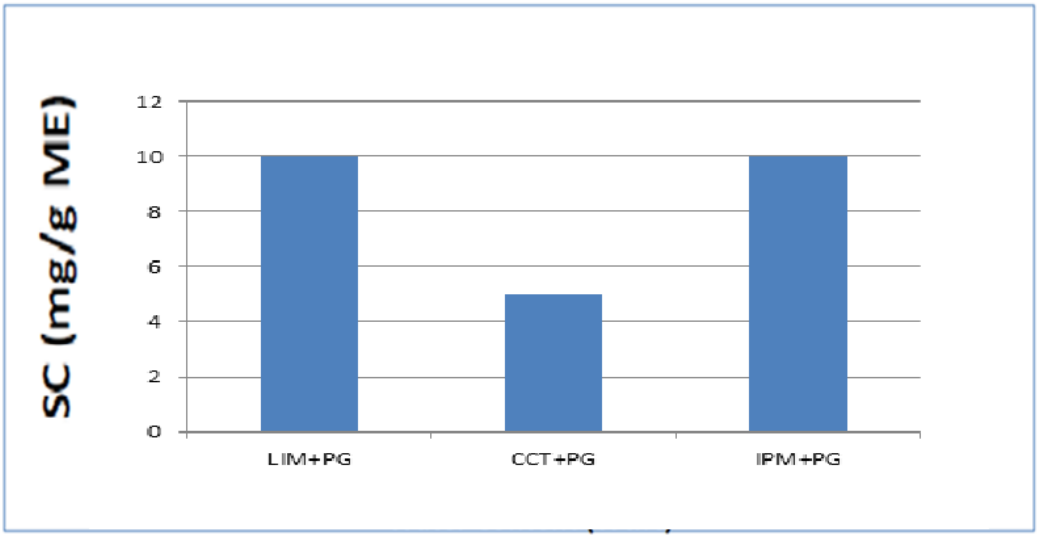

Figure 4.56: The solubilization capacity (SC) of cefuroxime axetil (mg drug / g microemulsion) as function of compounds content at 25°C.

In Figure 4.57**,** we will show the solubilization capacity (SC) of cefuroxime axetil (mg drug / g microemulsion) as function of compounds content at 25°C in the system: water / sucrose myristate M1695 / oil + glycerol .

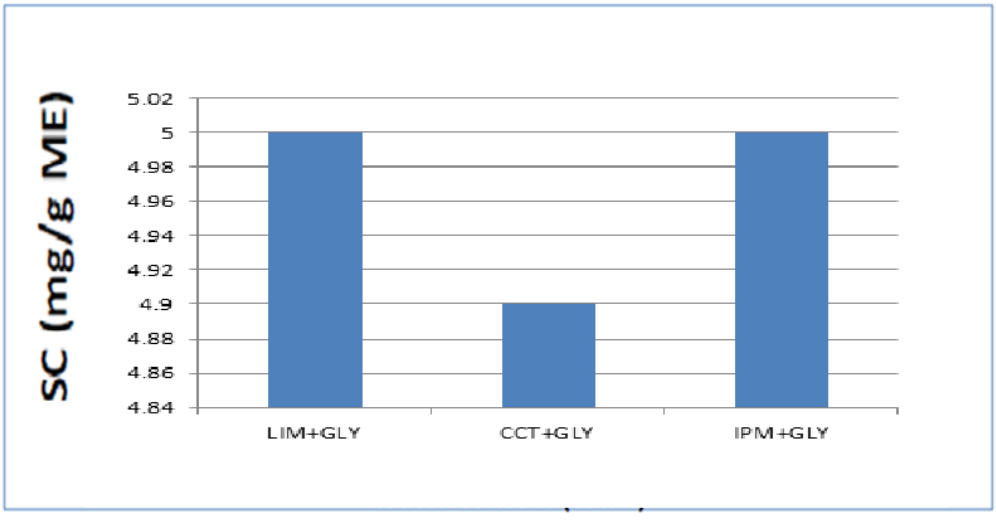

Figure 4.57: The solubilization capacity (SC) of cefuroxime axetil (mg drug / g microemulsion) as function of compounds content at 25°C.

The solubilization capacity of cefuroxime axetil in microemulsion systems was higher than at any single component that formed the microemulsion.

4.3.2 Solubilization capacity in water / sucrose myristate M1695 / peppermint + cosurfactants

4.3.2.a Water / sucrose myristate M1695 / peppermint + ethanol

The solubilization capacity (SC) of cefuroxime axetil at 25°C as function of aqueous phase content along the dilution line N60 in the system: water / sucrose myristate M1695 / peppermint + ethanol is presented in Table 4.29 and Figure 4.7.

Table 4.29**:** The solubilization capacity (mg drug / g microemulsion) for the system: water / sucrose myristate M1695 / peppermint + ethanol at different water contents, along the dilution line N60 presented in Figure 4.7.

	SC(mg drug / g microemulsion)
Water content (Wt.%)	**25°C**
0	**12**
10	**12**
20	**12**
30	**12**
40	**12**
50	**12**

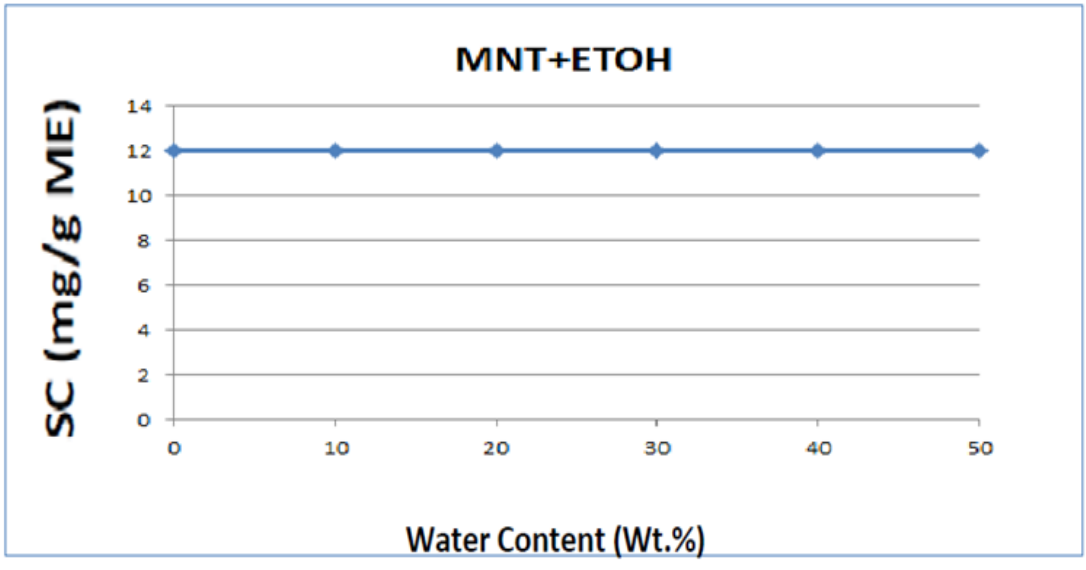

Figure 4.58: The solubilization capacity (SC) of cefuroxime axetil (mg drug / g microemulsion) as function of water content, in the system: water / sucrose myristate M1695 / peppermint + ethanol, along the dilution line N60 in the phase diagrams presented in Figure 4.7 at 25°C.

The solubilization capacity stable at all percentage of water content.

4.3.2.b Water / sucrose myristate M1695 / peppermint + propylene glycol

The solubilization capacity (SC) of cefuroxime axetil at 25°C as function of aqueous phase content along the dilution line N60 is presented in Table 4.30 and Figure 4.13**.** Two different regions can be identified the phase diagrams is presented in Figure 4.59.

Table 4.30**:** The solubilization capacity (mg drug / g microemulsion) for the system: water / sucrose myristate M1695 / peppermint + propylene glycol at different water contents, along the dilution line N60 presented in Figure 4.13.

	SC(mg drug / g microemulsion)
Water content (Wt.%)	**25°C**
0	**12**
10	**12**
20	**9**
30	**9**

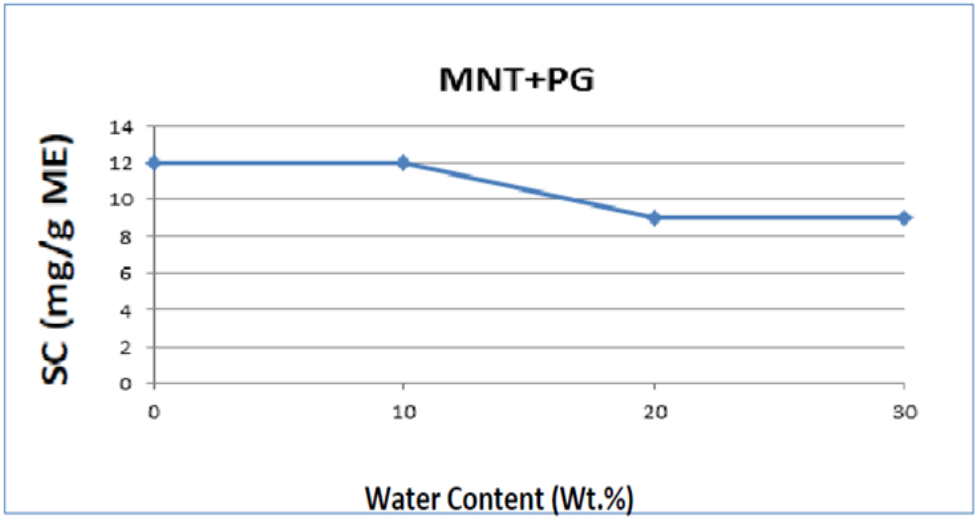

Figure 4.59: The solubilization capacity (SC) of cefuroxime axetil (mg drug / g microemulsion) as function of water content in the system: water / sucrose myristate M1695 / peppermint + propylene glycol, along the dilution line N60, in the phase diagrams presented in Figure 4.13 at 25°C.

In the first region, The solubilization capacity starts staple. Its 12mg/g microemulsion at water content equal 0 wt.% to water content equal 10 wt.%. In the second region, the solubilization capacity decreases dramatically from 12mg/g at water content equal 10 wt.% to about 9mg/g microemulsion at water content equals 20 wt.%. In the third region, the solubilization capacity returns stable 9mg/g microemulsion at water content equals 20 wt.% to water content equals 30 wt.%.

4.3.2.d Water / sucrose myristate M1695 / peppermint + glycerol

The solubilization capacity (SC) of cefuroxime axetil at 25°C as function of aqueous phase content along the dilution line N60 is presented in Table 4.31 and Figure 4.14**.** Two different regions can be identified the phase diagrams is presented in Figure 4.60.

Table 4.31: The solubilization capacity (mg drug / g microemulsion) for the system: water / sucrose myristate M1695 / peppermint + glycerol at different water contents, along the dilution line N60 presented in Figure 4.19.

	SC(mg drug / g microemulsion)
Water content (Wt.%)	**25°C**
0	**15**
10	**15**
20	**15**
30	**15**
40	**12**

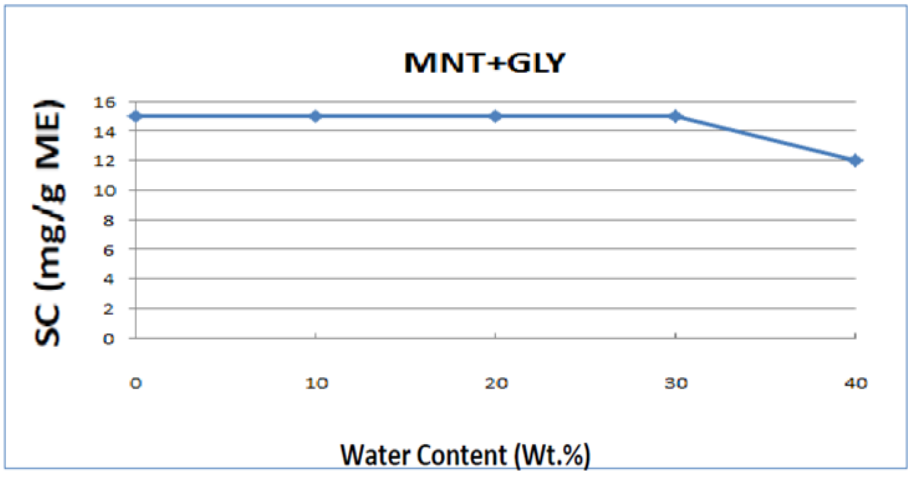

Figure 4.60: The solubilization capacity (SC) of cefuroxime axetil (mg drug / g microemulsion) as function of water content in the system: water / sucrose myristate M1695 / peppermint + glycerol, along the dilution line N60 in the phase diagrams presented in Figure 4.19 at 25°C.

In the first region, the solubilization capacity starts staple. It is 15mg/g microemulsion at water content equal 0 wt.% to water content equal 30 wt.%. In the second region, the solubilization capacity decreases dramatically from 15mg/g at water content equal 30 wt.% to about 12mg/g microemulsion at water content equals 400 wt.%.

As shown in Tables 4.8, 4.9, 4.10 and 4,11, the system: water / sucrose myristate M1695 / peppermint + glycerol has the lowest value of N_S – BSO where N_S the surfactant chain length and N_S – BSO the difference between surfactant chain and (oil chain length + alcohol chain length) as empirical Bansal, Shah, O'Connell (BSO), they concluded that the maximum amount of water which may be solubilized in such a microemulsion is reached when the oil chain length (carbon number), N_O, added to that of the cosurfactant (alcohol) chain length, N_A, is equal to the surfactant chain length, N_S, i.e. $N_S = N_O + N_A$ then when this value increases, the water solubilization decrease, and chain length compatibility decreases. From the result printed in Tables 4.29, 4.30, 4.31 and Figures 4.63, 4.64, 4.65, the system: water / sucrose myristate M1695 / peppermint + glycerol has the highest value of cefuroxime axetil solubilization because they have the lowest value of N_S – BSO, so when the N_S – BSO decreases, the solubilization capacity increases and chain length compatibility increases.

4.3.3 Cefuroxime axetil solubilization capacity in water / sucrose myristate M1695 / R (+)-limonene oil + cosurfactants

4.3.3.a Water / sucrose myristate M1695 / R (+)-limonene + ethanol

The solubilization capacity (SC) of cefuroxime axetil at 25°C as function of aqueous phase content along the dilution line N60 is presented in Table 4.32 and Figure 4.8**.** Two different regions can be identified in the phase diagrams presented in Figure 4.61.

Table 4.32: The solubilization capacity (mg drug / g microemulsion) for the system: water / sucrose myristate M1695 / R (+)-limonene + ethanol at different water contents, along the dilution line N60 presented in Figure 4.8.

	SC(mg drug / g microemulsion)
Water content (Wt.%)	**25°C**
0	**18**
10	**15**
20	**15**
30	**15**
40	**12**
50	**6**
60	**6**
70	**6**
80	**6**
90	**6**

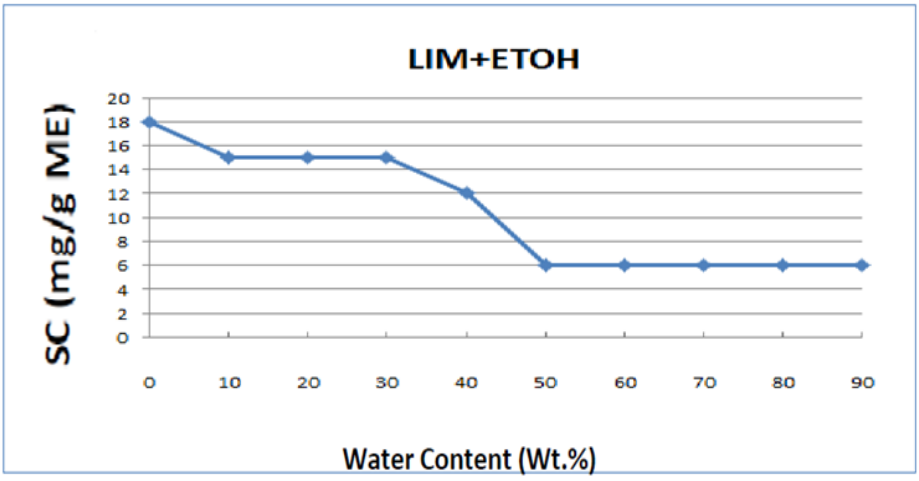

Figure 4.61: The solubilization capacity (SC) of cefuroxime axetil (mg drug / g microemulsion) as function of water content in the system: water / sucrose myristate M1695 / R (+)-limonene + ethanol, along the dilution line N60 in the phase diagrams presented in Figure 4.8 at 25°C.

The solubilization capacity decreases from 18mg/g microemulsion at water content equal 0 wt.% to about 15mg/g at water content equal 10 wt.% in the first region. In the second region, the solubilization capacity stable 15mg/g microemulsion at water content equals 10 wt.%, to water content equals 30 wt.%. After that, the solubilization capacity decreases from 15mg/g microemulsion at water content equal 30 wt.% to about 6 mg/g at water content equal 50 wt.% and this is in the third region. In the fourth region, the solubilization capacity is stable 6mg/g microemulsion at water content equals 50 wt.%, to water content equals 90 wt.%.

4.3.3.b Water / sucrose myristate M1695 / R (+)-limonene + propylene glycol

The solubilization capacity (SC) of cefuroxime axetil at 25°C as function of aqueous phase content along the dilution line N60 is presented in Table 4.33 and Figure 4.14. Two different regions can be identified in the phase diagrams presented in Figure 4.62.

Table 4.33: The solubilization capacity (mg drug/ g microemulsion) for the system: water / sucrose myristate M1695 / R (+)-limonene + propylene glycol at different water contents, along the dilution line N60 presented in Figure 4.14.

	SC(mg drug/ g microemulsion)
Water content (Wt.%)	**25°C**
0	**15**
10	**18**
20	**18**
30	**18**
40	**18**
50	**15**
60	**15**
70	**6**
80	**6**
90	**6**

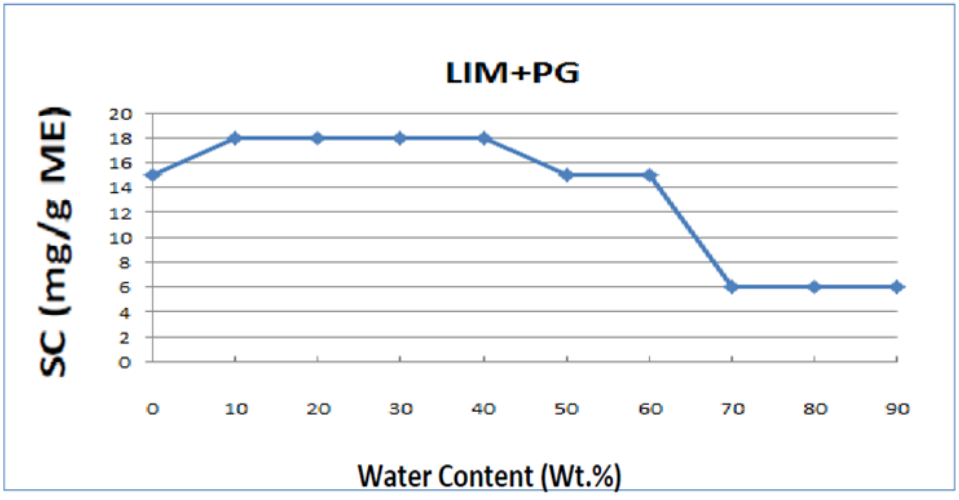

Figure 4.62: The solubilization capacity (SC) of cefuroxime axetil (mg drug / g microemulsion) as function of water content in the system: water / sucrose myristate M1695 / R (+)-limonene + propylene glycol, along the dilution line N60 in the phase diagrams presented in Figure 4.14 at 25°C.

The solubilization capacity increases from 15mg/g microemulsion at water content equal 0 wt.% to about 18mg/g at water content equal 10 wt.% in the first region. In the second region, the solubilization capacity is stable 18mg/g microemulsion at water content equals 10 wt.%, to water content equals 40 wt.%. After that, the solubilization capacity decreases from 18mg/g microemulsion at water content equal 40 wt.% to about 15 mg/g at water content equal 50 wt.% and this is in the third region. In the fourth region, the solubilization capacity is stable 15mg/g microemulsion at water content equals 50 wt.%, to water content equals 60 wt.% . In the fifth region, the solubilization capacity decreases from 15mg/g microemulsion at water content equal 60 wt.% to about 6 mg/g at water content equal 70 wt.%. After that, the solubilization capacity is stable 6mg/g microemulsion at water content equals60 wt.% to water content equals 90 wt.% and this is in the sixth region.

4.3.3.c Water / sucrose myristate M1695 / R (+)-limonene + glycerol

The solubilization capacity (SC) of cefuroxime axetil at 25°C as function of aqueous phase content along the dilution line N60 is presented in Table 4.34 and Figure 4.20**.** Two different regions can be identified in the phase diagrams presented in Figure 4.63.

Table 4.34: The solubilization capacity (mg drug / g microemulsion) for the system: water / sucrose myristate M1695 / R (+)-limonene + glycerol at different water contents, along the dilution line N60 presented in Figure 4.20.

	SC(mg drug / g microemulsion)
Water content (Wt.%)	**25°C**
0	**9**
10	**12**
20	**12**
30	**12**
40	**12**
50	**12**
60	**12**
70	**12**
80	**12**
90	**12**

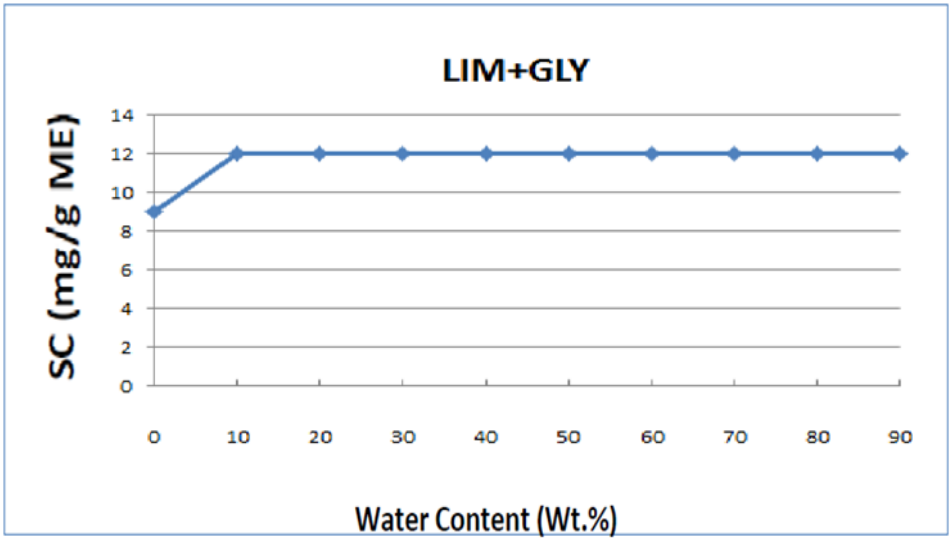

Figure 4.63: The solubilization capacity (SC) of cefuroxime axetil (mg drug / g microemulsion) as function of water content in the system: water / sucrose myristate M1695 / R (+)-limonene + glycerol, along the dilution line N60 in the phase diagrams presented in Figure 4.20 at 25°C.

The solubilization capacity increases from 9mg/g microemulsion at water content equal 0 wt.% to about 12mg/g at water content equal 10 wt.% in the first region. In the second region, the solubilization capacity is stable 12mg/g microemulsion at water content equals 10 wt.%, to water content equals 90 wt.%.

As shown in the result presented in Tables 4.32 ,4.33 ,4.34 and Figures 4.61, 4.62 and 4.63, the system: water / sucrose myristate M1695/ R (+)-limonene + glycerol, has the lowest solubilization capacity of cefuroxime axetil because glycerol has high values of molecular volume, this gives low viscous, low motion and high homogenized microemulsion, this causes also a decrease in solubilization capacity of cefuroxime axetil.

4.3.4 Cefuroxime axetil solubilization capacity in water / sucrose myristate M1695 / caprylic/capric triglyceride + cosurfactant

4.3.4.a Water / sucrose myristate M1695 / caprylic/capric triglyceride + ethanol

The solubilization capacity (SC) of cefuroxime axetil at 25°C as function of aqueous phase content along the dilution line N60 is presented in Table 4.35 and Figure 4.9**.** Two different regions can be identified in the phase diagrams presented in Figure 4.64.

Table 4.35: The solubilization capacity (mg drug / g microemulsion) for the system: water / sucrose myristate M1695/ caprylic/capric triglyceride + ethanol at different water contents, along the dilution line N60 presented in Figure 4.9.

	SC(mg drug / g microemulsion)
Water content (Wt.%)	**25°C**
0	18
10	18
20	21
30	18
40	18
50	18
60	18
70	21
80	21
90	18

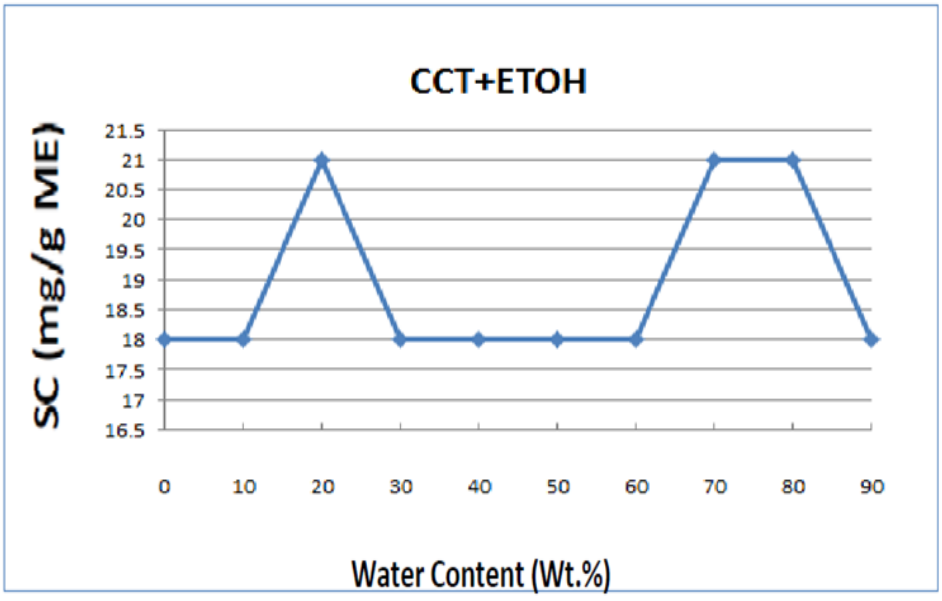

Figure 4.64: The solubilization capacity (SC) of cefuroxime axetil (mg drug / g microemulsion) as function of water content in the system: water / sucrose myristate M1695/ caprylic/capric triglyceride + ethanol, along the dilution line N60 in the phase diagrams presented in Figure 4.69 at 25°C.

In the first region, the solubilization capacity starts stable 18mg/g microemulsion at water content equals 0 wt.%, to water content equals 10 wt.%. After that, the solubilization capacity increases from 18mg/g microemulsion at water content equals 10 wt.% to about 21mg/g at water content equals 20 wt.% in the second region. In the third region, the solubilization capacity decreases from 21mg/g microemulsion at water content equals 20 wt.% to about 18 mg/g at water content equals 30 wt.%. After that, the solubilization capacity returns stable 18mg/g microemulsion at water content equals 30 wt.% to water content equals 60wt.% in the fourth region. After that, the solubilization capacity increases from 18mg/g microemulsion at water content equals 60 wt.% to about 21mg/g at water content equals 70 wt.% and in the fifth region. In the sixth, the solubilization capacity returns stable 21mg/g microemulsion at water content equals 70 wt.%, to water content equals 80 wt.%. After that, the solubilization

capacity decreases from 21mg/g microemulsion at water content equals 80 wt.% to about 18 mg/g at water content equals 90 wt.% in the seventh region.

4.3.4.b Water / sucrose myristate M1695 / caprylic/capric triglyceride + propylene glycol

The solubilization capacity (SC) of cefuroxime axetil at 25°C as function of aqueous phase content along the dilution line N60 presented in Table 4.36 and Figure 4.15**.** Two different regions can be identified in the phase diagrams presented in Figure 4.65.

Table 4.36: The solubilization capacity (mg drug / g microemulsion) for the system: water / sucrose myristate M1695/ caprylic/capric triglyceride + propylene glycol at different water contents, along the dilution line N60 presented in Figure 4.15.

	SC(mg drug / g microemulsion)
Water content (Wt.%)	25°C
0	12
10	12
20	12
30	15
40	12
50	12
60	15
70	9
80	9
90	9

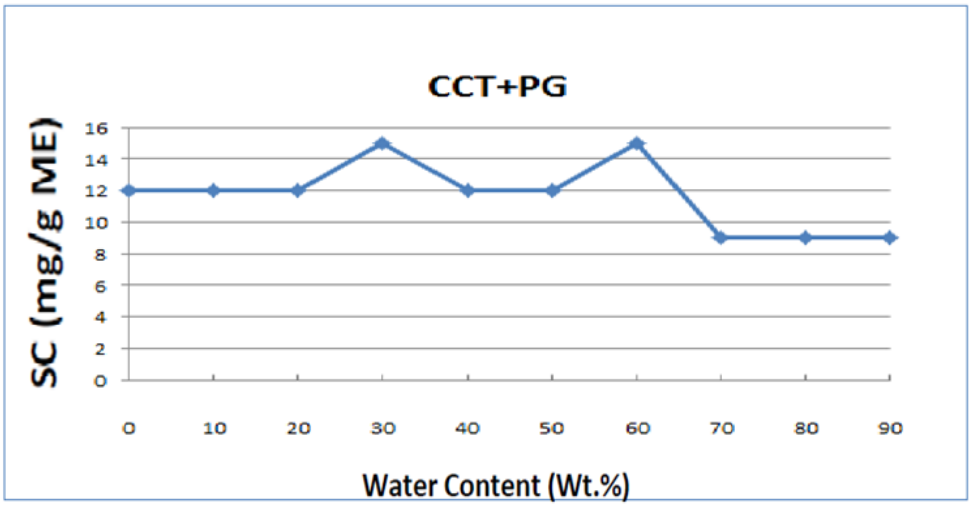

Figure 4.65: The solubilization capacity (SC) of cefuroxime axetil (mg drug / g microemulsion) as function of water content in the system: water / sucrose myristate M1695/ caprylic/capric triglyceride + propylene glycol, along the dilution line N60 in the phase diagrams presented in Figure 4.15 at 25°C.

In the first region, the solubilization capacity starts stable 12mg/g microemulsion at water content equals 0 wt.%, to water content equals 20 wt.%. After that, the solubilization capacity increases from 12mg/g microemulsion at water content equals 20 wt.% to about 15mg/g at water content equals 30 wt.% in the second region. In the third region, the solubilization capacity decreases from 15mg/g microemulsion at water content equals 30 wt.% to about 12 mg/g at water content equals 40 wt.%. After that, the solubilization capacity returns stable 12mg/g microemulsion at water content equals 40 wt.% to water content equals 50wt.% in the fourth region. After that, the solubilization capacity increases from 12mg/g microemulsion at water content equals 50 wt.% to about 15mg/g at water content equals 60 wt.% in the fifth region. In the sixth region, the solubilization capacity decreases from 15mg/g microemulsion at water content equals 60 wt.% to about 9 mg/g at water content equals 70 wt.%. After that, the solubilization capacity returns stable 9mg/g microemulsion at water content equals 70 wt.% to water content equals 90 wt.% in the seventh region.

4.3.4.c Water / sucrose myristate M1695 / caprylic/capric triglyceride + glycerol

The solubilization capacity (SC) of cefuroxime axetil at 25°C as function of aqueous phase content along the dilution line N60, presented in Table 4.37 and Figure 4.21. Two different regions can be identified in the phase diagrams presented in Figure 4.66.

Table 4.37: The solubilization capacity (mg drug / g microemulsion) for the system: water / sucrose myristate M1695 / caprylic/capric triglyceride + glycerol at different water contents, along the dilution line N60 presented in Figure 4.21.

	SC(mg drug / g microemulsion)
Water content (Wt.%)	25°C
0	12
10	12
20	12
30	12
40	12
50	12
60	9
70	9
80	9
90	9

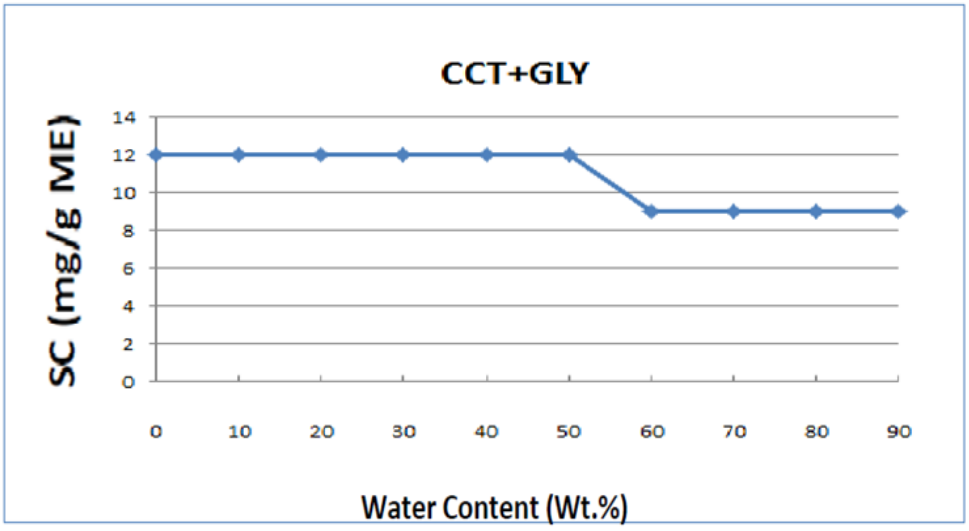

Figure 4.66: The solubilization capacity (SC) of cefuroxime axetil (mg drug / g microemulsion) as function of water content in the system: water / sucrose myristate M1695 / caprylic/capric triglyceride + glycerol, along the dilution line N60 in the phase diagrams presented in Figure 4.21 at 25°C.

In the first region, the solubilization capacity starts stable 12mg/g microemulsion at water content equals 0 wt.%, to water content equals 50 wt.%. In region two, the solubilization capacity decreases from 12mg/g microemulsion at water content equals 50 wt.% to about 9 mg/g at water content equals 60wt.%. After that, the solubilization capacity returns stable 9mg/g microemulsion at water content equals 60 wt.%, to water content equals 90wt.%, in region three.

As shown in Tables 4.8, 4.9, 4.10 and 4,11, the system: water / sucrose myristate M1695 / caprylic/capric triglyceride+ ethanol has the lowest value of N_S – BSO where N_S the surfactant chain length and N_S – BSO the difference between surfactant chain and (oil chain length + alcohol chain length) as empirical Bansal, Shah, O'Connell (BSO), they concluded that the maximum amount of water which may be solubilized in such a microemulsion is reached when the oil chain length (carbon number), N_O, added to that the cosurfactant, alcohol, chain length, N_A, is equal to the surfactant chain length, N_S, i.e. $N_S = N_O + N_A$ then when this value

increases the water solubilization decreases, and chain length compatibility decreases. From the result presented in Tables 4.35, 4.36, 4.37 and Figures 4.63, 4.64, 4.65, the system: water / sucrose myristate M1695 / caprylic/capric triglyceride+ ethanol has the highest value of cefuroxime axetil solubilization because they have the lowest value of N_{S-}BSO, so when the N_{S-} BSO decreases the solubilization capacity increases and chain length compatibility increases.

4.3.5 Cefuroxime axetil solubilization capacity in water / sucrose myristate M1695 / isopropyl myristate + cosurfactant

4.3.5.a Water / sucrose myristate M1695 / isopropyl myristate + ethanol

The solubilization capacity (SC) of cefuroxime axetil at 25°C as function of aqueous phase content along the dilution line N60 presented in Table 4.38 and Figure 4.10**.** Two different regions can be identified in the phase diagrams presented in Figure 4.67.

Table 4.38: The solubilization capacity (mg drug / g microemulsion) for the system: water / sucrose myristate M1695/ isopropyl myristate + ethanol at different water contents, along the dilution line N60 presented in Figure 4.10.

	SC(mg drug / g microemulsion)
Water content (Wt.%)	25°C
0	15
10	15
20	15
30	15
40	18
50	18
60	18
70	18
80	15
90	15

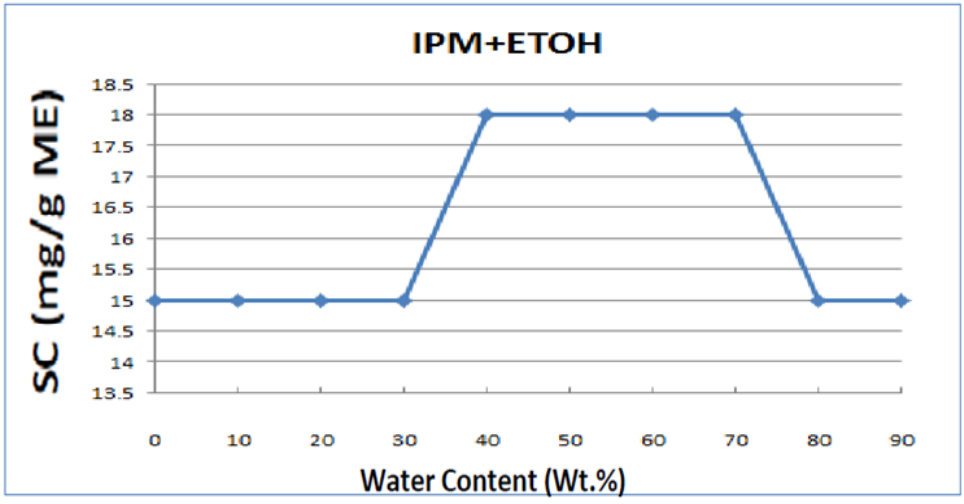

Figure 4.67: The solubilization capacity (SC) of cefuroxime axetil (mg drug / g microemulsion) as function of water content in the system: water / sucrose myristate M1695 / isopropyl myristate + ethanol, along the dilution line N60 in the phase diagrams presented in Figure 4.10 at 25°C.

In the first region, the solubilization capacity starts stable 15mg/g microemulsion at water content equals 0 wt.%, to water content equals 30 wt.%. After that, the solubilization capacity increases from 15mg/g microemulsion at water content equals 30 wt.% to about 18mg/g at water content equals 40 wt.% in the second region. In the third region, the solubilization capacity returns stable 18 mg/g microemulsion at water content equals 40 wt.% to water content equals 70 wt.%. After that, the solubilization capacity decreases from 18mg/g microemulsion at water content equals 70 wt.% to about 15 mg/g at water content equals 80 wt.% in the fourth region. After that, the solubilization capacity returns stable 15mg/g microemulsion at water content equals 80 wt.% to water content equals 90 wt.% in the fifth region.

4.3.5.b Water / sucrose myristate M1695 / isopropyl myristate + propylene glycol

The solubilization capacity (SC) of cefuroxime axetil at 25°C as function of aqueous phase content along the dilution line N60 presented in Table 39. and Figure 4.16. Two different regions can be identified in the phase diagrams presented in Figure 4.68.

Table 4.39: The solubilization capacity (mg drug / g microemulsion) for the system: water / sucrose myristate M1695 / isopropyl myristate + propylene glycol at different water contents, along the dilution line N60 presented in Figure 4.16.

	SC(mg drug / g microemulsion)
Water content (Wt.%)	**25°C**
0	15
10	15
20	21
30	18
40	18
50	18
60	18
70	21
80	21
90	18

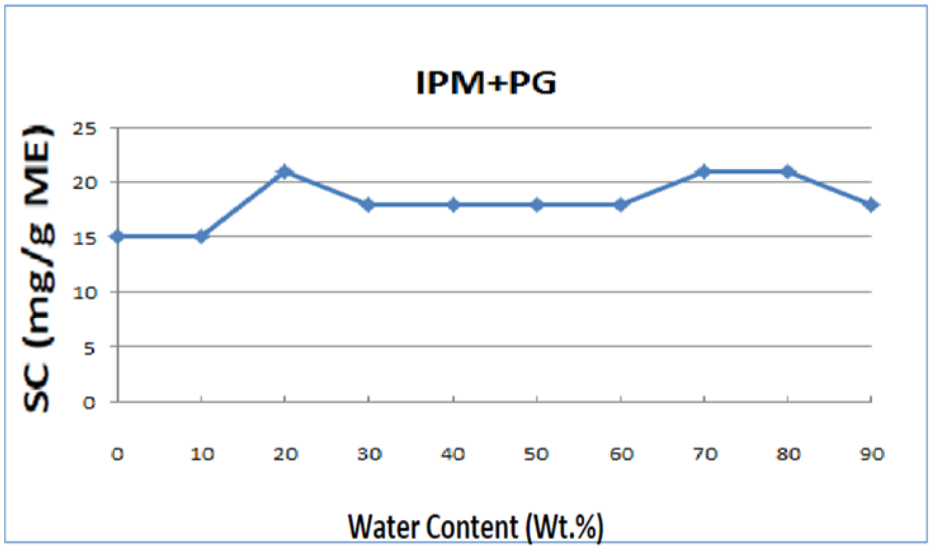

Figure 4.68: The solubilization capacity (SC) of cefuroxime axetil (mg drug / g microemulsion) as function of water content in the system: water / sucrose myristate M1695 / isopropyl myristate + propylene glycol, along the dilution line N60 in the phase diagrams presented in Figure 4.16 at 25°C.

In the first region, the solubilization capacity starts stable 15mg/g microemulsion at water content equals 0 wt.%, to water content equals 10 wt.%. After that, the solubilization capacity increases from 15mg/g microemulsion at water content equals 10 wt.% to about 21mg/g at water content equals 20 wt.% in the second region. In the third region, the solubilization capacity decreases from 21mg/g microemulsion at water content equals 20 wt.% to about 18 mg/g at water content equals 30 wt.%. After that, the solubilization capacity returns stable 18mg/g microemulsion at water content equals 30 wt.% to water content equals 60wt.% in the fourth region. After that, the solubilization capacity increases from 18mg/g microemulsion at water content equals 60 wt.% to about 21mg/g at water content equals 70 wt.% in the fifth region. In the sixth region, the solubilization capacity returns stable 21mg/g microemulsion at water content equals 70 wt.% to water content equals 80 wt.%. After that, the solubilization capacity decreases from 21mg/g microemulsion at water content equals 80 wt.% to about 18 mg/g at water content equals 90 wt.% in the seventh region.

4.3.5.c Water / sucrose myristate M1695 / isopropyl myristate + glycerol

The solubilization capacity (SC) of cefuroxime axetil at 25°C as function of aqueous phase content along the dilution line N60 presented in Table 4.40 and Figure 4.22**.** Two different regions can be identified in the phase diagrams presented in Figure 4.69.

Table 4.40: The solubilization capacity (mg drug / g microemulsion) for the system: water / sucrose myristate M1695 / isopropyl myristate + glycerol at different water contents, along the dilution line N60 presented in Figure 4.22.

	SC(mg drug / g microemulsion)
Water content (Wt.%)	**25°C**
0	12
10	12
20	12
30	12
40	12
50	12
60	12
70	12
80	12
90	12

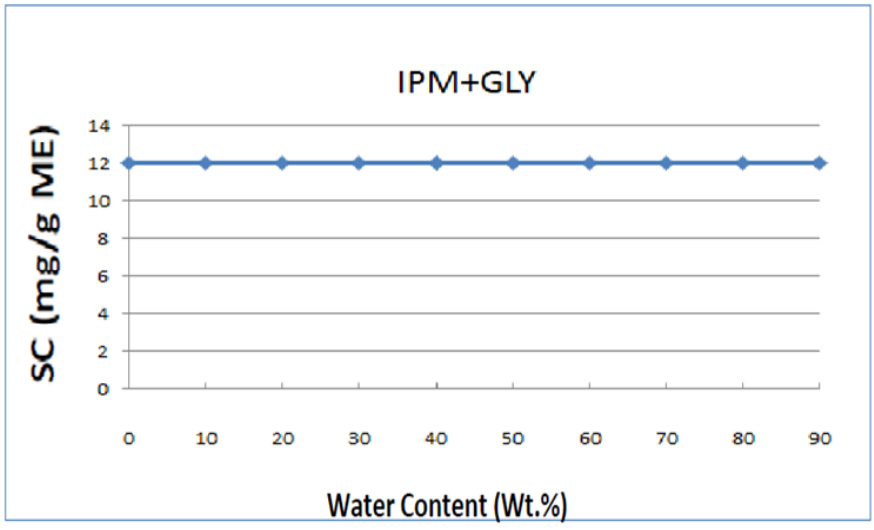

Figure 4.69: The solubilization capacity (SC) of cefuroxime axetil (mg drug / g microemulsion) as function of water content in the system: water / sucrose myristate M1695 / isopropyl myristate + glycerol along the dilution line N60 in the phase diagrams presented in Figure 4.22 at 25°C.

In this case, the solubilization capacity stable 12mg/g microemulsion at all percentages of water content.

As shown in Tables 4.10, 4.11, 4.12 and 4,13, the system: water / sucrose myristate M1695 / isopropyl myristate +(ethanol, propylene glycol) has the lowest value of N_S _ BSO than the system: water / sucrose myristate M1695 / isopropyl myristate + glycerol where N_S the surfactant chain length and N_S _ BSO the difference between surfactant chain and (oil chain length + alcohol chain length) as empirical Bansal, Shah, O'Connell (BSO), they concluded that the maximum amount of water which may be solubilized in such a microemulsion is reached when the oil chain length (carbon number), N_O, added to that the cosurfactant, alcohol, chain length, N_A, is equal to the surfactant chain length, N_S, i.e. $N_S = N_O + N_A$, then when this value increases the water solubilization decreases, and chain length compatibility decreases. From the result printed in Tables 4.38, 4.39, 4.40 and Figures 4.67, 4.68 and 4.69, the system: water / sucrose myristate M1695 / isopropyl myristate + (ethanol, propylene glycol) has the highest value of cefuroxime axetil solubilization because they have the lowest vale of N_S _ BSO, so when the N_S _ BSO decreases the solubilization capacity increases and chain length compatibility increases.

4.3.6 A comparative approach to drug solubilization

In this part of this study, we made a comparative approach on the drug solubilization. In the first part, we made the comparison based on the same type of oil and different types of cosurfactant to study the effect of the cosurfactant on the drug solubilization on the peppermint, R (+)-limonene, isopropyl myristate, and caprylic/capric triglyceride oil, then we made a comparison based on changing oil types with the same cosurfactant. After that, we will show the effect of changing water content on drug solubilization.

Values of solubilization capacity (SC) of cefuroxime axetil at 25°C as function of aqueous phase content along the dilution line N60 for the system: water / sucrose myristate M1695 / peppermint oil+ ethanol, propylene glycol and glycerol at different water contents presented in Table 4.41 and Figures 4.7, 4.13 and 4.19. The surfactant is sucrose myristate M1695 and different cosurfactants are used.

Table 4.41**:** A comparison of the solubilization capacity (mg drug / g microemulsion) for the system: water / sucrose myristate M1695 / peppermint oil + ethanol, propylene glycol, and glycerol at different water content, along the dilution line N60 presented in Figures 4.7, 4.13 and 4.19 at 25°C.

solubilization capacity (SC) of cefuroxime axetil			
water content %	MNT+ETOH	MNT+PG	MNT+GLY
0	12	12	15
10	12	12	15
20	12	9	15
30	12	9	15
40	12	0	12
50	12	0	0

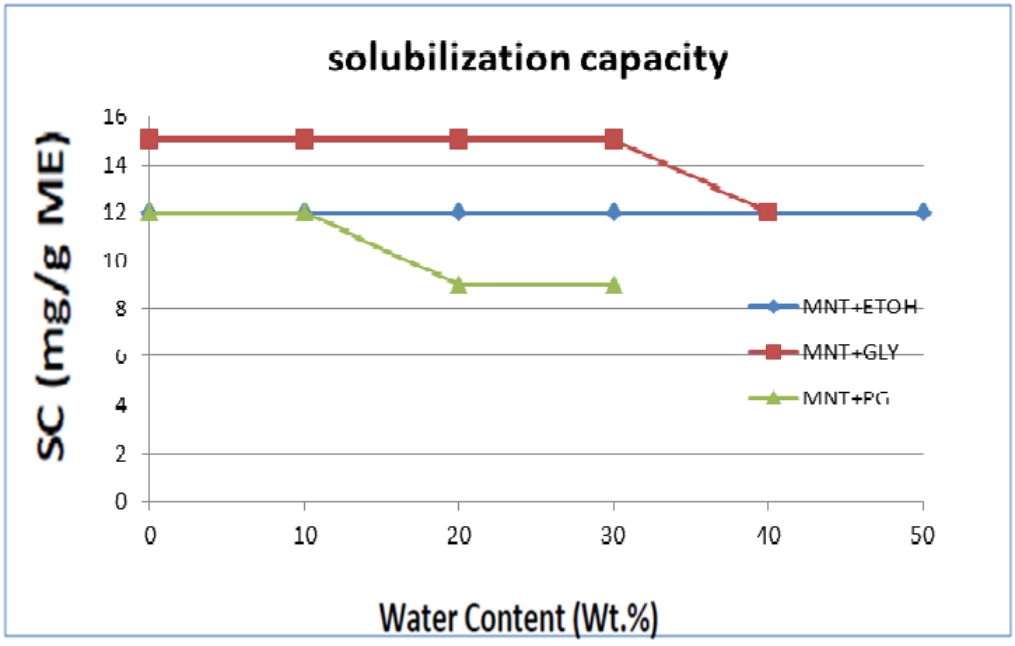

Figure 4.70: A comparison of the solubilization capacity of cefuroxime axetil (mg drug / g microemulsion) as function of water content in the system: water / sucrose myristate M1695 / peppermint oil+ ethanol, propylene glycol, and glycerol, along the dilution line N60 presented in Figures 4.7, 4.13 and 4.19 at 25°C.

Values of solubilization capacity (SC) of cefuroxime axetil at 25°C as function of aqueous phase content along the dilution line N60 for the system: water / sucrose myristate M1695 / R (+)-limonene oil + ethanol, propylene glycol, and glycerol at different water content presented in Table 4.42 and Figures 4.8, 4.14 and 4.20. The surfactant is sucrose myristate M1695 and different cosurfactants are used.

Table 4.42**:** A comparison of the solubilization capacity (mg drug / g microemulsion) for the system: water / sucrose myristate M1695/ R (+)-limonene oil+ ethanol, propylene glycol, and glycerol at different water contents, along the dilution line N60 presented in Figures 4.8, 4.14 and 4.20 at 25°C.

solubilization capacity (SC) of cefuroxime axetil			
water content.%	**LIM+ETOH**	**LIM+PG**	**LIM+GLY**
0	18	15	9
10	15	18	12
20	15	18	12
30	15	18	12
40	12	18	12
50	6	15	12
60	6	15	12
70	6	6	12
80	6	6	12
90	6	6	12

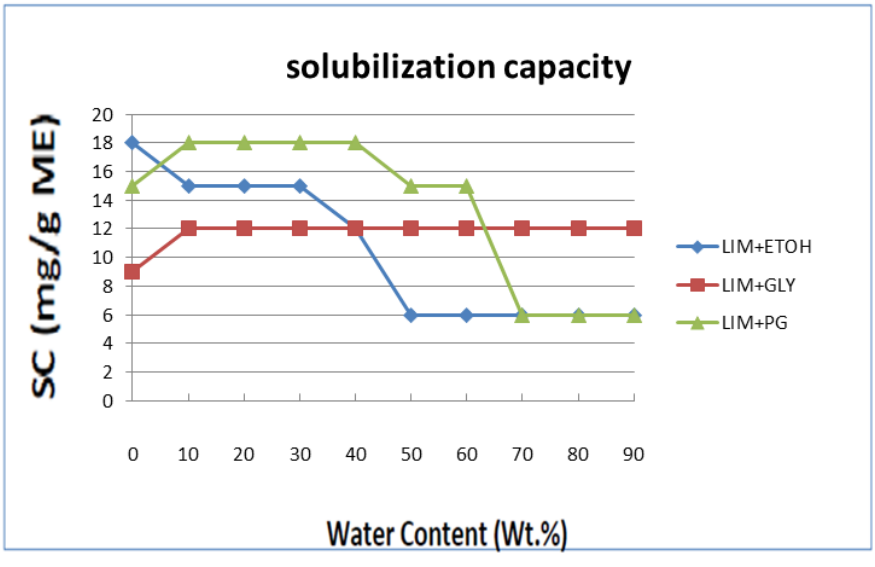

Figure 4.71: A comparison of the solubilization capacity of cefuroxime axetil (mg drug / g microemulsion) for the system: water / sucrose myristate M1695 / R (+)-limonene oil + ethanol, propylene glycol, and glycerol at different water contents, along the dilution line N60 presented in Figures 4.8, 4.14 and 4.20 at 25°C.

Values of solubilization capacity (SC) of cefuroxime axetil at 25°C as function of aqueous phase content along the dilution line N60 for the system: water / sucrose myristate M1695 / caprylic/capric triglyceride oil + ethanol, propylene glycol, and glycerol at different water contents presented in Table 4.43 and Figure 4.9, 4.15 and 4.21, the surfactant is sucrose myristate M1695 and different cosurfactants are used.

Table 4.43 **:** A comparison of the solubilization capacity (mg drug / g microemulsion) for the system: water / sucrose myristate M1695 / caprylic/capric triglyceride oil + ethanol, propylene glycol and glycerol at different water content, along the dilution line N60 presented in Figure 4.9, 4.15 and 4.21, at 25°C.

solubilization capacity (SC)			
water content.%	**CCT+ETOH**	**CCT+GLY**	**CCT+PG**
0	18	12	12
10	18	12	12
20	21	12	12
30	18	12	15
40	18	12	12
50	18	12	12
60	18	9	15
70	21	9	9
80	21	9	9
90	18	9	9

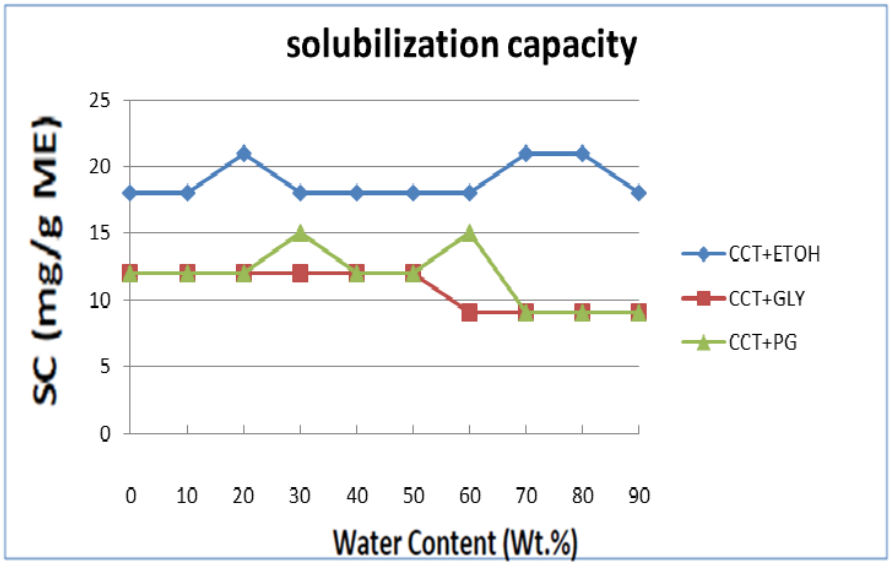

Figure 4.72: A comparison of the solubilization capacity of cefuroxime axetil (mg drug / g microemulsion) for the system: water / sucrose myristate M1695 / caprylic/capric triglyceride oil + ethanol, propylene glycol, and glycerol at different water content along the dilution line N60, presented in Figure 4.9, 4.15 and 4.21 at 25°C.

Values of solubilization capacity (SC) of cefuroxime axetil at 25°C as function of aqueous phase content along the dilution line N60 for the system: water / sucrose myristate M1695 / isopropyl myristate oil + ethanol, propylene glycol, and glycerol at different water contents presented in Table 4.44 and Figures 4.10, 4.22 and 4.16, the surfactant is sucrose myristate M1695 and different cosurfactants are used.

Table 4.44**:** A comparison of the solubilization capacity (mg drug / g microemulsion) for the system: water / sucrose myristate M1695 / isopropyl myristate oil + ethanol, propylene glycol and glycerol at different water content, along the dilution line N60 presented in Figures 4.10, 4.16 and 4.22 at 25°C.

solubilization capacity (SC)			
water content.%	**IPM+ETOH**	**IPM+GLY**	**IPM+PG**
0	15	12	15
10	15	12	15
20	15	12	21
30	15	12	18
40	18	12	18
50	18	12	18
60	18	12	18
70	18	12	21
80	15	12	21
90	15	12	18

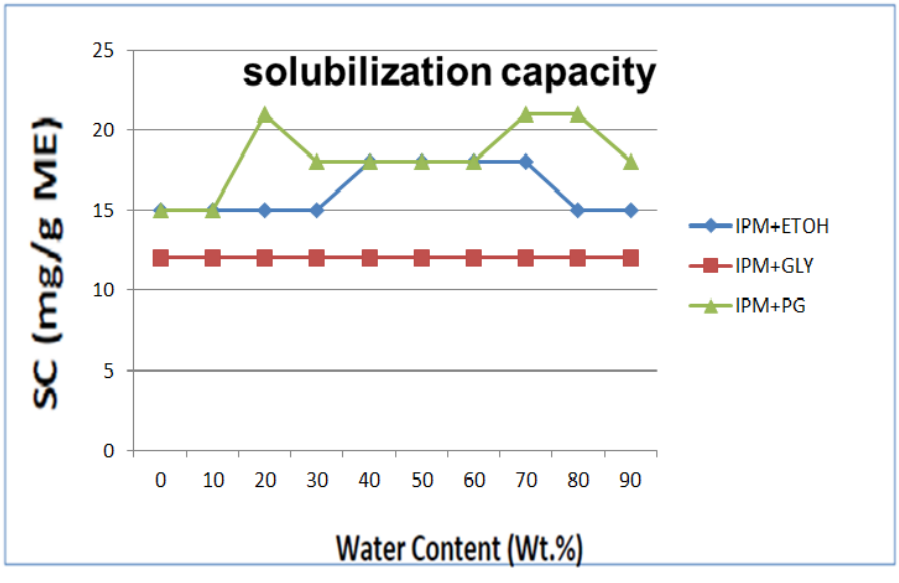

Figure 4.73: A comparison of the solubilization capacity of cefuroxime axetil (mg drug / g microemulsion) for the system: water / sucrose myristate M1695 / isopropyl myristate oil + ethanol, propylene glycol and glycerol at different water contents along the dilution line N60 presented in Figures 4.10, 4.16 and 4.22, at 25°C.

It is clear to show, in general, in all the systems. It was found that the solubilization curves for cefuroxime axetil showed different regions, a region at low water content arrange (0wt% to 30wt.%) which is a water in oil microemulsion. In this region, the solubilization capacity was the highest due to a high surface area and a high oil content. Second region which contains bicontinuous microemulsion and this region extents from 30wt% to 70wt% water content. In this region, the solubilization capacity almost remains constant due to the fact that surface area remains constant at this stage and finally the third region which contains oil in water microemulsion that extents from 70wt% to 100wt% water content. In this region, the solubilization capacity was sharply deceased due to that small amount of oil exists in the core of droplets and the interface became convex toward the oil resulting in very low solubility in the core and poor accommodation of the drugs at the hydrophilic interface.

In this section, we will study the solubilization capacity (SC) of cefuroxime axetil at 25°C for the system: water / sucrose myristate M1695 / different oil + cosurfactant, in order to determine the solubilization capacity (SC) of cefuroxime axetil.

Values of solubilization capacity (SC) of cefuroxime axetil at 25°C as function of aqueous phase content along the dilution line N60 for the system: water / sucrose myristate M1695 / peppermint, R (+)-limonene, isopropyl myristate, caprylic/capric triglyceride oil + ethanol at different water content presented in Table 4.45 and Figures 4.7, 4.8, 4.9 and 4.10, the surfactant is sucrose myristate M1695 and different oil types are used.

Table 4.45**:** A comparison of the solubilization capacity (mg drug / g microemulsion) for the system: water / sucrose myristate M1695 / peppermint, R (+)-limonene, isopropyl myristate, caprylic/capric triglyceride oil + ethanol at different water contents, along the dilution line N60 presented in Figures 4.7, 4.8, 4.9 and 4.10 at 25°C.

water content.%	**MNT+ETOH**	**LIM+ETOH**	**CCT+ETOH**	**IPM+ETOH**
10%	12	15	18	15
20%	12	15	21	15
40%	12	12	18	18
60%	0	6	18	18
80%	0	6	21	15

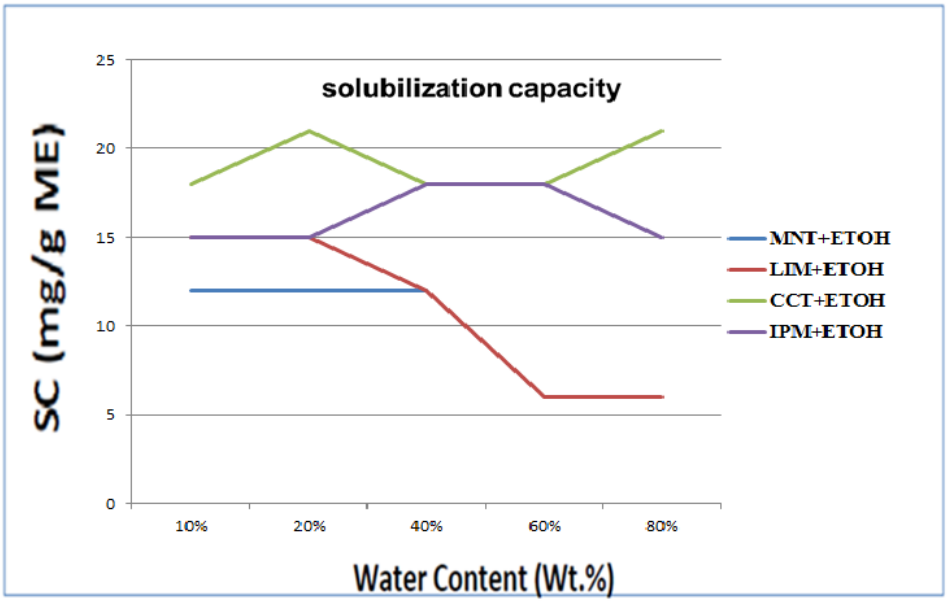

Figure 4.74: A comparison of the solubilization capacity of cefuroxime axetil (mg drug / g microemulsion) for the system: water / sucrose myristate M1695 / peppermint, R (+)-limonene, isopropyl myristate, caprylic/capric triglyceride oil + ethanol at different water contents along the dilution line N60 presented in Figures 4.7, 4.8, 4.9 and 4.10 at 25°C.

As shown in the result presented in Table 4.45 and Figure 4.74, the system: water / sucrose myristate M1695 / caprylic/capric triglyceride oil + ethanol have the maximum solubilization capacity of cefuroxime axetil because caprylic/capric triglyceride oil has the highest value of molecular volume. This gives low viscous, low motion and high stable microemulsion that causes an increase in solubilization capacity of cefuroxime axetil.

Values of solubilization capacity (SC) of cefuroxime axetil at 25°C as function of aqueous phase content along the dilution line N60 for the system: water / sucrose myristate M1695 / peppermint, R (+)-limonene, isopropyl myristate, caprylic/capric triglyceride oil + propylene glycol at different water contents presented in Table 4.46 and Figures 4.13, 4.14, 4.15 and 4.16, the surfactant is sucrose myristate M1695 and different oil types are used.

Table 4.46**:** A comparison of the solubilization capacity (mg drug / g microemulsion) for the system: water / sucrose myristate M1695 / peppermint, R (+)-limonene, isopropyl myristate, caprylic/capric triglyceride oil + propylene glycol at different water contents, along the dilution line N60 presented in Figures 4.13, 4.14, 4.15 and 4.16 at 25°C.

water content.%	**MNT+PG**	**LIM+PG**	**CCT+PG**	**IPM+PG**
10%	15	18	12	15
20%	15	18	12	21
40%	12	18	12	18
60%	0	15	15	18
80%	0	6	9	21

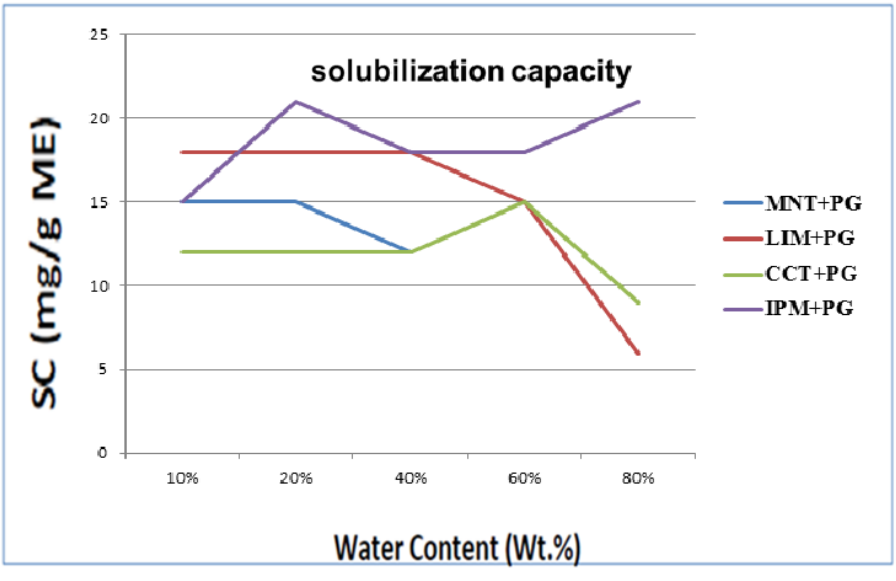

Figure 4.75: A comparison of the solubilization capacity of cefuroxime axetil (mg drug / g microemulsion) for the system: water / sucrose myristate M1695 / peppermint, R (+)-limonene, isopropyl myristate, caprylic/capric triglyceride oil + propylene glycol at different water contents, along the dilution line N60 presented in Figures 4.13, 4.14, 4.15 and 4.16, at 25°C.

As shown in Table 4.46 and Figure 4.75, the system: water / sucrose myristate M1695 / isopropyl myristate oil + propylene glycol, has the highest value of solubilization capacity of cefuroxime axetil because isopropylmyristate oil has linear structure, and contains (17) carbon number, they are like the surfactant chain length and structure, each carbon on oil bond to carbon on surfactant, this increases the stability and increases solubilization capacity. By adding propylene glycol to isopropyl myristate gives the maximum solubilization capacity because propylene glycol increases viscosity of microemulsion due to hydroxyl group (OH) found, and that causes to enhance stability of microemulsion.

Values of solubilization capacity (SC) of cefuroxime axetil at 25°C as function of aqueous phase content along the dilution line N60 for the system: water / sucrose myristate M1695 / peppermint, R (+)-limonene, isopropyl myristate, caprylic/capric triglyceride oil + glycerol at different water contents presented in Table 4.47 and Figures 4.19, 4.20, 4.21 and 4.22, the surfactant is sucrose myristate M1695 and different oil types are used.

Table 4.47**:** A comparison of the solubilization capacity (mg drug / g microemulsion) for the system: water / sucrose myristate M1695 / peppermint, R (+)-limonene, isopropyl myristate, caprylic/capric triglyceride oil + glycerol at different water contents, along the dilution line N60 presented in Figures 4.19, 4.20, 4.21 and 4.22 at 25°C.

water content.%	MNT+GLY	LIM+GLY	CCT+GLY	IPM+GLY
10%	15	12	12	12
20%	15	12	12	12
40%	12	12	12	12
60%	0	12	9	12
80%	0	12	9	12

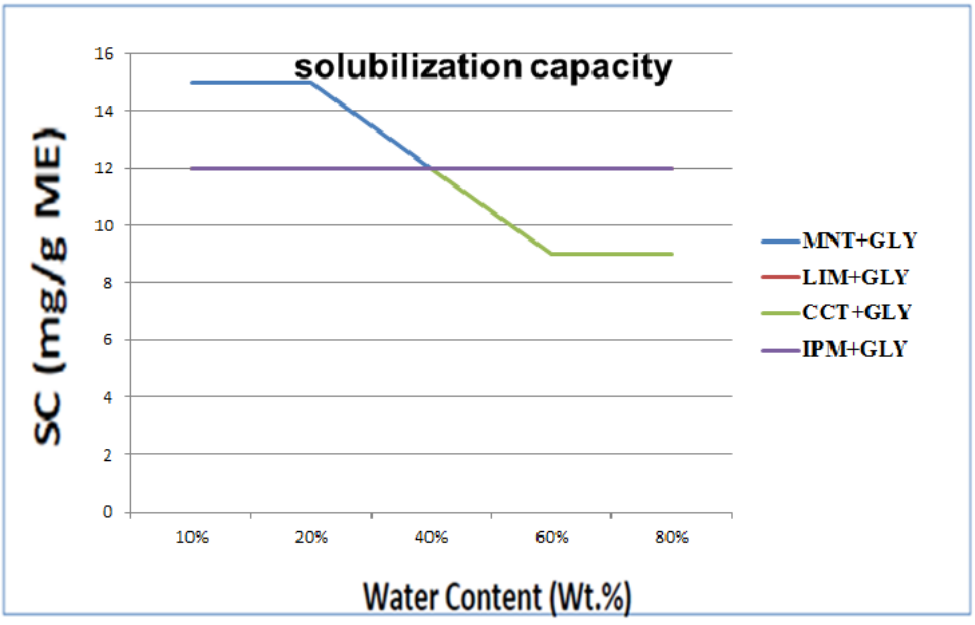

Figure 4.76: A comparison of the solubilization capacity of cefuroxime axetil (mg drug / g microemulsion) for the system: water / sucrose myristate M1695 / peppermint, R (+)-limonene, isopropyl myristate, caprylic/capric triglyceride oil + glycerol at different water contents, along the dilution line N60 presented in Figures 4.19, 4.20, 4.21 and 4.22 at 25°C.

As shown in Table 4.47 and Figure 4.76, the system: water / sucrose myristate M1695 / peppermint, R (+)-limonene, isopropyl myristate, caprylic/capric triglyceride oil + glycerol has the lowest value of solubilization capacity than other systems because they have the highest value of empirical Bansal, Shah, O'Connell (BSO) equation, increase the BSO causes a decrease in solubilization capacity and chain length compatibility decrease.

In this section, we will study the solubilization capacity (SC) of cefuroxime axetil at 25°C for the system: water / sucrose myristate M1695 / oil + cosurfactant, at water contents (10,20,40,60,80%) to determine the solubilization capacity (SC) of cefuroxime axetil.

Values of solubilization capacity (SC) of cefuroxime axetil at 25°C as function of aqueous phase content, along the dilution line N60 for the system: water / sucrose myristate M1695 / peppermint, R (+)-limonene, isopropyl myristate, caprylic/capric triglyceride oil + ethanol at

water contents (10,20,40,60,80%) presented in Table 4.48 and Figures 4.7, 4.8, 4.9 and 4.10, the surfactant is sucrose myristate M1695 and different oil types are used.

Table 4.48**:** A comparison of the solubilization capacity (mg drug / g microemulsion) for the system: water / sucrose myristate M1695 / peppermint, R (+)-limonene, isopropyl myristate, caprylic/capric triglyceride oil + ethanol at water contents (10,20,40,60,80%), along the dilution line N60 presented in Figures 4.7, 4.8, 4.9 and 4.10 at 25°C.

System	**10%**	**20%**	**40%**	**60%**	**80%**
MNT+ETOH	12	12	12	0	0
LIM+ETOH	15	15	12	6	6
CCT+ETOH	18	21	18	18	21
IPM+ETOH	15	15	18	18	15

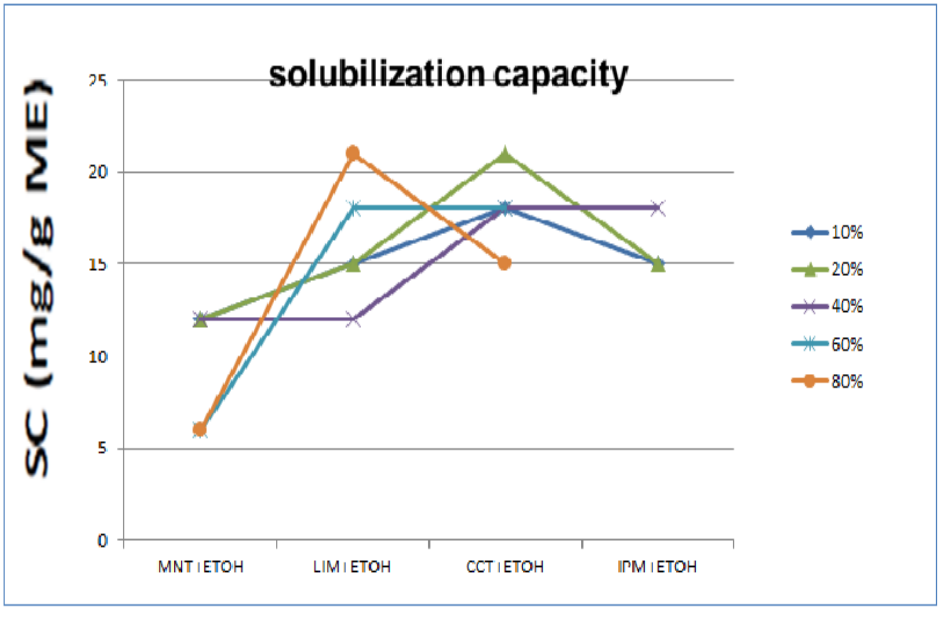

Figure 4.77: A comparison of the solubilization capacity of cefuroxime axetil (mg drug / g microemulsion) for the system: water / sucrose myristate M1695 / peppermint, R (+)-limonene, isopropyl myristate, caprylic/capric triglyceride oil + ethanol at water contents (10,20,40,60,80%) along the dilution line N60 presented in Figures 4.7, 4.8, 4.9 and 4.10 at 25°C.

Values of solubilization capacity (SC) of cefuroxime axetil at 25°C as function of aqueous phase content along the dilution line N60 for the system: water / sucrose myristate M1695 / peppermint, R (+)-limonene, isopropyl myristate, caprylic/capric triglyceride oil + propylene glycol at water content (10,20,40,60,80%) presented in Table 4.49 and Figures 4.13, 4.14, 4.15 and 4.16, the surfactant is sucrose myristate M1695 and different oil types are used.

Table 4.49**:** A comparison of the solubilization capacity (mg drug / g microemulsion) for the system: water / sucrose myristate M1695 / peppermint, R (+)-limonene, isopropyl myristate, caprylic/capric triglyceride oil + propylene glycol at water contents (10,20,40,60,80%), along the dilution line N60 presented in Figures 4.13, 4.14, 4.15 and 4.16 at 25°C.

System	10%	20%	40%	60%	80%
MNT+PG	15	15	12	0	0
LIM+PG	18	18	18	15	6
CCT+PG	12	12	12	15	9
IPM+PG	15	21	18	18	21

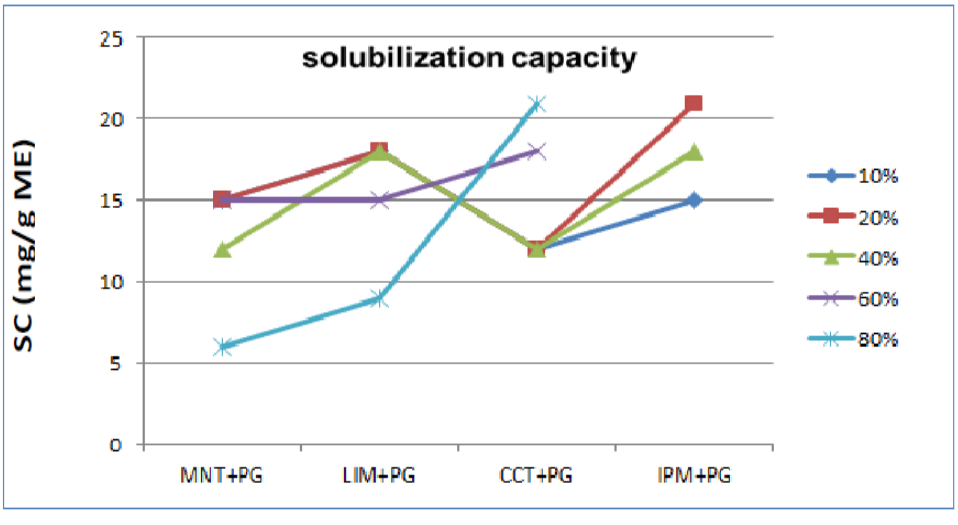

Figure 4.78: A comparison of the solubilization capacity of cefuroxime axetil (mg drug / g microemulsion) for the system: water / sucrose myristate M1695 / peppermint, R (+)-limonene, isopropyl myristate, caprylic/capric triglyceride oil + propylene glycol at water contents (10,20,40,60,80%) along the dilution line N60 presented in Figures 4.13, 4.14, 4.15 and 4.16 at 25°C.

Values of solubilization capacity (SC) of cefuroxime axetil at 25°C as function of aqueous phase content along the dilution line N60 for the system: water / sucrose myristate M1695 / peppermint, R (+)-limonene, isopropyl myristate, caprylic/capric triglyceride oil + glycerol at water contents (10,20,40,60,80%) presented in Table 4.50 and Figures 4.19, 4.20, 4.21 and 4.22, the surfactant is sucrose myristate M1695 and different oil types are used.

Table 4.50**:** A comparison of the solubilization capacity (mg drug / g microemulsion) for the system: water / sucrose myristate M1695 / peppermint, R (+)-limonene, isopropyl myristate, caprylic/capric triglyceride oil + glycerol at water contents (10,20,40,60,80%), along the dilution line N60 presented in Figures 4.19, 4.20, 4.21 and 4.22 at 25°C.

System	10%	20%	40%	60%	80%
MNT+GLY	15	15	12	0	0
LIM+GLY	12	12	12	12	12
CCT+GLY	12	12	12	9	9
IPM+GLY	12	12	12	12	12

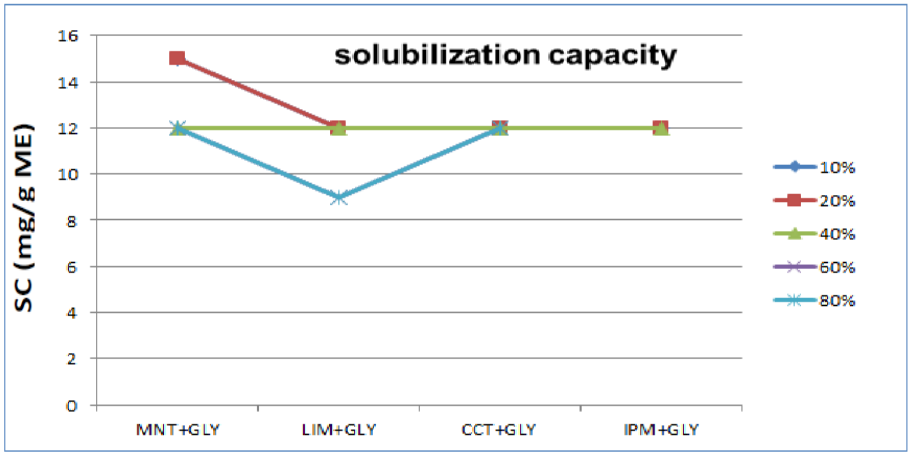

Figure 4.79: A comparison of the solubilization capacity of cefuroxime axetil (mg drug / g microemulsion) for the system: water / sucrose myristate M1695 / peppermint, R (+)-limonene, isopropyl myristate, caprylic/capric triglyceride oil + glycerol at water contents (10,20,40,60,80%) along the dilution line N60 presented in Figures 4.19, 4.20, 4.21 and 4.22 at 25°C.

It is clear in all the systems, it was found that the solubilization curves for cefuroxime axetil showed different regions, a region at low water content arrange (0wt% to 30wt.%) which is a water in oil microemulsion. In this region, the solubilization capacity was the highest due to high surface area and high oil content. A second region which contains bicontinuous microemulsion that extents from 30wt% to 70wt% water content. In this region, the solubilization capacity almost remains constant due to the fact that surface area remains constant at this stage , and the third region which contains oil in water microemulsion. This region extents from 70wt% to 100wt% water content. In this region, the solubilization capacity was sharply deceased due to that small amount of oil exists in the core of droplets and the interface becomes convex toward the oil resulting in very low solubility in the core and poor accommodation of the drugs at the hydrophilic interface.

5. Conclusions

In this work, new microemulsions were being developed using natural oils such as peppermint oil, R (+)-limonene oil, isopropylmyristate oil and common edible oils caprylic-capric triglyceride, new surfactants sucrose myristate M1695 in an aqueous solution water with or without added of cosurfactants such as ethanol, propionic acid, propylene glycol and glycerol.

In the following, we redraw the general conclusions varied from these subjects:

In this system, microemulsion systems based on single surfactants and a mixture of oil and cosurfactant. It is clear that the water solubilization capacity studied revealed that mixed oil and cosurfactant improve the water solubilization capacity in the microemulsions compared to the microemulsion systems based on single oil without cosurfactant. This mixture between oil and cosurfactant gives better interfacial solubilization (enhanced partitioning of the surfactant at the interface and this gives an increase in solubilization.

The chemical structure of oil affects water solubilization capacity. Cyclic oils, R(+)-limonene and peppermint, have the highest water solubilization capacity because cyclic structure tends to penetrate in the surfactant layer and widen the effective cross- sectional area per surfactant. Triglyceride oil, caprylic-capric triglyceride, and linear oil isopropylmyristate have low water solubilization than cyclic oil because of their high molecular volume and so the ability to penetrate the interfacial film is very low and does not assist to obtain the optimum curvature of surfactants, increase molecular volume and effective carbon number causes a decrease in water solubilization. Different comparative studies have been done on this study to see the effect of changing the types and percentages of the oils and cosurfactants.

Cosurfactants do play an important role in solubilizing. The roles of alcohol in microemulsions is to delay the occurrence of liquid crystalline phases, to increase the fluidity of the interfacial layer separating oil and water, to decrease the interfacial tension between the

microemulsion phase and excess oil and water and to increase the disorder in these interfacial layers as well as their dynamic character, so adding cosurfactant ethanol, glycerol, propylene glycol and propionic acid to the system improves the water solubilization capacity of the microemulsions and makes the system more organized. Hydroxyl group found in cosurfactant causes an increase of interaction with water, this gives enhance curvature of droplets size, decreases interfacial tension and gives an increase in monophasic area A_T %.

Different factors affect water solubilization, phase diagram and the total monophasic region A_T, these factors are:

- Effective carbon number.

- Molecular volume.

- Atom available for lipophilic interaction.

- Atom available for lipophilic interaction.

- The empirical BSO equation.

- The spontaneous curvature and elasticity of the interfacial film (R-ratio).

The empirical BSO (Bansal, Shah, O'Connell) equation which was derived as an empirical condition for maximum water solubilization in microemulsions stabilized by anionic surfactants in relation to the cosurfactant, alcohol, and oil chain lengths, i.e. $N_S = N_O + N_A$, where N_S, N_O, N_A are the surfactant chain lengths, oil and alcohol, respectively, was re-examined for this type of surfactants. This study demonstrates that a maximum water solubilization is obtained when the $N_S = (N_O + \_3) + N_A$ for N_S is greater than 14; when N_S is less than 14, this equation cannot predict the maximum water solubilization.

They concluded that the maximum amount of water which may be solubilized in such a microemulsion is reached when the oil chain length (carbon number), N_O, added to that of the cosurfactant (alcohol) chain length, N_A, is equal to the surfactant chain length, N_S, i.e. $N_S = N_O + N_A$. In the following, this is known as the BSO equation.

The changes of water solubilization in the studied systems, all other parameters remaining unchanged, should be the same as with the alcohol chain length. For the N_S effect, the chain length of the lipophilic tail of the surfactant, which increases the molar volume of the lipophilic tail of the surfactant with a short cosurfactant, results in an increase in oil penetration into the alkyl chains of the surfactant. This increases the attractive interaction potential, thereby suppressing the elasticity leading to smaller water droplets and lowering water solubilization.

We have shown in this study that the BSO equation and the concept of chain length compatibility can predict, within some limits, conditions for maximum solubilization in the presence of polyol nonionic surfactants. Limitations on their predictive capacity are that the cosurfactant, alcohol, not too soluble in either water or oil. The maximum water solubilization can be predicted using the BSO equation with approximate calculation based on the length of the main chain of oil when the oil is branched.

Two solubilization maxima can be explained in terms of additional membrane rigidity effect on the Rc curve and in terms of enhanced flattening of the interface effect on the Ro curve.

For example, increasing the chain length of the alcohol N_A when the molar volume of the oil in the system is small, will increase the oil penetration into the alkyl chains of the surfactant and the penetration of cosurfactant into the palisade layers. This will cause the interface to become more curved, thereby favoring decrease of Ro and the formation of small water in oil microemulsion droplets. On the other hand, decreased oil penetration decreases the attractive interaction potential, thereby increasing Rc. These competing effects lead to maximum solubilization, as observed experimentally.

Decreasing the length of the surfactant tail will result in a decrease in oil penetration into the alkyl chains of the surfactant, which causes the interface to become less curved, thereby favoring the growth of spontaneous curvature and the formation of larger water in oil microemulsion droplets.

Microemulsions formulated according to these strategies, low surfactant levels, have advantages of very high microemulsification capacity, low surfactant residue and low cost. This approach has been used to reduce the cost and improve the performance of several consumer product formulations, forming surfactants, in combination with indigenous cosurfactants. This strategy has been used to identify improved, simple, novel routes to solubilize industrially useful materials such as Cefuroxime Axetil .

Properties of microemulsions can be determined using various techniques such as electrical conductivity.

In this research, we study effects of changing the relative amounts of microemulsion components on the transport, diffusion and structural properties of these self-assemblies were investigated using electrical conductivity. The electrical conductivity measurements are performed to determine the type of microemulsion droplets formed i.e. water-in-oil, bicontinues, or oil-in-water, these structures are influenced both by the water to oil ratio and by the preferred curvature of the surfactant, which results from the interactions of the surfactant layer with the oil and water phases.

We concluded that the electrical conductivity increases as the water volume fraction increases, where the system is water in oil microemulsion, the high values of electrical conductivity at high-water volume fractions are explained by the fact that the sodium chloride ions are present in the external phase, which is the water. These results permit to distinguish between water in oil and oil in water microemulsions, then electrical conductivity starts decreasing, where the system is oil in water microemulsion. The electrical conductivity increases when temperature increases, this is due to the increase in kinetic energy which causes an increase in the collision between droplet and increases of movement of ions. By raising the temperature, the collision probability between the droplets increases and the opening and reforming of droplets will increase the mobility of water and the electrical conductivity will again rise with the temperature. In addition, the possibility of percolation becomes larger and the formation of water channels will also increase the electrical conductivity of the system.

According to the percolation model, the conductivity remains low up to a certain volume fraction of water at constant temperature, when the temperature reaches a value T_c at constant water volume fraction, or when the water-to-surfactant molar ratio increases. It must be emphasized that these conducting water-in-oil droplets, below volume fraction, are isolated from each other embedded in nonconducting continuum oil phase and hence contribute very little to the conductance. However, as the volume fraction of water reaches the percolation threshold volume fraction, some of these conductive droplets begin to contact each other and form clusters which are sufficiently close to each other. The number of such clusters increases very rapidly above the percolation threshold volume fraction, giving rise to the observed changes of properties, in particular to the increase of electrical conductivity. The electrical conductivity, r above volume fraction, has been attributed to the transfer of counter ions from one droplet to another through water channels opening between droplets during sticky collisions through transient merging of droplets.

The solubility of cefuroxime axetil in these microemulsion systems was investigated by dissolving in microemulsion. Microemulsion has unique properties that include high mutual solubilization of water and oil, that increase the solubility of active pharmaceutical ingredients cefuroxime axetil, the mixing of different types of oils with cosurfactant enhanced the solubilization capacity significantly. This interesting observation was explained by a hypothesis assuming non-ideal mixing of the oil and their penetration into surfactant layers. These formulations should help to improve the bioavailability of poorly soluble drugs.

The solubilization capacity of cefuroxime axetil in microemulsion systems was higher than any single component that formed the microemulsion. It was found that the solubilization curves for cefuroxime axetil showed different regions, a region at low water content (0wt% to 30wt.%), which is a water in oil microemulsion. In this region, the solubilization capacity was the highest due to high surface area and high oil content. Another region which contains bicontinuous microemulsion and this region extents from 30wt% to 70wt% water content. In this region, the solubilization capacity almost remains constant due to the fact that surface area remains constant at this stage. Another region which contains oil in water microemulsion and this region extents from 70wt% to 100wt% water content. In this region, the solubilization capacity was sharply deceased due to that small amount of oil exists in the core

of droplets and the interface becomes convex toward the oil resulting in very low solubility in the core and poor accommodation of the drugs at the hydrophilic interface.

The solubilization capacity of cefuroxime axetil highly depends on the composition of the microemulsion system. The presence of alcohol as a cosurfactant and the oil type and its penetration at the interface both greatly affect the degree of cefuroxime axetil solubilization. The solubilization capacity of cefuroxime axetil depends on the microstructure, which means that the microemulsion type strongly influenced by the extent of cefuroxime axetil solubilization.

The drug interacts at the interface with the microemulsion components at any specific microstructure of the investigated vehicles and affects the water contents at which the transitions from water in oil to bicontinuous to oil in water microemulsions, so the drug release kinetics from these microemulsions should be affected. The drug remains solubilized at the interface upon dilution with water and is oriented with its hydrophilic part facing the water. In many of the formulations the drug is soluble in the concentrated capsule, but it precipitates at once if diluted with water. Our formulations are based on nonionic surfactants and therefore are more resistant to low pH and can survive the stomach dilution and acidity.

We can conclude that microemulsion system helps increasing the solubility of the hydrophobic drug with the help of hydrophobic component of microemulsion and lipophilic part of the surfactant.

From all the above, we can conclude:

1- Microemulsions are clear dispersions of at least three components: a polar and non-polar liquid phases usually (water or brine and oil) and surfactant.

2- Microemulsions systems consist of oil, water and surfactant molecules, that brings down the water / oil interfacial tension (IFT) to a very low value. The IFT between oil and water is reduced to a very low value by the presence of an amphiphile but if

amphiphile don't bring the IFT down to the required very low value, we must add another substance to obtain the required IFT for the formation of a stable microemulsion such as short chain alcohols, cosurfactant, when microemulsions were prepared by using these components with cosurfactant the optimum amount of water solubilization increased with increasing the cosurfactant content.

3- The total monophasic region A_T of cyclic oil is more than A_T to triglyceride oils and linear oil.

4- Increase the molecular volume and atom available for effective carbon number causes a decrease in water solubilization and (the total monophasic region A_T).

5- Using isopropylmyristate oil with propylene glycol has greatly affected the solubilization of water in the mixture to prepare microemulsion, where the maximum amount of water miscible with the system was considerably remarkable compared to that when using propylene glycol with water with oil.

6- Solubility of cefuroxime axetil in microemulsions systems was investigated by dissolving in microemulsion.

7- Solubility of cefuroxime axetil in microemulsions containing oil + cosurfactant as lipophilic phase was markedly higher than that in single oil without presence of cosurfactant.

8- The maximum water solubilization obtained in this study was when the system contains water + sucrose myristate M1695 + propylene glycol as a cosurfactant.

9- The minimum water solubilization obtained in this study was when the system contains water + sucrose myristate M1695 + propionic acid as a cosurfactant.

10- The microemulsion system helps increasing the solubility of the hydrophobic drug with the help of hydrophobic component of microemulsion and lipophilic part of the surfactant.

11- Increasing the chain length of the alcohol N_A when the molar volume of the oil in the system is small, will increase the oil penetration into the alkyl chains of the surfactant and the penetration of cosurfactant into the palisade layers. This will cause the interface to become more curved, thereby favoring decrease of Ro and the formation of small water in oil microemulsion droplets. On the other hand, decreased oil penetration decreases the attractive interaction potential, thereby increasing Rc. These competing effects lead to maximum solubilization, as observed experimentally.

12- Decreasing the length of the surfactant tail will result in a decrease in oil penetration into the alkyl chains of the surfactant, which causes the interface to become less curved, thereby favoring the growth of spontaneous curvature and the formation of larger water in oil microemulsion droplets.

13- The maximum amount of water which may be solubilized in such a microemulsion is reached when the oil chain length (carbon number), N_O, added to that of the cosurfactant, alcohol, chain length, N_A, is equal to the surfactant chain length, N_S, i.e. $N_S = N_O + N_A$. This is known as the BSO equation.

Finally, microemulsions have been used in a variety of technological applications, including environmental protection, nanoparticle formation, personal care product formulations, drug delivery systems and chemical reaction media. These microemulsions could be used to improve the solubility of active pharmaceutical ingredients (cefuroxime axetil) and other natural food compound which are insoluble in water and poorly soluble in vegetable oils.

References

- Abuin. E.B, Rubio. M.A, Lissi.E.A, Solubility of Water in Water-in-Oil Microemulsions Stabilized by Cetyltri methyl ammonium: Effects of the Surfactant Counterion, the Nature and Composition of the Oil, and the Salinity of the Droplets, Journal Colloid Interface Science 158: 129-132, (1993).

- Adams. D.H, Wood .M.J, Farre. D, Oral cefuroxime axetil clinical pharmacology and comparative dose studies in urinary tract infection. Journal of Antimicrobial Chemotherapy 16: 359-366, (1985).

- Akira. Y, Junichi. M, Ritsuko. H, Takashi. Y, Isamu. S, Matsuhisa. I, and Susumu. M, Mechanism of Action of Cephalosporins and Resistance Caused by Decreased Affinity for Penicillin-Binding Proteins in Bacteroides fragilis.Journal of Antimicrobial agents and chemotherapy 32: 1848-1853, (1988).

- Attwood. D, Microemulsion, In Colloidal Drug Delivery Systems; Kreuter, Journal (ed.); Marcel Dekker: New York, 31–71 (1994).

- Bagwe. R. P, Kanicky. J. R, Palla. B. J, Patanjali. P. K, and Shah. D. O, Improved drug delivery using microemulsions: Rationale, recent progress, and new horizons. Crit. Rev. Ther. Drug Carr. Syst 18: 77–144, (2001).

- Bansal. V.K, Shah. D.O, O'Connell. J.P, Influence of alkyl chain length compatibility on microemulsion structure and solubilization, Journal Colloid Interface Science 75: 462–475, (1980).

- Berghenholtz. J, Romagnoli. A, and Wagner. N, Viscosity, microstructure, and interparticle potential of AOT/H2O/n-decane inverse microemulsions, Langmuir 11: 1559–1570, (1995).

- Biais. J, Clin. B, Laolanne. P, in Microemulsions: Structure and Dynamics (Eds: S. E. Friberg, P. Bothorel), CRC Press, Boca Raton, FL ,Ch. 1, (1987).

- Bord. F, Cametti. C, Chen. S.H, Rouch. J, F. Sciortino, P. Tartaglia, The static electrical conductivity of water in oil microemulsions below percolation threshold, Physica 231: 161-167, (1996).

- Bourrel. M, Schechter .R.S (Eds.), Microemulsions and Related Systems: Formulation, Solvency and Physical Properties, Marcel Dekker, New York, 30: 127, (1988).

- Brusseau. M.L, Sabatini. D.A, Gierke.J.S, and Annable. M.D, (Eds.) Innovative Subsurface Remediation, Field Testing of Physical, Chemical, and Characterization Technology; ACS, American Chemical Society, Washington. DC.725: 49-63 (1999).

- Bumajdad. A, and Eastoe. J, Conductivity of water in oil microemulsions stabilized by mixed surfactant. Journal Colloid Interface Science, 274: 268–276, (2004).

- Cametti. C, Codastefano. P, Tartaglia. P, Chen. S. H, and Rouch, Electrical conductivity and percolation phenomena in water-in-oil microemulsions. Journal of Physics and Chemistry of Solids45: 5358–5361 (1992).

- Chiellini. C, Coceani. N, Bresciani. M, Cadelli. G.C, Magarotto. L, and Carli. F, Incorporation of insoluble drugs into composite oil/polymer micro particles using an oily system, in: Proceedings of the 19th Pharmaceutical Technology Conference and Exhibition, Baveno-Stresa, Lago Maggiore, Italy. 11–13, 58–63, (2000).

- Eicke, H.F., Meier, W., Hammerich, H. (1994) Langmuir Conductive Flow Parameters of Mixed Nonionic Surfactants Microemulsions Journal of Dispersion Science and Technology, 10: 2223–2227.

- De Campo. L, Yaghmur. A, Garti. N, Leser. M.E, Folmer. B, and Glatter. O, Five-component food-grade microemulsions: Structural characterization by SANS, Journal Colloid Interface Science 274: 251–267, (2004).

- Fanun. M, Wachtel. E, Antalek. B, Aserin. A, and Garti. N, A Study of the microstructure of four-component sucrose ester microemulsions by SAXS and NMR. Journal Colloids and Surfaces. A, 180: 173–186, (2001).

- Fanun. M, Salah Al-Diyn. W, Temperature effect on the phase behavior of the systems water/sucrose laurate/ ethoxylated-mono-di-glyceride / oil" Journal of Dispersion Science and Technology 27: 1119-1127, (2006a).

- Fanun. M, and Salah Al-Diyn. W, Electrical conductivity and self diffusion NMR studies of the system :Water/sucrose laurate/ethoxylated mono-di-glyceride/isopropylmyristate systems. Colloids Surf. A:Physicochem. Eng. Aspects 277: 83–89, (2006b).

- Fanun. M, Structure probing of water/mixed nonionic surfactants/caprylic capric triglyceride. Journal of Molecular Liquids133: 22–27, (2007).

- Fanun. M, Salah Al-Diyn. W, Structural transitions in the system water /mixed nonionic surfactants/ R (+)-limonene studied by electrical conductivity and self diffusion-NMR" Journal of Dispersion Science and Technology 28: 165-174, (2007).

- Fanun. M, Propylene glycol and ethoxylated surfactant effects on the phase behavior of water/sucrose stearate/oil systems. Journal of Dispersion Science and Technology, 28: 1244-1253, (2007).

- Fanun. M, Microemulsions: Properties and Applications. Surfactants Science Series, Boca Raton, FL: Taylor & Francis/CRC Press,144 (2008a).

- Fanun. M, Conductive Flow Parameters of Mixed Nonionic Surfactants Microemulsions. Journal of Dispersion Science and Technology, 29:10,1426 -1434, (2008)

- Fanun. M (Ed.), Microemulsions: Properties and Applications, Taylor and Francis/CRC Press, Boca Raton, (2009).

- Fanun. M, Microemulsions with Nonionic Surfactants and Mint Oil, Journal Colloid and Interface Science, 3: 9-14, (2010).

- Feldman. Y, Kozlovich. N, Nir. I, Garti.N, Archpov. V, Idiyatullin. Z, Zuev. Y, and Fedotov, Fractals, diffusion, and relaxation, in disordered complex system V: Journal of Physical Chemistry. 100: 3745–3748, (1996).

- Garti. N, Aserin. A, Ezrahi. S, Proceeding of the International Conference on Tribology, Bulgaria, pp. 107–127, (1994).

- Garti. N, Aserin. A, Ezrahi. S, Wachtel. E, Adsorption and Aggregation of Surfactants in Solution Journal Colloid and Interface Science. 169, 428, (1995).

- Garti. N, Aserin. A , Fanun. M, Water Science for Food Health A Physicochem. Eng. Asp.164 ,27, (2000a).

- Garti. N, Clement. V, Fanun. M, Leser. M.E, Some characteristics of sugar ester nonionic microemulsion in new of possible food application, Journal Agriculture and Food Chemistry , 48: 3945-3965, (2000b).

- Garti. N, Fanun. M, Aserin. A, Antalek, and Wachtel. E, A study of the microstructure of four-component sucrose ester microemulsions by SAXS and NMR, Journal Colloids and Surfaces. A, 180:173-186, (2001).

- Gasco. M.R, Gallarate. M, Pattarino. F, In vitro permeation of azelaic acid from viscosized microemulsions, Int. Journal Pharm, 10: 193–196, (1991).

- Gillberg. G, Lehtinen. H, and Friberg. S. E, IR and NMR investigation of the conditions determining the stability of microemulsions, Journal Colloid and Interface Science, 33: 40–49, (1970).

- Glatter. O, Orthaber. D, Stradner. A, Scherf. G, Fanun. M, Garti. N, Clément. V,and Leser. M.E, Sugar-ester nonionic microemulsion: Structural characterization, Journal Colloid Interface Science. 241:215–225, (2001).

- Hou. M.j, Shah. D.O, Langmuir, 3,1086, (1987).

- Hsiao. Ho, Sheu, Preparation of microemulsions using polyglycerol fatty acid esters as surfactant for dielivery of protein drugs. Journal of Pharmaceutical Science, 85: 138-143, (1996).

- Kahlweit. M, Busse. G, and Winkler. J, Electrical conductivity in microemulsion, Journal of Chemical Physics, 99: 5605–5614, (1993).

- Kahlweit. M, Strey. R, and Busse. G, Microemulsions: A qualitative thermodynamic approach. Journal of Chemical Physics, 94: 3881–3894, (1990).

- Kahlweit. R, Strey. R, Busse. G, Effect of Alcohols on the Phase-Behavior of Microemulsions, Journal of Chemical Physics. 95: 5344-5350, (1991).

- Kahlweit. M, Strey. R, Schomacker. R, and Hasse. D, General patterns of the phase behavior of mixtures of water, nonpolar solvents, amphiphiles, and electrolytes. 2.Langmuir, 5: 305–315,(1989).

- Keith. B, Holten. M.D, and Edward. M, Onusko. M.D, Appropriate Prescribing of Oral Beta-Lactam Antibiotics Am Fam Physician. 62,: 611-620, (2000).

- Kumar. P, Mittal. K.C (Eds.), Handbook of Microemulsions Science and Technology, Marcell Dekker, New York, 499: 1-12, (1999).

- Kunieda. H, Nakano. A, Akimura. M, The effect of mixing of surfactants on solubilization in a microemulsion system, Journal Colloid Interface Science, 170: 78-84, (1995).

- Kunieda. H, Nakano. A, Pes. M, Effect of oil on the solubilization in microemulsion systems including nonionic surfactant mixture, Langmuir, 11: 3302-3306, (1995).

- Kunieda. H, Shinoda. k, Phase behavior in Systems of nonionic surfactant/ water/ oil around the hydrophilic-lipophilic-balance –temperature (HLB-tempreture) Journal Dispersion Science and Technology, 3: 233-244, (1982).

- Kunieda. H, Solans. C (Eds.), Industrial Applications of Microemulsions, Marcel Dekker, Inc., New York, 227-246, (1996).

- Kunieda. H, Yamagata. M, Mixing of nonionic surfactants at water –oil interface in microemulsions, Langmuir, 9: 3345-3351, (1993).

- Lapasin. R, Grassi. M, Coceani. N, Effects of polymer addition on the rheology of O/W microemulsions, Rheol. Acta 40 (2),185–192, (2001).

- Lawrence. M.J, and Rees. G.D, Microemulsion-based media as novel drug delivery systems, Adv. Drug Deliv. Rev, 45:89–121,(2000).

- MacKay. R.A, Agarwal .R, Handbook of Microemulsion Science and Technology Journal Colloid and Interface Science. 65 ,225, (1978).

- Malmsten. M: Microemulsions: Fundamentals and applied aspects; Kumar, P.; Mittal, K. L., Eds.; Marcel Dekker, Inc.: New York, (1996).

- Matsumoto. S. P, and Sherman. P, The viscosity of microemulsions. Journal Colloid and Interface Science, 30:525–536, (1969).

- Mehta. S.K, Bala. K, Tween based microemulsions: a percolation study. Fluid Phase Equilibria,172: 197-209, (2000).

- Moulik. S.P, and Paul. B.K, Structure, dynamics and transport properties of microemulsions Adv. Journal Colloid and Interface Science, 78: 99–195, (1998).

- Müller. R. H, Benita. S, Böhm. B, Emulsions and Nanosuspensions for the Formulation of Poorly Soluble Drugs, Medpharma GmbH Scientific Publishers, Stuttgart, 31-65, (1998).

- Muller. R. H, and Keck.C. M, Challenges and solutions for the delivery of biotech drugs—A review of drug nanocrystal technology and lipid nanoparticles. Journal Biotechnology, 113: 151–170, (2004).

- Nighute. A. B, Bhise S. B: Preparation and evaluation of microcrystalsof cefuroxime axetil. International Journal of Pharm Tech Research CODEN (USA) 1 : 424 -430, (2009).

- Ogino. K, Abe (Eds.) Mixed Surfactant Systems, Surfactant Science Series 46, Marcel Dekker, Inc. New York,(1992).

- Olsson. U, Shinoda. K, and Lindman. B, Change of the structure of microemulsions with the hydrophile lipophile balance of nonionic surfactant as revealed by NMR self-diffusion studies. Journal Phys. Chem.90: 4083–4088, (1986).

- Osborne. D.U, Ward. A.J, and O'Neill. K.J, Microemulsions as topical drug delivery vehicles. I. Characterization of a model system, Drug Dev. Ind. Pharm. 14 : 1203–1219, (1998).

- Papadimitriou. V, Sotiroudis. T.G, and Xenakis. A, Olive oil microemulsions: Enzymatic activities and structural characteristics, Langmuir, 23: 2071–2077, (2007).

- Paul. B, Mitra. R, Water solubilization capacity of mixed reverse micelles: Effect of surfactant component, the nature of the oil, and electrolyte concentration, Journal of Colloid and Interface Science, 288: 261–279, (2005).

- Pes. M.A, Aramaki. K, Nakamura. N, and Kunieda. H, Temperature-insensitive microemulsions a sucrose mono alkanoate system. Journal Colloid and Interface Science, 178: 666–672, (1996).

- Ponton. A, Bose. T. K, and Delbos. G, Trends in Colloid and Interface Science XI. Journal of Chemical Physics, 94: 6879–6886, (1991).

- Prince. L.M, Microemulsions: Theory and Practice, New York, Academic Press, (1977).

- Ray. S, Bisal. S, and Moulik. S, Studies on structure and dynamics of microemulsions II: Viscosity behavior of water-in-oil microemulsions. Journal Surfactant Science. Technology, 8: 191–208, (1992).

- Rosen. M.J, Surfactants and Interfacial Phenomena; John Wiley & Sons: New York,1-32,(1989).

- Roy. K, Huang. S, and Leong. K, Nanoparticle mediated oral gene delivery for DNA vaccination, Proc. Int. Symp. Control Release. Bioact. Mater. 26,134–135, (1999).

- Sabatini. D.A, and Knox. R.C, (Eds.) Transport and Remediation of Subsurface Contaminants, Colloidal, Interfacial and Surfactant Phenomena; ACS Symposium Series 491, American Chemical Society, Washington, DC,1: 1-251, (1992).

- Safran. S.A, Grest. G.S, and Bug. A, Webman, I. In Microemulsion Systems, edited by H. Rosano and M. Clausse; New York: Marcel Dekker; pp. 235–245, (1987).

- Salazar-Alvarez. G, Björkman. E, Lopes. C, Eriksson. A, Svensson S, and Muhammed. M Synthesis and nonlinear light scattering of microemulsions and nanoparticle suspensions, Journal Nanoparticle Res, 9: 647–652, (2007).

- Shah. D.O, Bansal. V.K, Chan. K.S, and Hsich. C.W. Improved Oil Recovery by Surfactants and Polymer Flooding; Shah, D.O. and Schecter, R.S. (eds.); Academic: New York, 293: 55-92, (1977).

- Soderman. O, and Nyden. M, NMR in microemulsions. NMR translational diffusion studies of a model microemulsion. Colloids Surfactant. A: Physicochem. Eng. Aspects 158: 273–280, (1999).

- Solans. C, and Kunieda. H, (Eds.) Industrial Applications of Microemulsions. Surfactant Science Series, Marcel Dekker, New York, 66, (1997).

- Song. S, Labhasetwar. V, Cui.X, Underwood. T, and Levy. R.J, Arterial uptake of biodegradable nanoparticles forintravascular local drug delivery: results with an acute dog model, Journal Control Release 54: 201–211, (1998).

- Szekeres. S, Acosta. E, Sabatini.D.A, and Harwell. J.H, Modeling solubilization of oil mixtures in anionic microemulsions: II. Mixtures of polar and non-polar oils Journal of Colloid and Interface Science, 294: 222-233, (2006).

- Tenjarla. S, Microemulsions: An overview and pharmaceutical applications. Crit. Rev. Ther. Drug Carr. Syst, 16: 461–525, (1999).

- Texter. J, (Ed.) Reactions and Synthesis in Surfactant Systems. Surfactant Science Series, Marcel Dekker, New York, 100,(2001).

- Thevenin. M.A, Grossiord. J.L, and Poelman. M.C, Sucrose esters/cosurfactant microemulsion systems for transdermal delivery: assessment of bi–continuous structures. Int. Journal Pharma, 137: 177–186, (1996).

- Thiele. L, Rothen-Rutishauser. B, Wunderli-Allenspach. H, Merkle. H.P, and Walter. E, Particle-uptake by monocyte-derived dendritic cells in vitro: evaluation of particle size and surface characteristics, Proc. Int. Symp. Control Release Bioact. Mater. 26, 163–164,(1999).

- Yaghmur. A, De Campo. L, Aserin. A, Garti. N, and Glatter. O, Structural characterization of five-component food grade oil-in-water nonionic microemulsions, Journal Physical Chemistry Chemical Physics 6 :1524–1533, (2004).

- Viswanathan. N.B, Thomas. P.A, Pandit. J.K, Kulkarni. M.G, and Mashelkar. R.A, Preparation of non-porous microspheres with high entrapment efficiency of proteins by a (water-in-oil)-in-oil emulsion technique, Journal Control Release, 58, 9–20, (1999).